1976

Decay schemes for mass separated 136I, and 138I, and 137Xe

Warren Ralph Western
Iowa State University

INFORMATION TO USERS

This material was produced from a microfilm copy of the original document. While the most advanced technological means to photograph and reproduce this document have been used, the quality is heavily dependent upon the quality of the original submitted.

The following explanation of techniques is provided to help you understand markings or patterns which may appear on this reproduction.

1. The sign or "target" for pages apparently lacking from the document photographed is "Missing Page(s)". If it was possible to obtain the missing page(s) or section, they are spliced into the film along with adjacent pages. This may have necessitated cutting thru an image and duplicating adjacent pages to insure you complete continuity.

2. When an image on the film is obliterated with a large round black mark, it is an indication that the photographer suspected that the copy may have moved during exposure and thus cause a blurred image. You will find a good image of the page in the adjacent frame.

3. When a map, drawing or chart, etc., was part of the material being photographed the photographer followed a definite method in "sectioning" the material. It is customary to begin photoing at the upper left hand corner of a large sheet and to continue photoing from left to right in equal sections with a small overlap. If necessary, sectioning is continued again — beginning below the first row and continuing on until complete.

4. The majority of users indicate that the textual content is of greatest value, however, a somewhat higher quality reproduction could be made from "photographs" if essential to the understanding of the dissertation. Silver prints of "photographs" may be ordered at additional charge by writing the Order Department, giving the catalog number, title, author and specific pages you wish reproduced.

5. PLEASE NOTE: Some pages may have indistinct print. Filmed as received.

University Microfilms International
300 North Zeeb Road
Ann Arbor, Michigan 48106 USA
St. John's Road, Tyler's Green
High Wycombe, Bucks, England HP10 8HR

Decay schemes for mass separated ^{136}I, ^{138}I, and ^{137}Xe

by

Warren Ralph Western

A Dissertation Submitted to the
Graduate Faculty in Partial Fulfillment of
The Requirements for the Degree of
DOCTOR OF PHILOSOPHY

Department: Physics
Major: Nuclear Physics

Approved:

Signature was redacted for privacy.

In Charge of Major Work

Signature was redacted for privacy.

For the Major Department

Signature was redacted for privacy.

For the Graduate College

Iowa State University
Ames, Iowa

1976

TABLE OF CONTENTS

LIST OF FIGURES

LIST OF TABLES

I. INTRODUCTION

The decays of several neutron-rich nuclides produced in fission are the subject of this work. These nuclides, ^{136}I, ^{137}Xe, and ^{138}I, are outlined with a solid border on a portion of the Chart of the Nuclides (1) shown in Figure 1. They have half-lives ranging from 6 seconds to 3.8 minutes. With the exception of ^{136}I, the daughters of these nuclides are unstable against beta decay. The decay energies, or Q-values, for these nuclei are greater than 4 MeV; therefore many excited states are expected to be populated in beta decay, and the corresponding gamma spectra may be quite complicated. No decay scheme for ^{138}I has been published previous to this work. Even though the decay of ^{136}I has been studied, no information exists on high-energy gamma transitions above 3400 keV.

The study of the decay of these nuclides is difficult since they have short half-lives, therefore many samples must be studied in order to obtain sufficient statistics. Access to a continuous means of producing these isotopes therefore constitutes an important advantage. Neutron-rich isotopes are conveniently produced by fission, but the number of different activities produced is large, therefore sophisticated techniques such as on-line mass separation are of great value in separating and identifying the activity of interest.

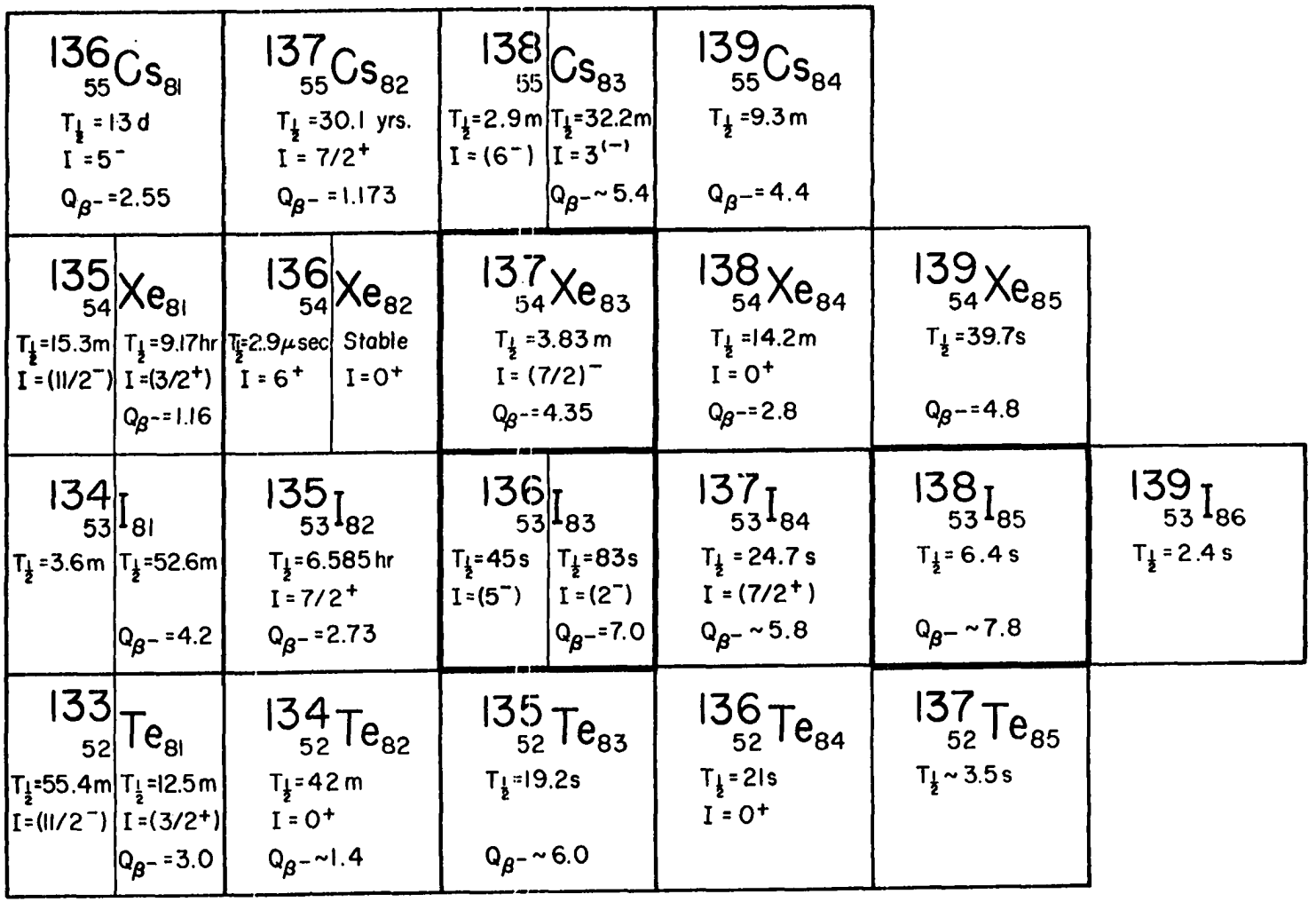

Figure 1. Section of the chart of nuclides showing the nuclides studied

Another reason for studying these nuclei is to advance the basic knowledge and understanding of nuclear systematics used in the development of nuclear theories. The knowledge gained is also important in the design of reactors and in reactor decay-heat calculations.

A. Advancement of Basic Knowledge

A basic reason for studying these decays is to extend the systematics of excited states for neutron-rich nuclei. The decays of the nuclides studied in this work represent an important source of information on the level structure of ^{136}Xe, ^{138}Xe, and ^{137}Cs and extend the knowledge of the N=82, and N=84 isotones and the Xe and Cs isotopes further into the neutron-rich side of stability.

It is important to note that all of these nuclides are near the magic numbers Z=50 and N=82, therefore the results are useful as a test of the shell model in this region. It is of interest to determine if a shell-model basis, consisting of only simple configurations of those particles outside the doubly magic core, is adequate to describe the low-lying states of these nuclides. A shell-model calculation is dependent on the nucleon-nucleon interaction and hence is an indication of the adequacy of the interaction used. In addition to providing a test of the shell model, these results assist in evaluating the possibility of collective motion in

this region. It is hoped that at some time all nuclides can be described and their properties predicted by a full shell-model calculation using an interaction which is consistent with nucleon-nucleon scattering results.

Finally, there is a need to resolve a number of disagreements among previous results on the decay of ^{136}I. A notable problem is the claim in one of the previous studies that there exists two excited isomeric states in ^{136}I that beta decay. Other investigators have reported only one.

B. Technological Applications

The primary application of the results of this research is in the design and modeling of fission reactors. The results relate both to the operation of the reactor and to its generation and diffusion of heat. A detailed intensity inventory of the beta and gamma radiation as a function of energy is needed for most of the radioactive fission products. The kinetic energy of an electron emitted in beta decay is absorbed in the vicinity of the fission fragment while the energy of the associated neutrino is completely lost. The volume affected by gamma radiation heating is very dependent on the energy of the transition and the design of the reactor. This work also demonstrates the feasibility of studying activities other than the inert gases and their daughters by using a uranyl stearate target with the TRISTAN

on-line isotope separator.

C. Survey of Earlier Work

The halogen fission products were among the first to be studied. In 1940 Strassmann and Hahn (2) identified two new iodine activities. They measured the half-lives to be 1.8 ± 0.4 minutes and 30 ± 6 seconds. These half-lives correspond to those of ^{136}I and ^{137}I, respectively. The decay of ^{138}I was first observed by Sugarman (3) in 1949. He measured the half-life of this activity to be 5.9 ± 0.4 seconds. The xenon fission products were also identified during this period. The first observation of ^{137}Xe decay was by Seelmann-Eggebert and Born (4) in 1943. They reported a half-life of 3.8 minutes.

The techniques of experimental nuclear physics progressed from half-life measurements with Geiger counters and measurements of the maximum gamma- and beta-decay energies, using absorbers, to NaI(Tl) and plastic scintillator detectors and small multichannel analyzers. During this period there were two studies of the gamma and beta transitions in the decay of ^{136}I (5,6), but only delayed neutron emission studies of the decay of ^{138}I.(7) Holm *et al.* (8) performed the only NaI(Tl) study of the decay of ^{137}Xe. This study was also the first for any of these isotopes in which a mass-separated source was used.

1. Previous studies of the decay of ^{136}I

The first study of the decay of ^{136}I using Ge(Li) detectors was by Lundan and Siivola (9) in 1968. Chemical separation was used to isolate the iodine activity produced in fission. A total of 21 gamma transitions were identified as belonging to the decay of ^{136}I with two more possibly belonging. Of these 23 transitions, 22 were placed in a level scheme consisting of 13 definite levels and two possible levels. The level scheme is supported by gamma-gamma coincidence data obtained from both a Ge(Li)-NaI(Tl) and a NaI(Tl)-NaI(Tl) experiment. This was the first study to postulate the existence of a short-lived isomeric state in ^{136}I in addition to the 83-second state. The value obtained for the half-life of the short-lived isomeric state was 40 ± 5 seconds, which was determined by measuring the decay of many of the transitions in a sequence of 64 successive spectra.

Carraz *et al.* (10) reported the results of an ^{136}I study in 1970. The iodine fission products were separated chemically. This study identified 15 gamma transitions as belonging to the decay of ^{136}I and placed all of them in a level scheme consisting of six definite excited levels and five possible excited levels. This level scheme is supported by gamma-gamma coincidence data from a Ge(Li)-NaI(Tl) system. Gates were placed in only three regions of the spectrum. A

measurement of the beta spectrum in coincidence with the first excited state transition gave a Q-value of 6.3 ± 0.2 MeV for the decay of ^{136}I. A delayed coincidence experiment between the 197-keV transition and the beta spectrum indicated a half-life of 2.8 ± 0.2 microseconds for the 1892-keV state of ^{136}Xe. Carraz et al. (10) measured the half-lives of the ^{136}I isomeric states by multiscaling the gamma transitions using a 20-second counting period for a total time of four minutes. The values obtained were 48 ± 1 seconds for the short half-life activity and 83 ± 3 seconds for the long half-life activity. There are other discrepancies between this work and the earlier work of Lundan and Siivola (9). These discrepancies include transition energies and intensities and levels included in the decay scheme.

Lundan (11) published a new study of the decay of ^{136}I in 1971. This revised study used the Studsvik isotope separator on-line to a reactor. The results were much more consistent with those of Carraz et al. than with his earlier study. He identified 21 gamma transitions as belonging to the decay of ^{136}I, and placed all of them in a level scheme consisting of 18 excited levels. Only three of these levels are the same as those he reported earlier, and nine of them are the same as reported by Carraz et al. The transition energies and intensities were consistent with the values obtained by Carraz et al., but the intensities were consider-

ably different from those he reported earlier. His level scheme is supported by gamma-gamma coincidence data obtained with two Ge(Li) detectors. In this study three half-lives were measured for the decay of ^{136}I. The values obtained were 48 ± 2 seconds, 83 ± 3 seconds, and 100 ± 3 seconds. The half-life measurements were obtained from multiscaling experiments in which gates were placed on seven peaks in one experiment and fifteen in the other. The time intervals were 8 seconds and 2 seconds with total measuring times of 1000 and 106 seconds respectively. The half-lives of all but a few weak peaks were also measured by following their intensities in a sequence of eight successive 4K spectra of 57-second duration each.

The most recent detailed study of the decay of ^{136}I was by Erten *et al.* (12) in 1971. The iodine activity was obtained by chemical separation from fission-product activities. In this study 21 transitions were identified and 17 of these were placed in a level scheme consisting of 14 excited levels. This level scheme is supported by gamma-gamma coincidence information obtained from a Ge(Li)-NaI(Tl) system. The half-lives of the isomeric states in ^{136}I were determined by following the decay of appropiate gamma transitions over a 6.5-minute period divided into 20-second intervals. Only two half-lives were observed, 45 seconds and 83 seconds. Even though the accepted Q-value is 6980 keV (if the 83 second ac-

tivity is regarded as the ground state of ^{136}I (13)), the highest energy gamma transition identified in any of these three studies is the 3949-keV transition in the study by Erten et al. (12). There are also discrepancies in the location of the excited states and in the number and placement of the gamma transitions. The coincidence results reported are in general agreement, but are subject to differences in interpretations because NaI(Tl) detectors were used for at least one side of the coincidence data and only a few windows were set.

Achterberg et al. (14) in 1972 reported a study of the internal-conversion coefficients of the low-energy transitions seen in the decay of ^{136}I. This study used the Buenos Aires on-line isotope separator, and coefficients and multipolarities were determined for two transitions.

The 197-, 381-, and 1313-keV transitions, which depopulate the 6^+, 4^+, and 2^+ members of the ^{136}Xe YRAST band, were observed in two studies of the fission products produced in the spontaneous fission of ^{252}Cf. The first study was of the isomeric transitions in fission fragments, reported by John et al. in 1970 (15). A four-parameter experiment was performed where the kinetic energy of the two fragments, the energy of the gamma transition, and the time delay between one of the fragments and the transition were recorded. The cascade was observed because the 6^+ is an

isomeric state with a measured half-life of about 3 microseconds. The other study measured the prompt gamma transitions emitted in spontaneous fission, and was reported by Cheifetz et al. (16) in 1971. In these studies fragment masses were identified from the kinetic energies of the fragments in coincidence with the gamma transitions. The elements were identified by the coincident K x-rays.

Edvardson and Norlin (17) reported in 1974 that the B(E2) value for the first-excited to ground-state transition in ^{136}Xe was 0.17 ± 0.03 e^2b^2. The lifetime of the first excited state at 1313 keV was reported to be 0.59 ± 0.15 picoseconds. These values were obtained from Coulomb excitation of stable ^{136}Xe.

In 1971, Wildenthal et al. (18,19) reported the results of a study of proton transfer reactions on the N=82 nuclei. Using the reactions ^{136}Xe(d,^{3}He)^{135}I and ^{136}Xe(^{3}He,d)^{137}Cs they deduced that the doubly-magic core of ^{132}Sn is not active in the ground state of ^{136}Xe. The experimentally determined spectroscopic factors from the DWBA calculation are directly related to the occupancy of the orbitals in the target nuclide. For ^{136}Xe, they concluded from the spectroscopic factors of the pickup reaction that the ratio of occupancy in the ground state is 85% $1g_{7/2}$ to 15% $2d_{5/2}$.

There have been two ^{136}Xe(p,p')^{136}Xe experiments which populated excited states of ^{136}Xe. The first of these was

the study of the isobaric analog resonances by Moore et al. (20) in 1970. In this study, 36 excited states of ^{136}Xe below 6.3 MeV were observed and possible spins and parities were assigned to the levels above 3.26 MeV. A second inelastic proton scattering experiment was reported by Sen et al. (21) in 1972. This study was designed to complement the study of Moore et al., by concentrating on the levels below 3.3 MeV. Fourteen levels below this energy were analyzed using the distorted-wave Born approximation. A collective complex form factor was used to obtain spins, parities and deformation parameters for these levels.

2. Previous studies of the decay of ^{138}I

Very little is known about the decay of ^{138}I and the levels of ^{138}Xe. Lundan and Anttila (22) observed one transition in the decay of ^{138}I in 1970. Kratz et al. (23) identified five transitions as belonging to the decay of ^{138}I in a survey of gamma-ray emission from short-lived Br and I isotopes. No attempt was made to construct a level scheme.

The only study of the levels of ^{138}Xe is the $^{252}Cf(SF)$ study by Cheifetz (16), discussed previously. In this study the transitions which depopulate the 4^+ and 2^+ members of the YRAST band were observed.

3. Previous studies of the decay of ^{137}Xe

The first study of the decay of ^{137}Xe in which Ge(Li) detectors were used was by Holm (24) in 1968. The ^{137}Xe fission fragments were obtained from a uranyl stearate target from which Xe gases emanate easily. An isotope separator on-line to the Nobel Institute 225-cm cyclotron was used to separate the xenon isotopes produced in the fission of ^{238}U. Nineteen well-established transitions were identified, and 14 additional very low-intensity transitions were reported. Of the 19 well-established transitions, 17 were placed in a level scheme consisting of nine excited levels and one possible level. This level scheme was supported by gamma-gamma coincidence data obtained with two NaI(Tl) detectors. The statistics of the coincidence data were poor due to the low intensity of all transitions except the one at 456 keV.

A more complete study of the decay of ^{137}Xe was reported by Monnand *et al.* (25) in 1975. The target in this study was a sample of heated $^{235}UO_2$. The ARIEL isotope separator facility was used to mass separate the xenon which emanated from the target. In this study 83 gamma transitions were identified. The proposed level scheme consists of 21 excited levels and two possible levels. A total of 55 transitions were placed in this decay scheme. The coincidence data used to construct the level scheme were obtained using two Ge(Li)

detectors and consisted of gates on six transitions.

The existence of a level at 848.5 keV was confirmed in a muon capture study by Lucas *et al.* (26) in 1973 and its transitions to the ground and the first excited states were observed. The reaction $^{138}Ba(\mu^-,n)^{137}Cs$ was used. This study demonstrated the feasibility of studying nuclear properties by muon capture. The multipolarity of the 456-keV transition from the first excited level to the ground state has been determined to be E2 ($\leq$10%M1) by Achterberg *et al.* (14) from internal-conversion measurements.

The character of the lowest levels in ^{137}Cs has been studied by Wildenthal *et al.* (18,19), in 1968 and 1971, using proton stripping and pickup reactions on ^{136}Xe and ^{138}Ba, respectively. Six levels were observed in the stripping reaction (19) below 2.2 MeV.

II. EXPERIMENTAL TECHNIQUES

A. The TRISTAN System

The nuclides studied were produced using the TRISTAN isotope separator, operating on-line to the Ames Laboratory Research Reactor (27,28,29). The system is shown in Figure 2 and a brief description is given below.

The fission products are produced when thermal neutrons from a beam external to the reactor are absorbed by uranium nuclei in a sample of uranyl stearate which has been enriched to 93% in ^{235}U. The asymmetric mass yield of fission fragments from thermal neutron induced fission of ^{235}U is shown in Figure 3. For the proton numbers 36 (Kr), 53 (I), and 54 (Xe) the cumulative fission yield, as a function of A, peaks near the mass numbers 90, 134 and 138 respectively. Thus the yield of ^{138}I is much less than that for ^{136}I.

The inert gas fission products which emanate efficiently from the stearate, and with fresh targets some iodine and bromine, are transported through a teflon transport line 1.4 meters long to the ion source. A sweep gas consisting of a mixture of helium with small amounts of stable krypton and xenon is used to assist in maintaining a discharge in the ion source and to monitor the focus and mass number of the separator ion beam.

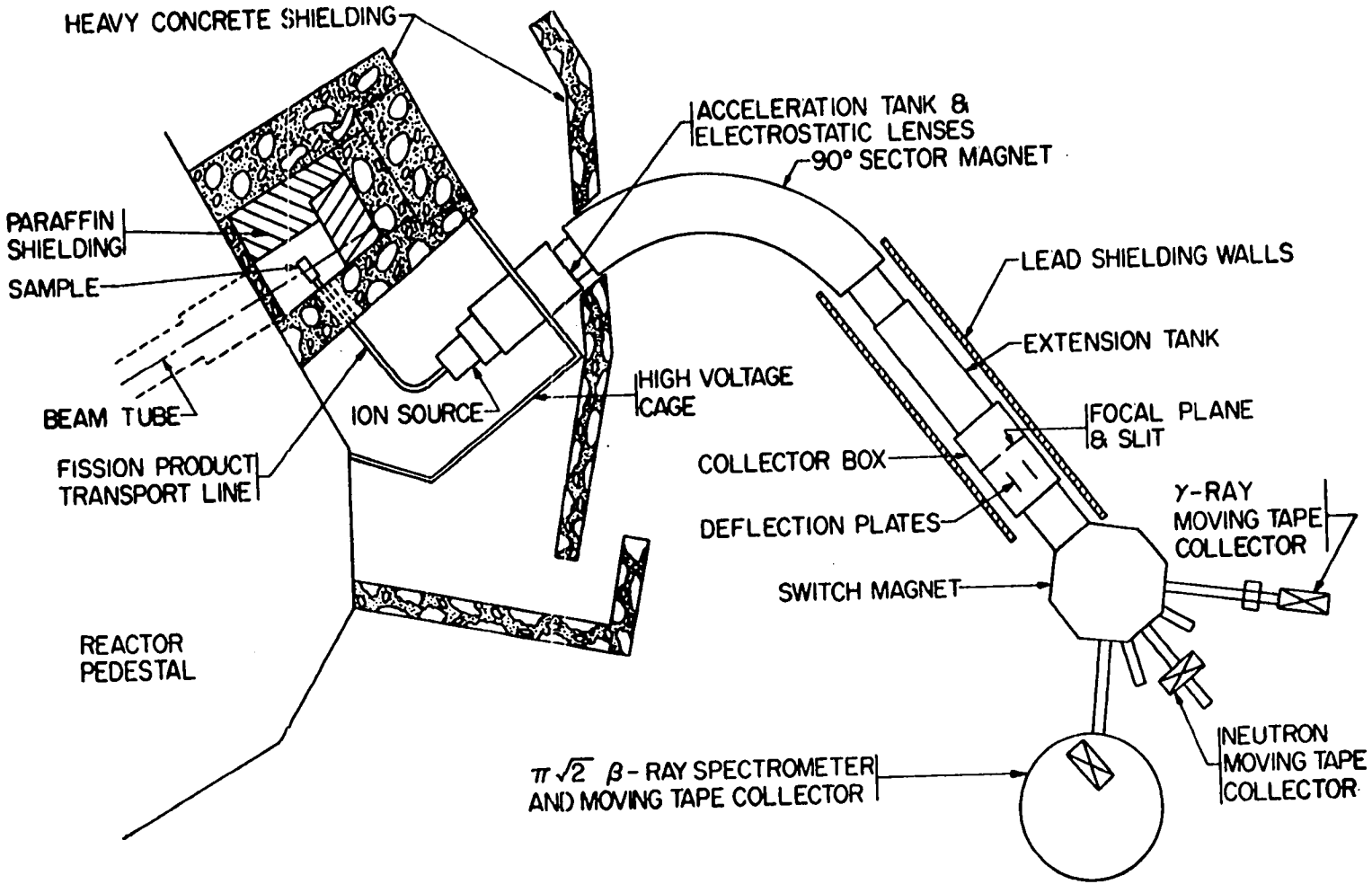

Figure 2. Schematic layout of the TRISTAN isotope separator facility

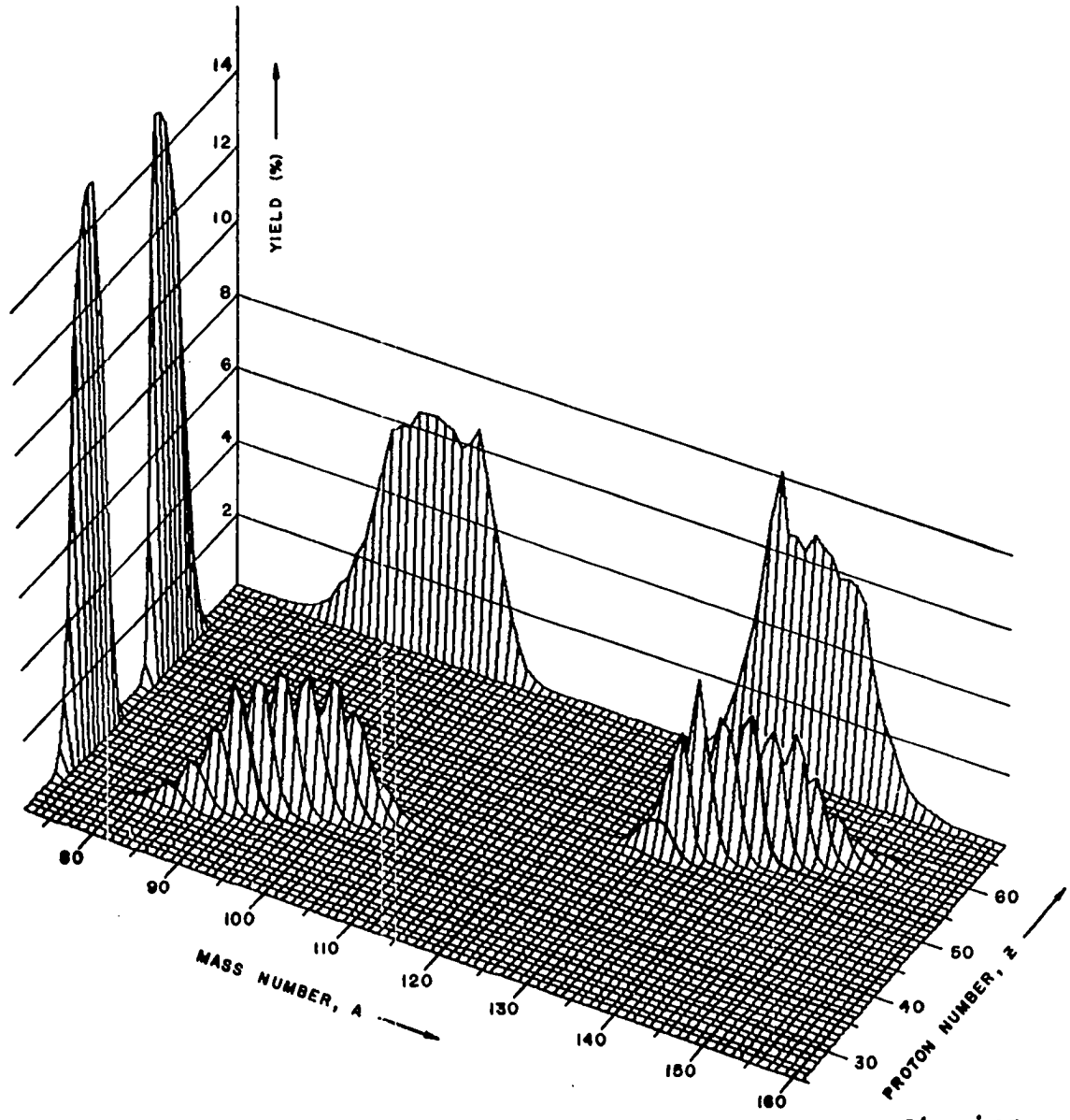

Figure 3. Fission product yield of ^{235}U for thermal neutron fission

After the sweep gas and the fissicn products are ionized they are accelerated through a potential of 50 kilovolts and focused by two electrostatic lenses before entering the 90° analyzing magnet of the separator. The mass-separated beam enters a collector box where the beam can be focused visually by observing the stable isotopes on a fluorescent screen. The desired mass can then be positioned in the center of the slit. Two parallel copper strips (pins) are positioned on opposite sides of a neighboring mass to provide beam position stabilization. These stabilization pins are ccnnected to the inputs of a differential amplifier/integrator system which detects any asymmetry in the beam current deposited on the pins and centers the beam between the pins by adjusting the accelerating potential.

The slit in the collector box is aligned with the entrance to a switching magnet. The magnet directs the selected isotope ion beam to the experimental station being used and helps to remove any residual neighboring mass or neutral contaminants from the beam. For this study the beam was directed to the moving tape collector (MTC).

In the MTC the beam is deposited on aluminized mylar tape. The deposited activity can be positioned in front of the detectors and later removed by means of a tape transport system. Two different MTC systems were used to obtain the data for this study. The initial data were obtained using

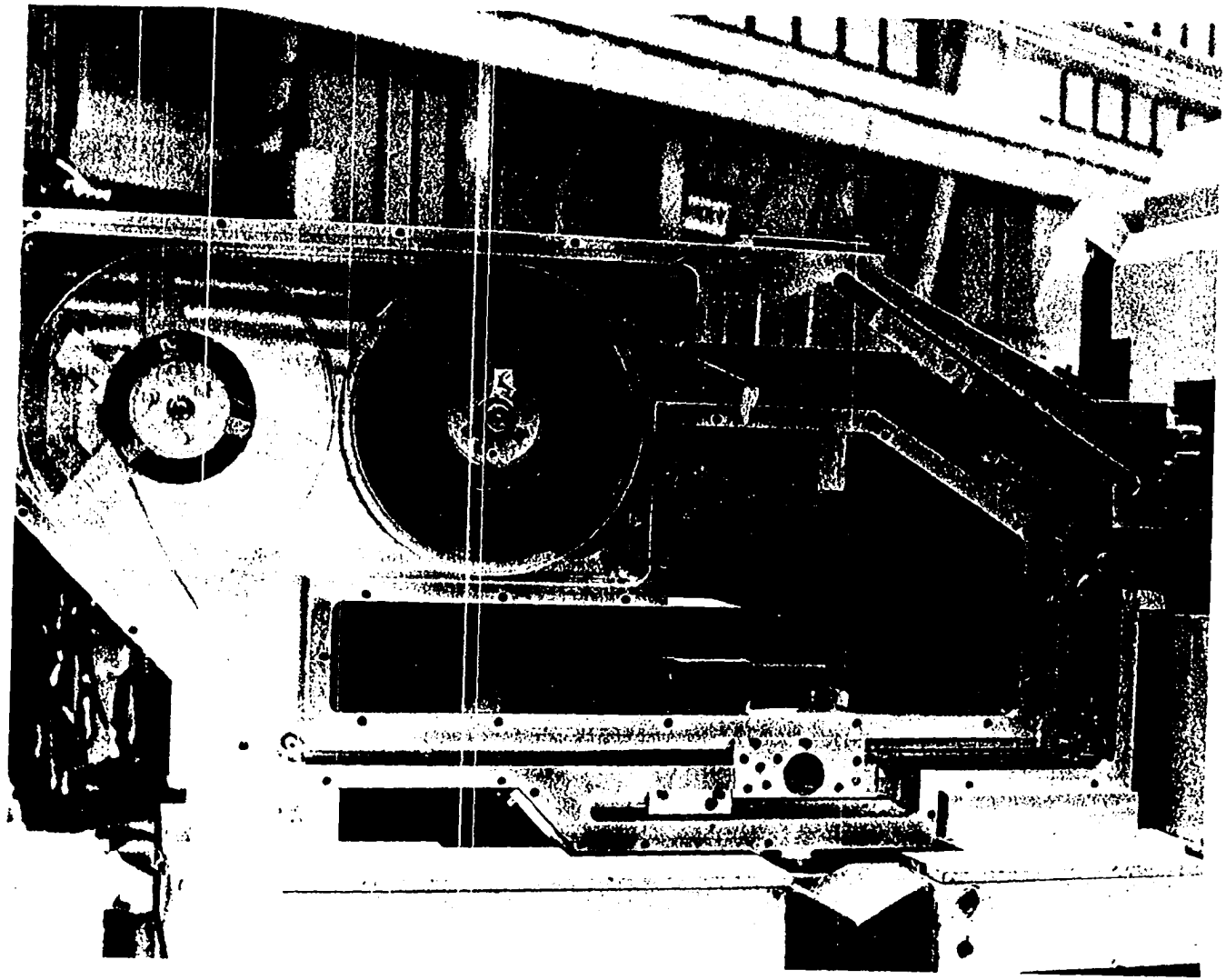

Figure 4. Photograph of second generation moving tape collector (MTC)

the second generation design (Figure 4) and the later data were taken using the third generation design (Figure 5). Both designs have detector ports at the point of deposit and at "downstream" ports which are used to study daughter activities. The purpose of the MTC is to enhance the ratio of the integrated activity of the desired nuclide to that of other nuclides of the same A. The operating cycle for the MTC and the data acquisition is controlled by the Daughter Analysis System (DAS) which determines the times for beam collection, delay, data accumulation, and tape motion. The computer code ISOBAR can be used to determine the values for these parameters which give the maximum enhancement of a specific member of the decay chain. A complete description of this code and the parameters involved is contained in a report by Norman *et al.* (30).

In this study the parent was the activity of interest, and the MTC was used to limit the build-up of the daughter. In studying iodine activity, xenon as well is deposited directly on the tape and also grows in from the iodine parent.

B. Separator Operation to Obtain Iodine Activity

Although a given stearate sample is used for about six months, the iodine emanates from the stearate for a period of only about three weeks. This occurs because iodine emanation is more dependent on the structure of the stearate material

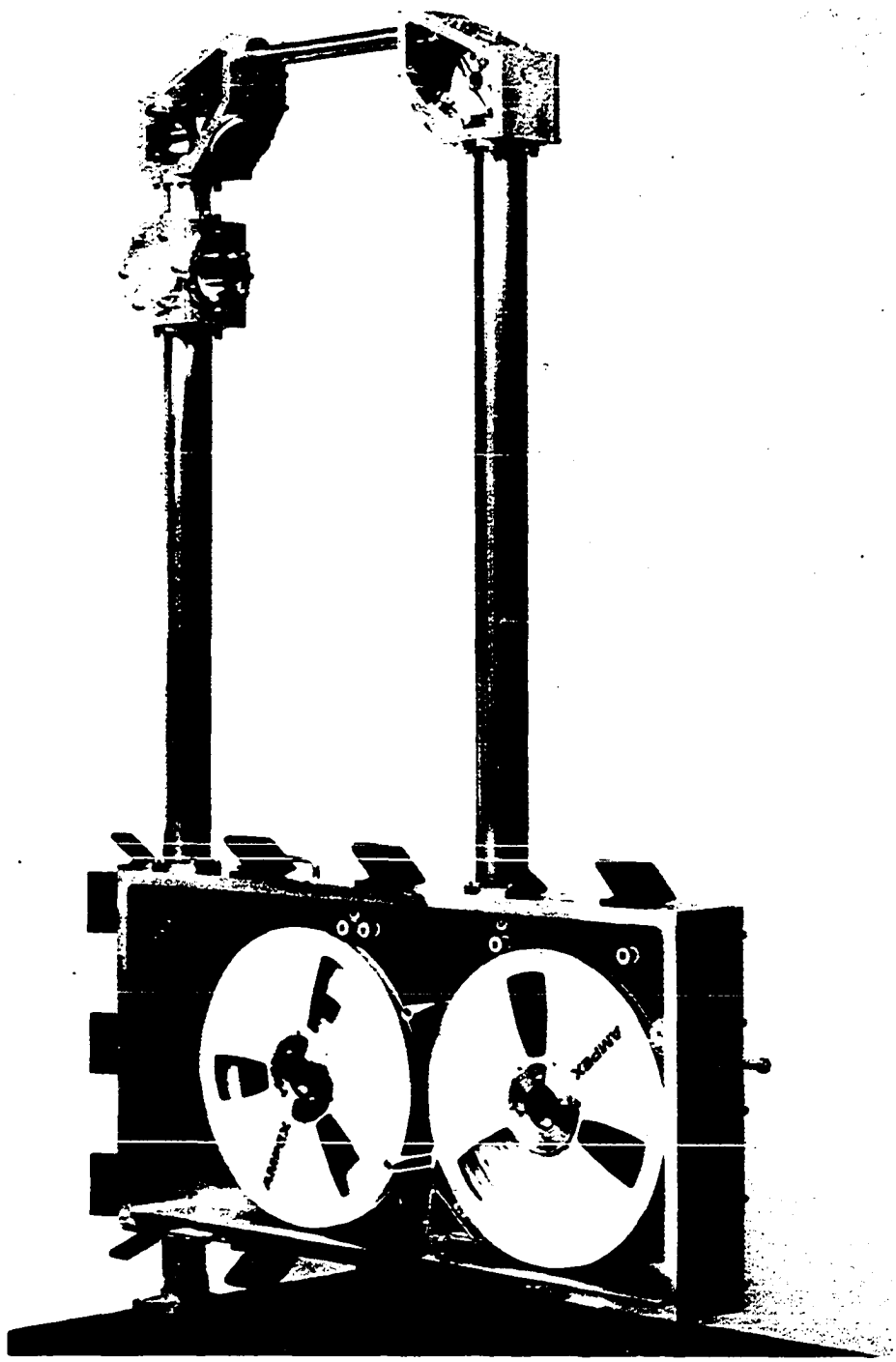

Figure 5. Photograph of third generation moving tape collector (MTC)

than inert-gas emanation and hence is more sensitive to radiation damage. This period also corresponds to the time of maximum hydride contamination during the use of a stearate sample.

The differential pump pressure increases 15 to 20 microtorr when the sample is initially irradiated, therefore a period of a day or two is required to outgas a new stearate sample. It is found that this pressure has to be 10 to 15 microtorr before any iodine activity can be observed, and that the maximum activity is obtained when the pressure added by the support gas is minimal.

A current of 41 to 42 amperes through the filament of the ion source was used for the iodine experiments in this study, since this relatively high filament current was required to obtain maximum iodine activity. The other ion source operating parameters did not have unique values which gave maximum activity. A typical set of values for the other parameters is about 330 milliamperes for the current through the ion source magnet, 45 volts for the anode voltage, and 3.8 kilovolts for the extractor voltage.

The ^{136}I activity (the daughter ^{136}Xe is stable) obtained after about 160 seconds of beam collection was about 8 kcps using an 11% Ge(Li) detector. The higher iodine masses are more difficult to study for several reasons. The xenon daughters are not stable and emanate more readily than iodine

thus making it impossible to get a relatively clean spectrum. Also the fission yield is lower compared to the yield of xenon, and the ratio decreases for the higher masses. Finally, the iodine isotopes have shorter half-lives, therefore the emanation and transport times are more important. An attempt was made to observe the 2.4-second ^{139}I activity but no peaks could be identified.

C. Data Acquisition

Three different types of measurements were performed in this study. They were gamma singles, gamma-gamma coincidence, and gamma multiscale measurements. In all of these experiments the detectors used were large volume true-coaxial detectors manufactured by Ortec. The characteristics of these detectors are summarized in Table I.

1. Gamma-ray singles measurements

A block diagram of the equipment used to obtain gamma singles measurements is shown in Figure 6. The equipment used and typical settings which gave the best results are described in the following paragraphs.

The bias voltage for the detector was supplied by a battery pack, and the power for the preamplifier was supplied by NIM bins. A Tennelec TC 203BLR amplifier was usually used to process the preamplifier signal. The values of the pulse-shape time constant which gave the best resolution were

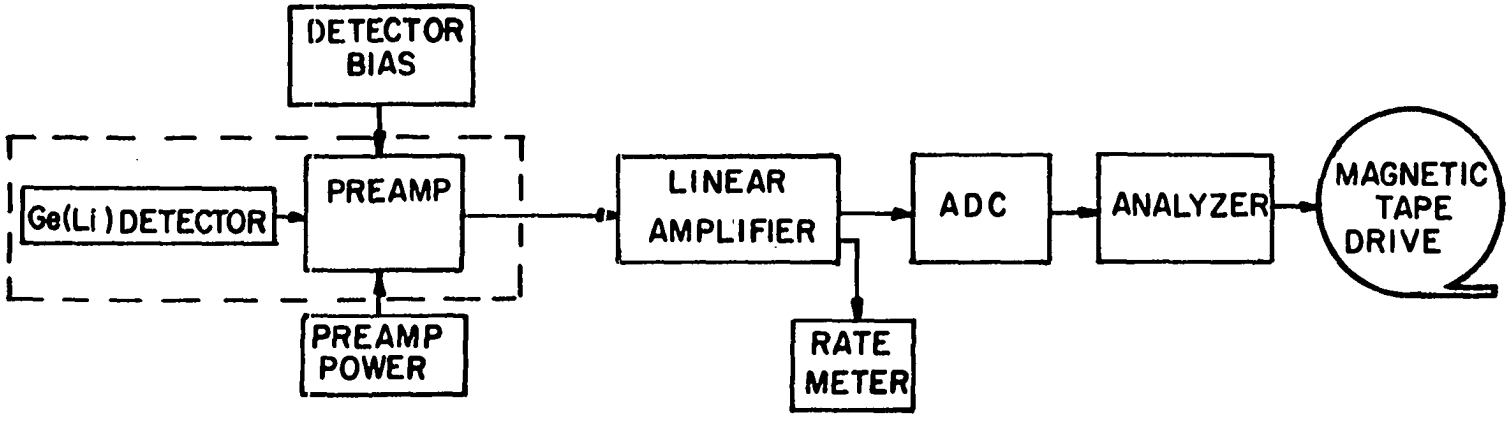

Figure 6. Block diagram of gamma singles electronics

Table I. Detectors used in this study

Detector	A	B
Active volume	57.3 cm^3	58.2 cm^3
Resolution	2.7 keV at 1.33 MeV	2.7 keV at 1.33 MeV
Efficiency	11.8%	9%
Peak-Compton ratio	34:1	28:1
Absorbing layers	0.5 mm Al 1.0 mm teflon .64 cm plexiglass	0.5 mm Al 1.0 mm teflon .64 cm plexiglass
Bias voltage	1890 volts	2500 volts

either 2 or 4 microseconds. The amplifier was direct coupled to the ADC except when a restorer/rejector unit was used.

A Canberra Model 1464 Baseline Restorer/Rejector unit was used in a few of the spectra obtained for this work. A typical shaping time constant used was 2 microseconds.

Geoscience Model 8050 8K ADC's were used in this work. Pile-up rejection and logarithmic baseline restoration were used with time constants of either 6.4 or 12.8 microseconds. In most cases a full 8K spectrum was obtained.

The analyzer used in these experiments was a Technical Measurements Corporation 16K analyzer which has a memory capacity of $10^5 - 1$ counts per channel. The resulting

spectra were recorded on seven-track magnetic tape for subsequent computer analysis. Usually the memory was erased after a spectrum was recorded. The individual spectra were added together by an IBM 360/65 computer using codes which could perform gain shift and overflow corrections.

Four types of spectra were obtained using the same apparatus settings for each activity studied. The first type was a spectrum of the unknown activity. The location of the detector and the DAS parameters were chosen to enhance the activity of interest. This spectrum required the longest collection time, because good statistics are important to observe and measure accurately the energies and intensities of the weak transitions.

In order to calibrate the energies in the above spectrum, it is necessary to have a spectrum in which calibration source activities are included along with the activity studied. The values obtained for the more intense transitions in this calibration-plus-unknown spectrum are then used to calibrate the urknown spectrum.

The third type of spectrum is called the calibration spectrum and consists of calibration activities only. The purpose of this spectrum is to map the differential nonlinearity of the system and to obtain the relative efficiency curve for the detector. This spectrum contains calibration sources in addition to those used in the calibration-plus-

unknown spectrum, in order to more completely map the nonlinearity and detector efficiency.

Finally either a background spectrum or a spectrum measured under different MTC conditions was obtained to assist in identifying peaks that were the result of either background or contaminant activity. The separator is used but the activity is stopped at the screen in the collector box if a background spectrum is desired. If positive identification of the weak unknown peaks is to be made, the time required for collecting this spectrum is similar to that for the unknown spectrum.

Parameters for the singles measurements associated with the ^{136}I decay study are given in Table II. The ^{135}I hydride and a few other contaminants were identified from the ^{135}I spectrum. Other contaminants were identified by comparison of the unknown spectra A and B and the calibration-plus-unknown spectrum D.

Because these three spectra were obtained at different times and under different conditions, a comparison of the relative intensities of the transitions in these spectra revealed systematic differences depending on which isomeric state populated the level. This difference was used to suggest half-life asssignments for those transitions which were not directly measured by multiscale techniques.

Table II. Gamma-ray run parameters for the ^{136}I decay study

Spectrum	A	B	C[1]	D
Range (keV)	30 - 4075	200 - 5500	50 - 6300	35 - 1340
Length	8K	8K	8K	4K
Duration	5.33 hr	33 hr	12 hr	1.5 hr
Count Rate	2.5 kcps[2]	8 kcps[2]	8 kcps[3]	3 kcps[2]
DAS Cycle	15 min[4]	160 sec[4]	13.5 hr[5]	20 min[4]
Calibration Activities	^{56}Co, ^{226}Ra ^{57}Co, ^{228}Th	^{56}Co ^{226}Ra	^{56}Co ^{226}Ra	^{57}Co, ^{192}Ir ^{182}Ta, ^{133}Ba
MTC	2nd[6]	2nd[6]	2nd[6]	3rd[6]

[1]A spectrum of ^{135}I used to identify hydride and other contaminants.
[2]The approximate count rate at the end of source deposition.
[3]Estimated count rate at the beginning of the counting period.
[4]The DAS cycle was to count during deposition and then move the tape.
[5]The DAS cycle was, deposit activity for 30 minutes, delay for 1 hour, and count for 12 hours.
[6]The generation of MTC used for the experiment. Detector A (see Table I.) was used at the parent port of the MTC and the amplifier was a Tennelec TC 203BLR.

The details of the ^{138}I decay study are given in Table III. Most of the peaks observed in the ^{138}I spectra were not the result of that activity. The iodine peaks were identified by determining the ratio of the areas of the peaks in the unknown to their area in the delayed spectrum. The relative efficiency curve for the ^{138}I study was obtained from the areas of the ^{138}Xe and ^{138}Cs peaks in the unknown spectrum (31,32). The prompt and delayed ^{138}I spectra were measured simultaneously.

Table IV contains the details of the ^{137}Xe singles measurements. These spectra were obtained after iodine had ceased to emanate from the stearate. The daughter activity ^{137}Cs was not observed except as a background contaminant, since it has a low specific activity. It was especially important to have the background spectra since ^{137}Xe decay is almost completely dominated by the 456-keV transition, and most of the other transitions are very weak in comparison. The calibration-plus-unknown spectrum B was used to determine the energy of the 456-keV transition. Spectra D and E were obtained using a Pb absorber to enhance weak high-energy transitions and reduce the dead time due to the 456-keV transition.

Table III. Gamma-ray run parameters for the ^{138}I decay study

Spectrum	A	B
Range (keV)[1]	100 - 4100	100 - 4100
Duration	14.2 hours	14.2 hours
Count Rate[2]	11 kcps	11 kcps
DAS Cycle	Deposit and count for 24 seconds	24 sec deposit 12 sec delay 12 sec count
Calibration Activities	^{138}Xe, ^{138}Cs	^{138}Xe, ^{138}Cs
MTC Port[3]	Parent	Daughter

[1]The length of these spectra was 8K.
[2]The approximate value of the maximum count rate during the counting part of the DAS cycle.
[3]Detectors are described in Table I. The amplifiers used were Tennelec TC 203BLR amplifiers. The third generation MTC was used for these spectra.

Table IV. Gamma-ray run parameters for the ^{137}Xe decay study

Spectrum	A	B[1]	C	D[2]	E[2]
Range (keV)	64 - 4100 [3]	64 - 4100 [3]	64 - 4100 [3]	360 - 4400 [3]	360 - 4400 [3]
Duration	16.5 hr	36 min	16.7 hr	42 hr	36 hr
Count Rate	1.1 kcps[4]	1 kcps[4]		3.2 kcps[4]	
DAS Cycle	D = 2.5s, C = 92s [5]	D = 1s, C = 100s [5]	bkg	D = 13s, C = 11s [6]	bkg
Calibration Activities	^{192}Ir ^{198}Au ^{56}Co	^{192}Ir ^{198}Au		^{56}Co	
MTC	2nd[7]	2nd[7]	2nd[7]	3rd[7]	3rd[7]
Restorer/ Rejector	Yes	Yes	Yes	No	No
Amplifier	Ortec 452	Ortec 452	Ortec 452	Tennelec 203BLR	Tennelec 203BLR

[1]The purpose of this calibration-plus-unknown spectrum was to determine accurately the energy of the 456-keV transition.
[2]These spectra were obtained through an absorber consisting of 7 mm of Pb followed by 2 mm of Cd.
[3]The length of these spectra was 8K channels.
[4]Count rate at the end of deposition.
[5]The DAS cycle was to deposit activity for time D followed immediately by counting for time C.
[6]For this cycle counting occurred during the deposition time D as well as during time C.
[7]The generation of MTC used. Detector A was used at the parent port of the MTC.

2. Multiscale measurements

Multiscale data on the decay of ^{136}I were obtained in order to determine the number of isomeric states in ^{136}I, confirm the assignment of transitions to the two isomers in ^{136}I decay, and measure the half-lives associated with this decay. The energy range from 170 keV to 2500 keV was spanned in three separate sets of data consisting of 32 successive 512-channel spectra obtained after the deposition of the iodine activity. A block diagram showing the equipment used and the connections between the units is shown in Figure 7. A brief description is given below.

All of the equipment with the exception of the detector, the amplifier, the DAS, and the magnetic tape unit were manufactured by Technical Measurements Corporation. The data acquisition cycle was controlled by the DAS. After a source had been deposited and the beam deflected, the DAS generated an external start pulse for the TMC 204 Multiscale module and moved the tape at the end of the multiscale cycle.

The multiscale module was inserted into a TMC 12-bit Model 242 Input Unit. The output was a bit pattern which was incremented after a preset time period. The desired time interval was obtained by setting the dwell time of the multiscale module and specifying the bits retained with the 12-bit input unit.

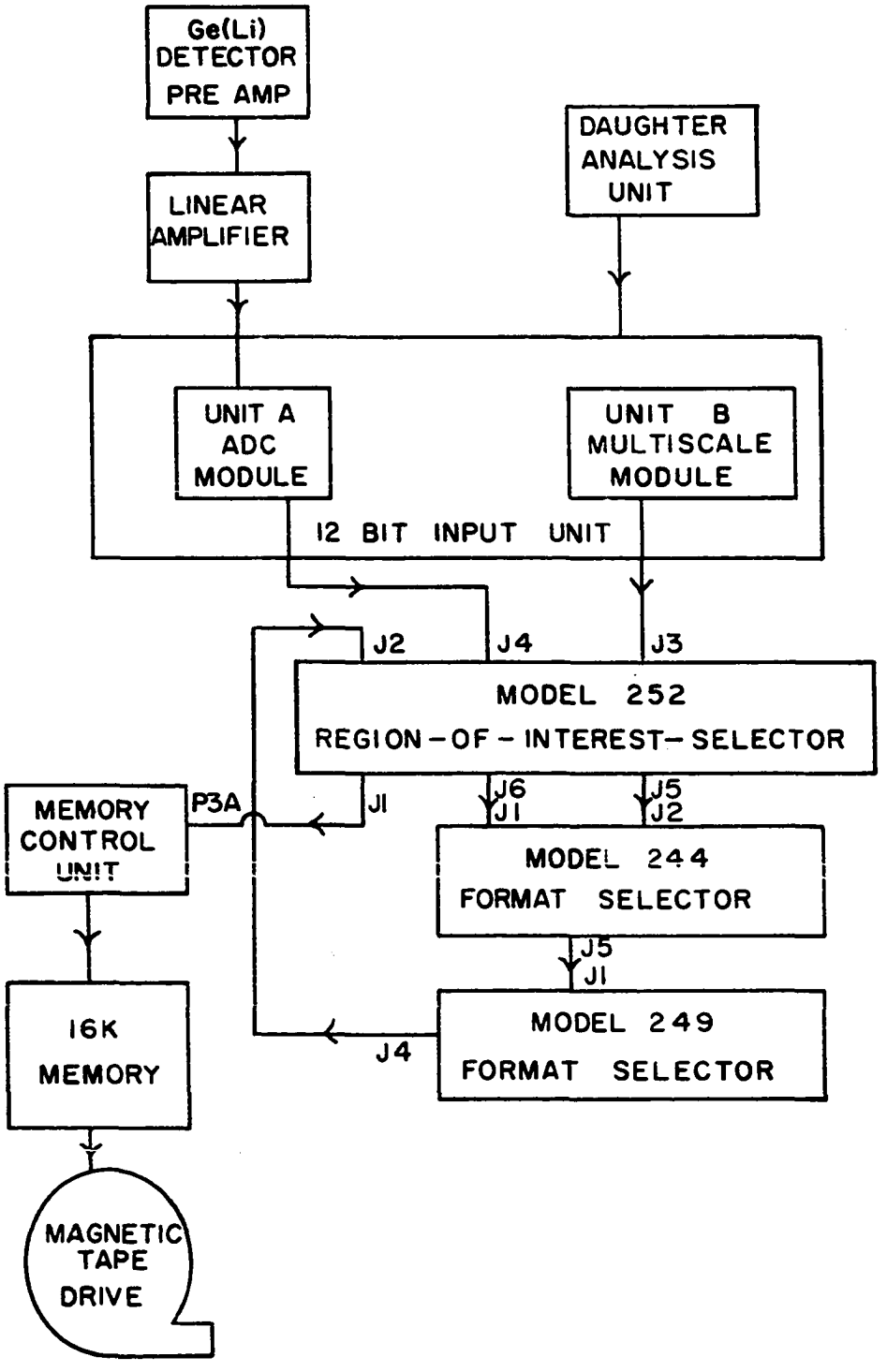

Figure 7. Block diagram of gamma multiscale electronics

One of the large Ge(Li) detectors was used at the parent port of the seccnd generation MTC, and the output was amplified by a Tennelec TC 203BLR amplifier. The bipolar output of the amplifier was routed to a Model 217A, 4K ADC which was inserted into the 12-bit unit. This ADC contains a live-time channel-zero pulser which was used to obtain intensity corrections for the dead time of the ADC. The length of the spectrum was set on the ADC and was 512 channels for these data.

The energy and multiscale bit patterns were routed through the TMC Model 252 Region-of-Interest Selector (which was used in the bypass mode) to the Model 244 Format Selector. This unit generates the correct memory address by combining the time-interval number from the multiscale unit (5 bits) with the channel number from the ADC (9 bits) to create a 14-bit memory address. The apportionment of the bits from the two inputs in the 14-bit output is specified with the address division switch. The setting used was 128-32, but the actual division resulting from this setting is 512-32 because of a modification of the switch made for this experiment. The single output of the format selectcr was routed through the Model 249 Format Selector and the region-of-interest selector in order to be properly interfaced with the memory control unit. The data were recorded on magnetic tape as 16K data sets for later computer analysis with codes specifically

designed for these data. These codes are described in the Appendix.

Because of the limited number of channels in the spectrum associated with each time interval, three different sets of data over different energy ranges were obtained. The first spanned the range of 170 to 760 keV and used a time interval of 16 seconds. The activity was deposited for 1 minute before counting for 8.6 minutes, after which the tape was moved. This cycle was repeated about 94 times for a total run time of about 15.5 hours.

It was determined that the best method to shift the energy region for the second set of data was to raise the base line on the ADC. With this approach, channel zero of each time interval continued to provide an indication of the live-time during the time interval. The energy region was from about 740 keV to 1330 keV and the time interval was 32 seconds. This interval was obtained by setting the multiscale unit to 2^7 steps with a dwell time of 8 seconds and dropping the 2 least significant bits. In the DAS cycle the activity was deposited for 2 minutes and then multiscaled for 17.1 minutes before moving the tape. This cycle was repeated 79 times for a total time of 26 hours.

The third energy range of 1500 to 2500 keV was obtained by lowering the gain of the amplifier and adjusting the baseline of the ADC. The length and the number of time

intervals were the same as in the previous energy range. The DAS cycle was the same except that the deposition time was 2.2 minutes. A total of 24 hours was required to obtain the 72 cycles contained in this data.

3. Gamma-gamma coincidence measurements

A block diagram for the coincidence apparatus is shown in Figure 8. The two detectors used are described in Table I. For each detector one of the preamplifier outputs was used to determine if a coincidence had occurred, and the other output was used for energy analysis. The equipment used in the coincidence experiments is listed in Table V.

Table V. Equipment used in coincidence experiments

Timing filter amplifiers	Ortec Model 454
Constant-fraction timing discriminators	Ortec Model 453
Time-to-pulse-height converter	Ortec Model 437
Single channel analyzer	Canberra Model 1430

Constant-fraction timing was used because the timing signal which results is amplitude and rise-time compensated. This compensation was obtained by gating the logic pulse on

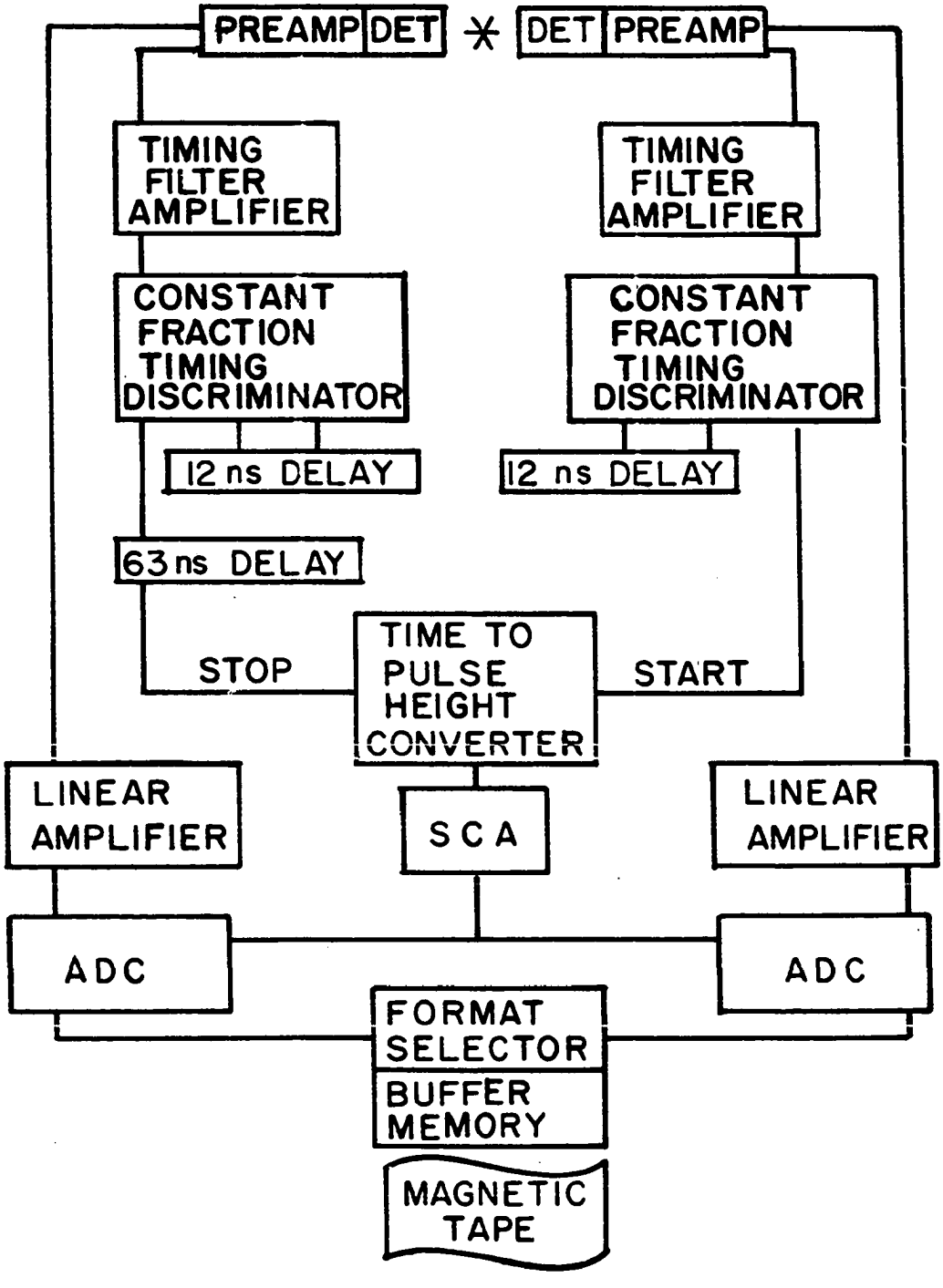

Figure 8. Block diagram of gamma coincidence electronics

the crossover pcint of a pulse which is the sum of the attenuated original pulse plus the one obtained from the original pulse by inversion and delay (by 12 nanoseconds). A more complete description of this timing technique is given by D. A. Gedcke and W. J. McDonald.(33,34) The two logic pulses were used as start and stop signals for the time-to-pulse-height converter and the ccincidence window (typically 60 nanoseconds) was determined by the width of the Single Channel Analyzer (SCA) window. The output of the SCA was used to gate the two ADC's. A Delay Amplifier was sometimes required on the energy pulse to obtain the proper time interval at the ADC's between the arrival of the gating pulse and the energy signal. The ADC's were used in the 8K mode with 2 to 1 compression so that the resulting coincidence array was 4096 by 4096 channels. The individual coincidence events were stored on magnetic buffer tape for later analysis using either the TMC analyzer or the IBM 360/65 computer. The details of the coincidence experiments are given in Table VI.

Table VI. Gamma-gamma coincidence measurements

Mass	136	137	138
Elements	I	I & Xe	I & Xe
Energy Matrix[1] (MeV,MeV)	(4.1,2.0)	(4.1,2.0)	(4.1,2.0)
Duration	16 hours	43 hours	44 hours
Number of Events	5 million	6 million	10 million
Count Rate[2]	8 kcps	14 kcps	12 kcps
DAS Cycle Length[3]	600 sec	25 sec	18 sec
MTC[4]	2nd	2nd	3rd

[1]The first and second values are the upper limits for the A and B sides of the coincidence events respectively.
[2]The maximum count rate during the DAS cycle.
[3]The DAS cycle was to count during deposition and then to move the tape.
[4]The generation of MTC used. The parent port was used.

III. DATA ANALYSIS

Experiments in nuclear spectroscopy generate very large amounts of data and require computer analysis to obtain complete and accurate decay schemes. Several computer codes have been developed by TRISTAN experimenters to facilitate analysis of the data, some of which are described in greater detail in the Appendix.

A. Transition Energies and Intensities

The data from the analyzer were stored on magnetic tape and recorded at frequent intervals to minimize gain-shift distortions of the peak shapes and overflow corrections. The computer code DISKRITE was used to add these spectra together and transfer the sum onto a private disk pack. This code performed overflow and gain-shift corrections while summing the spectra.

The spectra were analyzed to determine the peak centroids and areas using the computer codes PEAKFIND (35) and SKEWGAUS (36). The output from these two codes included plots of the fits, punched card output of the parameters, and errors associated with each peak in the fit. The plots were used to determine the quality of the fits. The output cards

were used as input for the codes ENERGY and DRUDGE which determined the energies and intensities respectively.

The procedure for determining the energies using the code ENERGY is described below. A weighted least-squares straight line for the energy as a functicn of channel number was obtained for both the calibration and the calibration-plus-unknown spectra using calibration peaks that were present in both spectra. The nonlinearity of the system with respect to this LSQ line was obtained from the calibration spectrum and was assumed to be the same for the other spectra. Weighted least-squares polynomial fits of degrees two through seven were made of the nonlinearity curve, and the best one was used for the nonlinearity.

The least-squares line for the calibration-plus-unknown spectrum was used to obtain the straight-line energies of the well-defined unknown peaks. These straight-line energies were used to obtain the least-squares straight line in the unknown spectrum associated with the nonlinearity curve.

The ratios of the double- and single-escape peak areas to the area of the full-energy peak were determined from known escape peaks. The ratios as a function of energy along with the calculated energies were used by the computer code DRUDGE to identify possible single- and double-escape peaks in the unknown spectrum. The escape peaks were used to extend the energy calibration for energies greater than the

3.548-MeV ^{56}Co transition.

A bootstrapping process to extend the energy calibration was an important part of the energy analysis for the ^{136}I data, since a large proportion of the transitions were above 3.5 MeV. The calculation of the energy of the full-energy peak from the bootstrapping was performed with the assistance of the code ENERGY. A weighted average of the photopeak energy obtained from both the single- and double-escape peaks was used to extend the range of the energy calibration. With this extended range the energies of other escape peaks were determined and the energy calibration extended still further. Seven such iterations were performed to extend the energy calibration up to 5.4 MeV for the ^{136}I data.

A relative efficiency curve for photon detection was obtained from the calibration spectra using the peak areas and known relative intensities of gamma rays from the calibration sources. The curve was extended above the highest energy calibration transition by assuming that the curve is a straight line on a log-log plot for energies greater than 2 MeV. The computer code DRUDGE was used to convert the peak areas in the unknown spectrum into relative intensities. The normalization used was 1000 for the most intense transition. For most transitions studied the intensity corrections for internal conversion were less than the uncertainties in the intensities.

A few high-energy peaks were observed in the ^{136}I data for which the expected escape peaks were not observed. It was assumed that these peaks were double-escape peaks and the areas of the photopeaks were deduced from the escape-peak ratios in order to determine the relative intensities.

Two different normalizations were required for the ^{136}I data. The 1321-keV transition was used for the transitions resulting from the decay of the low-spin state and the 381-keV transition for those of the high-spin state. No isomeric transition was identified, and most transitions appear to have cnly one half-life. The most intense transition (1313 keV) contained both half-lives. The multiscale data were used to relate the intensity of these two components to the 381- and 1321-keV normalizations. The final normalizations were 1000 for the short and long half-life components of the 1313-keV transition.

B. Multiscale Data

The ^{136}I multiscale data were recorded on magnetic tape as 16K data sets. An old transfer program was modified to sum these data sets and to store the sum on the private disk pack for computer analysis. Plots were obtained of the energy spectra associated with the sum of the first three and the last five time intervals. These plots were used to determine the placement of windows that were set on the peaks of

interest and on the background above and below the peaks. A computer code used these windows to obtain the live-time corrected areas of the peaks as a function of time. The calculation of these corrected areas is described in the Appendix. The code provided punched card output and fit the data to a single half-life. The punched card output was used with a different code if more than one half-life was needed to fit the decay curve.

Only two transitions were found to contain significant amounts of both the ground-state and isomeric-state activities. Some other peaks were found to contain a component of constant activity. These components were attributed to contaminants.

C. Gamma-Gamma Coincidence Data

A plot was obtained of the coincidence profiles. The two profiles are the pulse-height spectra obtained from the respective ADC's gated by the output of the coincidence circuitry. From these plots gates were determined for all transitions of interest. Two gates were used for each transition. One was centered on the peak, and the other was placed above the peak to identify coincidences due to the Compton background. Events within the appropriate gates were assembled by the computer code BUFFTAPE which is capable of processing up to 255 gates simultaneously. The resulting co-

incidence spectra were recorded on magnetic tape by the code. This tape was read using the code BUFFREAD, and both the peak and the background gates were plotted. The code BRUTAL was used in some cases to obtain listings of the spectra and areas of some of the larger peaks.

The plots or listings were examined to identify coincidences. If the peak was significantly larger in the peak gate than in the background gate, then the coincidence was called definite. If it was only slightly larger or statistics were poor, then it was called a possible coincidence.

D. Identification of Contaminants

Contaminant peaks were identified using several different techniques. In one of these techniques the unknown spectrum was compared to a background spectrum. This was used for the ^{137}Xe decay study. In the ^{136}I study a spectrum of ^{135}I was used, because hydride contamination from mass 135 was the most serious problem.

Another method used was to compare spectra obtained using different MTC enhancements. Peaks which were not seen in both spectra or did not change in concordance with known peaks were considered to be contaminants. Other techniques included identification from the known results of other fission product decays and, in the ^{136}I study, identification of half-life as determined from the multiscale data.

The nature of contamination varied widely with the nuclide studied. The cleanest spectra were obtained in the ^{137}Xe decay study. Almost all of the contaminant activities observed were those associated with reactor background; ^{60}Co, ^{40}K, ^{41}Ar, and some ^{137}Cs. The only observed transition in the spectrum associated with the operation of the TRISTAN system was the intense ^{138}Cs transition at 1436 keV. The spectrum obtained using a Pb absorber contained a few peaks associated with ^{140}La and ^{140}Ba activity.

The iodine decay studies contained substantial amounts of hydride contamination from the lower iodine masses. The contaminant activities identified in the ^{136}I decay study included ^{134}I, ^{135}I, and ^{135}Xe. The multiscale data were used to identify a few other long-lived transitions and determine the amount of contamination in some of the ^{136}I peaks.

The ^{138}I spectra contained the largest amount of contamination. Most of the activity observed was ^{138}Xe and ^{138}Cs. Other activity observed included the adjacent masses ^{137}Xe and ^{139}Xe, hydride contamination from ^{137}I, and ^{136}I from the delayed neutron emission of ^{137}I.

E. Construction of the Level Scheme

A review of the literature and systematics was completed prior to the construction of the level scheme. From this review and the singles and coincidence results of this work,

a preliminary level scheme was constructed. This scheme was extended using the computer code LVLSURCH. The final decision on whether a proposed level was accepted depended on several factors, most of which are contained in a confidence index (CI) which is defined as:

$$CI = N_g + 2N_c + N_{pc}$$

where N_g is the total number of transitions populating and depopulating the level, N_c is the number of definite coincidences, and N_{pc} is the number of possible coincidences. Levels were accepted if the confidence index was three or greater.

F. Spin and Parity Assignments for Levels

Beta feeding to the levels was calculated using the computer code LEAF, and the log*ft* values were calculated using the code LOGFT. It was not possible to measure the ground-state beta branching with an equilibrium spectrum, because xenon emanates from the stearate along with the iodine.

For the ^{136}I decay study, some transitions were multiply placed. Since the intensity associated with each placement could not be determined, two calculations of the beta branching and log*ft* values were performed. The multiply placed transitions were assumed to have their full intensity at all placements in one calculation and zero intensity at

all placements in the other. If the two values obtained were within uncertainties, an average was used, otherwise the values were interpreted as limits for the actual value.

Whenever possible, limits were placed on the spin and parity assignments on the basis of deduced log*ft* values, observed gamma transitions and systematics. The rules for assignments based on log*ft* values are those of Raman and Gove (37). A summary of these rules is presented in Table VII.

Table VII. Rules for spin and parity assignments based on log*ft* values

Log*ft* Values	Spin Change	Parity Change
Z < 80 Log*ft* < 5.9	J = 0,1	No
Z > 80 Log*ft* < 5.1	J = 0,1	No
Logf_1t < 8.5	J = 0,1	Yes or No
Log*ft* < 11.0	J = 0,1 or J = 2	Yes or No Yes
Log*ft* < 12.8	J = 0,1,2	Yes or No

IV. EXPERIMENTAL RESULTS AND DECAY SCHEMES

For each activity studied, figures of gamma singles and coincidence spectra and the proffered level scheme are given. In the level scheme figure, a solid dot at the extremity of a transition was used if at least one definite coincidence was observed, and a hollow dot was used if only a possible coincidence was observed. A table of the observed transition energies, relative intensities and their placements is given. Other tables presented include coincidence results, a comparison of the results of this work to previous studies and beta branching deduced from the log*ft* values.

A. Decay of ^{136}I

A singles spectrum (spectrum A of Table II.) for energies less than 1340 keV is shown in Figure 9 and a spectrum (spectrum B of Table II.) for energies greater than 1350 keV is shown in Figure 10. Contaminant activities observed included ^{135}I, ^{135}Xe, ^{137}Xe and the reactor background activites ^{41}Ar and ^{60}Co. The energies, intensities and placements of the observed gamma transitions are given in Table VIII. It was not possible to determine the half-life of some transitions from either multiscale measurements, placement in the level scheme or comparison of relative intensities in spectra A and B of Table II. The intensities of

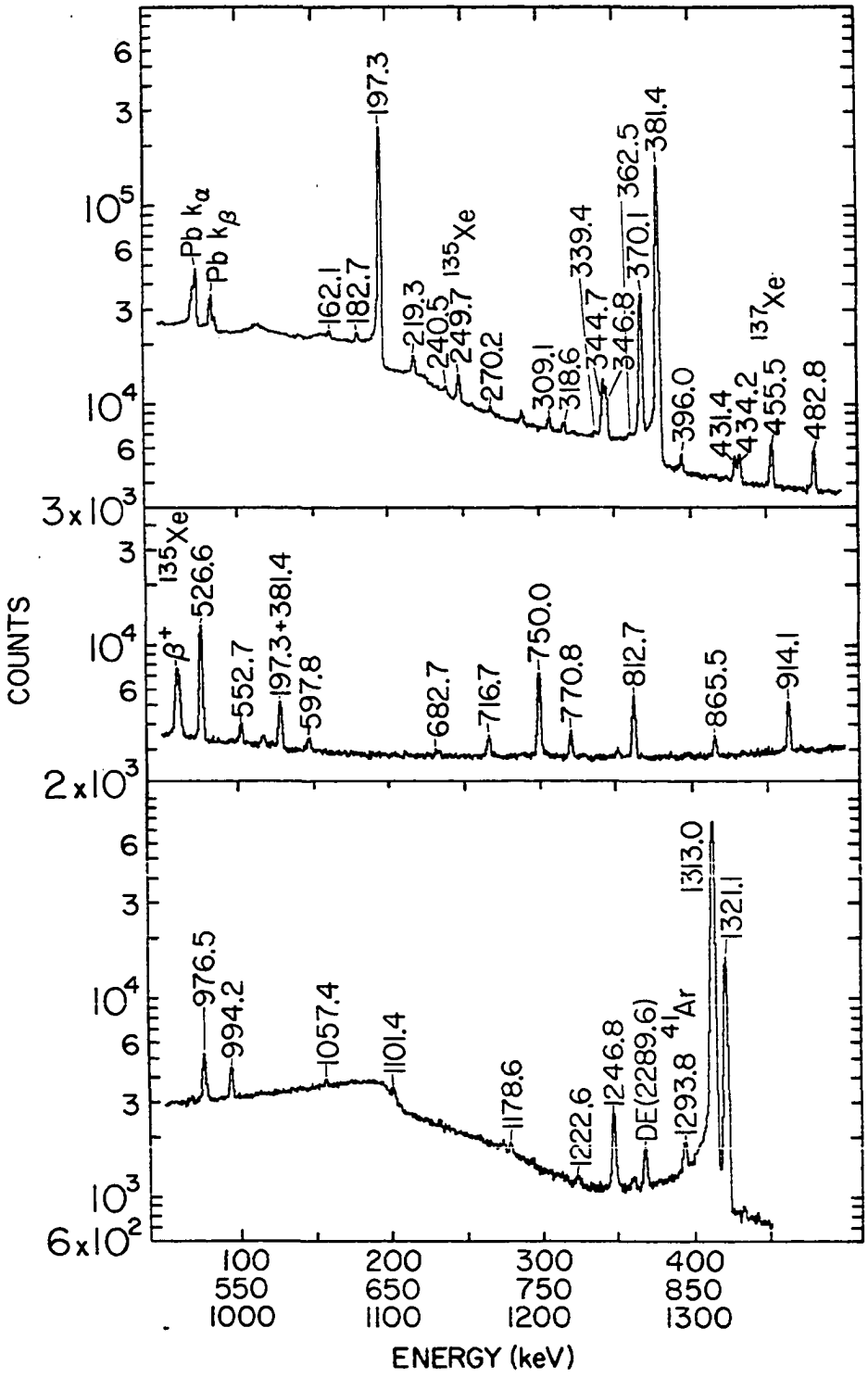

Figure 9. Spectrum of gamma rays with energies less than 1340 keV from the decay of ^{136}I

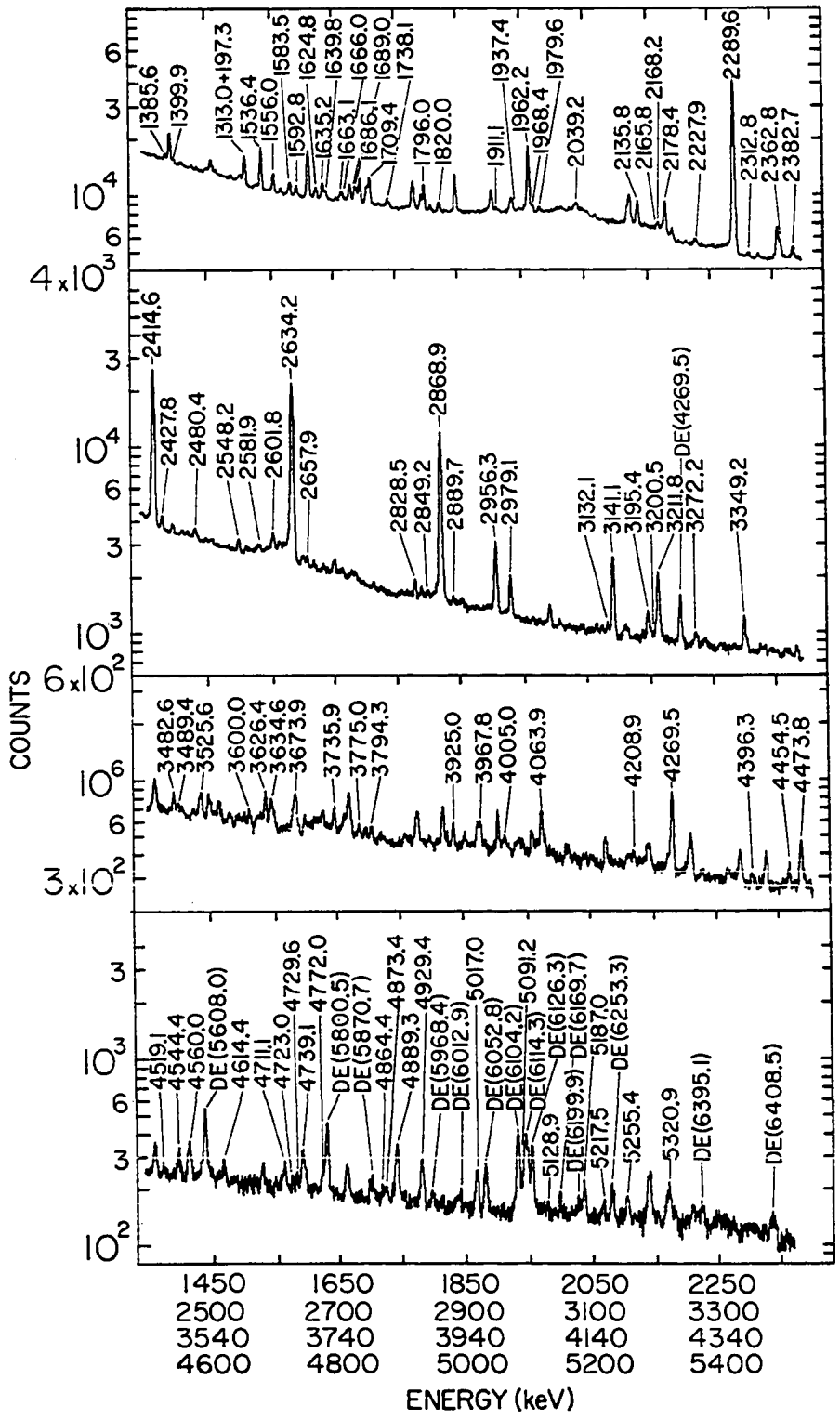

Figure 10. Spectrum of gamma rays with energies greater than 1350 keV from the decay of ^{136}I

Table VIII. Gamma transitions observed in ^{136}I decay

Energy (keV)	Relative Intensity 45 second Activity[1]	85 second Activity[2]	Halflife Unknown[3]	Placement
164.12 ± 0.16	4.3 ± 0.9			2609 --> 2444
182.7 ± 0.2	7.4 ± 0.9			2444 --> 2262
197.33 ± 0.05	783. ± 45.			1892 --> 1694
219.33 ± 0.15		12.3 ± 1.0		2634 --> 2415
240.5 ± 0.2		3.4 ± 0.7		2849 --> 2609
270.2 ± 0.3		3.1 ± 0.8		2560 --> 2289
309.1 ± 0.2		5.1 ± 0.5		2869 --> 2560
318.6 ± 0.2	5.1 ± 0.4			2444 --> 2126
339.4 ± 0.2	2.6 ± 0.5			2465 --> 2126
344.72 ± 0.10		36. ± 3.		2634 --> 2289
346.81 ± 0.10	30.1 ± 1.8			2609 --> 2262
362.5 ± 0.4		1.9 ± 0.3		3212 --> 2849
370.13 ± 0.06	175. ± 10.			2262 --> 1892
381.37 ± 0.06	998. ± 55.			1694 --> 1313
396.0 ± 0.2		6.4 ± 0.8		4269 --> 3873
				4454 --> 4058
431.38 ± 0.12	6.3 ± 1.9	3.0 ± 1.0		2126 --> 1694
434.18 ± 0.11		11.9 ± 0.9		2560 --> 2126
482.80 ± 0.10	17.5 ± 0.9			2609 --> 2126

[1]Intensity normalized to 1000 for the 45-second component of the 1313-keV transition.
[2]Intensity normalized to 1000 for the 85-second component of the 1313-keV transition.
[3]Same normalization as for the 85-second activity.

Table VIII. (continued)

Energy (keV)	Relative Intensity 45 second Activity[1]	85 second Activity[2]	Halflife Unknown[3]	Placement
552.69 ± 0.14	8.4 ± 0.6			2444 --> 1892
597.8 ± 0.2		5.4 ± 0.6		3873 --> 3275
682.7 ± 0.3			2.8 ± 0.4	
716.7 ± 0.3	9.8 ± 0.7			2609 --> 1892
750.05 ± 0.07	58. ± 4.			2444 --> 1694
770.75 ± 0.15	12.8 ± 0.8			2465 --> 1694
812.63 ± 0.08	26. ± 9.	13. ± 4.		2126 --> 1313
865.5 ± 0.3		9.6 ± 0.8		2560 --> 1694
914.1 ± 0.2	35. ± 2.			2609 --> 1694
976.5 ± 0.2		40. ± 3.		2289 --> 1313
994.2 ± 0.2		24.2 ± 1.3		4269 --> 3275
1057.4 ± 0.4		4.3 ± 0.7		4269 --> 3212
1101.4 ± 0.3		7.2 ± 1.1		2415 --> 1313
1178.6 ± 0.3		3.3 ± 0.5		4454 --> 3275
1222.6 ± 0.4			2.3 ± 0.4	
1246.84 ± 0.10		34.0 ± 1.8		2560 --> 1313
1313.02 ± 0.10	1000.	1000.		1313 --> 0
1321.08 ± 0.10		372. ± 26.		2634 --> 1313
1385.6 ± 0.4	1.8 ± 0.3			3830 --> 2444
1399.9 ± 0.5		1.6 ± 0.4		4269 --> 2869
1536.41 ± 0.10		19.4 ± 1.1		2849 --> 1313
1555.97 ± 0.15		7.0 ± 0.5		2869 --> 1313
1583.5 ± 0.2		3.8 ± 0.5		3873 --> 2289
1592.8 ± 0.2	2.5 ± 0.3			4058 --> 2465
1624.8 ± 0.3		3.5 ± 0.5		4474 --> 2849

Table VIII. (continued)

Energy (keV)	Relative Intensity 45 second Activity[1]	85 second Activity[2]	Halflife Unknown[3]	Placement
1635.2 ± 0.2		5.6 ± 0.6		4269 --> 2634
1639.8 ± 0.5			2.8 ± 0.6	
1663.1 ± 0.8			1.0 ± 0.4	
1666.0 ± 0.4		2.6 ± 0.4		2979 --> 1313
1686.1 ± 0.3			4.6 ± 0.5	
1689.0 ± 0.3			3.9 ± 0.5	
1709.4 ± 0.2		10.4 ± 0.7		4269 --> 2560
1738.1 ± 0.3			2.4 ± 0.4	
1796.0 ± 0.2	6.9 ± 0.5			4058 --> 2262
1820.0 ± 0.3		3.2 ± 0.4		4454 --> 2634
1911.1 ± 0.4		1.4 ± 0.3		4545 --> 2634
1937.4 ± 0.5	2.1 ± 0.4			3830 --> 1892
1962.2 ± 0.3		34.2 ± 1.9		3275 --> 1313
1968.4 ± 0.4		2.5 ± 0.4		4947 --> 2979
1979.6 ± 0.3		2.0 ± 0.3		4269 --> 2289
2039.2 ± 0.4		2.4 ± 0.4		4454 --> 2415
2135.8 ± 0.2	6.9 ± 0.5			3830 --> 1694
2165.8 ± 1.5	0.7 ± 0.6			4058 --> 1892
2168.2 ± 1.1		1.2 ± 0.8		5017 --> 2849
2178.4 ± 0.2	8.8 ± 0.6			3873 --> 1694
2227.9 ± 0.5			.6 ± 0.4	
2289.6 ± 0.2		156. ± 8.		2289 --> 0
2312.8 ± 0.5			1.0 ± 0.2	4947 --> 2634
				6186 --> 3873
2362.8 ± 0.3	4.1 ± 0.4			4058 --> 1694

Table VIII. (continued)

Energy (keV)	Relative Intensity 45 second Activity[1]	85 second Activity[2]	Halflife Unknown[3]	Placement
2382.7 ± 0.3		3.2 ± 0.4		5017 --> 2634
2414.6 ± 0.2		102. ± 5.		2415 --> 0
2427.8 ± 0.3			2.7 ± 0.4	
2480.4 ± 0.4			2.0 ± 0.4	
2548.2 ± 0.4		1.9 ± 0.4		5760 --> 3212
2581.9 ± 0.7			0.8 ± 0.2	6412 --> 3830
2601.8 ± 0.9		1.8 ± 0.9		5017 --> 2415
2634.2 ± 0.2		101. ± 5.		2634 --> 0
2657.9 ± 0.4		1.4 ± 0.2		4947 --> 2289
				5218 --> 2560
2828.5 ± 0.3		1.5 ± 0.2		6104 --> 3275
2849.2 ± 0.7		0.5 ± 0.2		2849 --> 0
2889.7 ± 0.7			0.6 ± 0.2	
2868.9 ± 0.2		59. ± 3.		2869 --> 0
2956.3 ± 0.2		10.8 ± 0.6		4269 --> 1313
2979.1 ± 0.3		4.6 ± 0.4		2979 --> 0
3132.1 ± 0.5			0.73 ± 0.15	
3141.1 ± 0.3		10.4 ± 0.6		4454 --> 1313
3195.4 ± 0.4		2.5 ± 0.3		5321 --> 2126
3200.5 ± 1.0			0.7 ± 0.3	5760 --> 2560
				6412 --> 3212

Table VIII. (continued)

Energy (keV)	Relative Intensity 45 second Activity[1]	85 second Activity[2]	Halflife Unknown[3]	Placement
3482.6 ± 0.4			1.36 ± 0.14	5608 --> 2126
				6091 --> 2609
3489.4 ± 0.5			0.70 ± 0.12	
3525.6 ± 0.6		1.7 ± 0.4		6395 --> 2869
3600.0 ± 0.6	0.62 ± 0.13			5862 --> 2262
3626.4 ± 0.4			2.5 ± 0.2	6091 --> 2465
				6186 --> 2560
3634.6 ± 0.5		1.8 ± 0.2		4947 --> 1313
				5760 --> 2126
3673.9 ± 0.5		2.5 ± 0.2		5800 --> 2126
3735.9 ± 0.5	0.89 ± 0.14			5862 --> 2126
3775.0 ± 1.0		0.40 ± 0.18		6409 --> 2634
				6624 --> 2849
3794.3 ± 0.6			0.72 ± 0.18	
3925.0 ± 0.4			1.21 ± 0.19	6186 --> 2262
3967.8 ± 0.5			1.41 ± 0.18	6412 --> 2444
4005.0 ± 0.8			0.8 ± 0.2	
4063.9 ± 0.4		2.5 ± 0.3		6624 --> 2560
4208.9 ± 0.5		0.69 ± 0.17		6624 --> 2415
4269.5 ± 0.2		5.3 ± 0.3		4269 --> 0
4396.3 ± 0.8	0.30 ± 0.09			6091 --> 1694
4454.5 ± 0.7		0.60 ± 0.15		4454 --> 0
4473.8 ± 0.3		2.0 ± 0.2		4474 --> 0
4519.1 ± 1.0		0.22 ± 0.10		5832 --> 1313
4544.4 ± 0.5		0.86 ± 0.17		4545 --> 0

Table VIII. (continued)

Energy (keV)	Relative Intensity 45 second Activity[1]	85 second Activity[2]	Halflife Unknown[3]	Placement
4560.0 ± 0.4			1.41 ± 0.18	
4614.4 ± 0.6			0.74 ± 0.14	
4711.1 ± 0.4		0.8 ± 0.2		4711 --> 0
4723.0 ± 1.4			0.19 ± 0.11	
4729.6 ± 0.8			0.40 ± 0.11	
4739.1 ± 0.5		1.6 ± 0.2		6053 --> 1313
4772.0 ± 0.8			0.55 ± 0.14	
4864.4 ± 0.6			0.36 ± 0.09	
4873.4 ± 0.9			0.28 ± 0.12	6186 --> 1313
4889.3 ± 0.4			2.2 ± 0.3	
4929.4 ± 0.3		1.71 ± 0.18		6624 --> 1694
5017.0 ± 0.3		1.30 ± 0.14		5017 --> 0
5091.2 ± 0.6			0.54 ± 0.12	
5128.9 ± 1.1			0.41 ± 0.15	
5187.0 ± 0.4			1.04 ± 0.18	
5217.5 ± 1.1		0.4 ± 0.14		5218 --> 0
5255.4 ± 0.9			0.58 ± 0.14	
5320.9 ± 0.3		1.1 ± 0.2		5321 --> 0
5608.0 ± 0.4		2.2 ± 0.5		5608 --> 0
5800.5 ± 0.4		1.9 ± 0.4		5800 --> 0
5870.7 ± 1.2		0.4 ± 0.3		5870 --> 0
5968.4 ± 1.0		0.21 ± 0.18		5968 --> 0
6012.9 ± 1.0		0.22 ± 0.18		6013 --> 0
6052.8 ± 0.5		0.8 ± 0.2		6053 --> 0
6104.2 ± 0.6		2.0 ± 0.4		6104 --> 0

Table VIII. (continued)

Energy (keV)	Relative Intensity 45 second Activity[1]	85 second Activity[2]	Halflife Unknown[3]	Placement[4]
6114.3 ± 0.7		1.0 ± 0.3		6114 --> 0
6126.3 ± 0.5		1.4 ± 0.4		6126 --> 0
6169.7 ± 0.8		0.21 ± 0.06		6170 --> 0
6199.9 ± 1.3		0.17 ± 0.08		6200 --> 0
6253.3 ± 0.8		0.50 ± 0.15		6253 --> 0
6395.1 ± 1.1		0.24 ± 0.09		6395 --> 0
6408.5 ± 1.2		0.28 ± 0.10		6409 --> 0

these transitions were normalized to 1000 for the component of the 1313-keV transition populated by the 85-second iodine activity. This normalization was chosen because most such transitions are of high energy and probably decay to the ground state or a low-spin excited state.

A few transitions were placed twice in the decay scheme. Both placements are shown in the table with the second placement immediately following the first. The listed intensity is the full intensity of the peak. The doubly-placed transitions are at 396, 2313, 2658, 3483, 3626, 3635, and 3775 keV.

Comparisons of the relative intensities obtained in this work with values reported in previous beta decay studies are given in Tables IX. and X. for the 45-second and 85-second activities respectively. The peak at 3248 keV, which has been reported in previous decay studies (11,12) as a gamma transiton was identified in this study as the double-escape peak for the 4270-keV transition.

The possible 100-second isomeric state observed by Lundan (11) was not seen in this work. The decay curves associated with five transitions populated by the 85-second activity are shown in Figure 11. Lundan (11) reported the 1321-keV and 1536-keV transitions as being populated by only the 100-second isomeric state, the 1247-keV transition by only the 85-second state, and the 2289- and 2415-keV transi-

Table IX. Comparison of gamma intensities[1] with previous studies of the 45-second isomer of ^{136}I

Energy (keV)	This Work	Carraz et al. (10)	Lundan (11)	Erten et al. (12)
164	4.3 ± 0.9			
183	7.4 ± 0.9			
197	783. ± 45.	850 ± 50	770 ± 50	713 ± 71
220				40 ± 4
319	5.1 ± 0.4			
339	2.6 ± 0.5			
347	30.1 ± 1.8			
370	175. ± 10.	190 ± 20	130 ± 20	167 ± 17
381	998. ± 55.	980 ± 60	1000 ± 50	1000 ± 100
431	6.3 ± 1.9			
434		weak		
483	17.5 ± 0.9			
553	8.4 ± 0.6			
717	9.8 ± 0.7			
750	58. ± 4.			
771	12.8 ± 0.8			
813	26. ± 9.			
914	35. ± 2.			
1313	1000.	1000	1000	1000
1386	1.8 ± 0.3			
1536		weak		
1593	2.5 ± 0.3			
1796	6.9 ± 0.5			
1937	2.1 ± 0.4			
2136	6.9 ± 0.5			
2166	0.7 ± 0.6			
2178	8.8 ± 0.6			
2363	4.1 ± 0.4			

[1]Intensities normalized to 1000 for the 45-second component of the 1313-keV transition.

Table X. Comparison of gamma intensities[1] with previcus studies of the 85-second isomer of ^{136}I

Energy (keV)	This Work	Carraz et al. (10)	Lundan (11)	Erten et al. (12)
219	12.3 ± 1.0	20 ± 2	10	
240	3.4 ± 0.7			
270	3.1 ± 0.8			
309	5.1 ± 0.5			
345	36. ± 3.	60 ± 6	31	29 ± 3
363	1.9 ± 0.3			
396	6.4 ± 0.8			
431	3.0 ± 1.0			
434	11.9 ± 0.9	15		
481			9	
598	5.4 ± 0.6			
751				11 ± 1
813	13. ± 4.		22	
866	9.6 ± 0.8			
976	40. ± 3.	60 ± 6	34	53 ± 5
994	24.2 ± 1.3			
1057	4.3 ± 0.7			
1101	7.2 ± 1.1			
1247	34.0 ± 1.8		42	32 ± 3
1179	3.3 ± 0.5			
1313	1000.	1000	1000	1000
1321	372. ± 26.	440 ± 44	320	368 ± 37
1400	1.6 ± 0.4			
1536	19.4 ± 1.1	40 ± 4	17	27 ± 3
1556	7.0 ± 0.5			
1584	3.8 ± 0.5			
1625	3.5 ± 0.5			
1635	5.6 ± 0.6			
1640	2.8 ± 0.6			
1666	2.6 ± 0.4			
1686	4.6 ± 0.5			
1709	10.4 ± 0.7			27 ± 3

[1]Intensities normalized to 1000 for the 85-second component of the 1313-keV transition.

Table X. (continued)

Energy (keV)	This Work	Carraz et al. (10)	Lundan (11)	Erten et al. (12)
1820	3.2 ± 0.4			
1911	1.4 ± 0.3			
1962	34.2 ± 1.9	50 ± 5	32	38 ± 4
1968	2.5 ± 0.4			
1980	2.0 ± 0.3			
2039	2.4 ± 0.4			
2168	1.2 ± 0.8			
2290	156. ± 8.	180 ± 18	145	168 ± 17
2383	3.2 ± 0.4			
2415	102. ± 5.	110 ± 11	90	101 ± 10
2480	2.0 ± 0.4			
2548	1.9 ± 0.4			
2602	1.8 ± 0.9			
2634	101. ± 5.	120 ± 12	110	101 ± 10
2658	1.4 ± 0.2			
2828	1.5 ± 0.2			
2849	0.5 ± 0.2			
2870	59. ± 3.	70 ± 7	56	60 ± 6
2956	10.8 ± 0.6		10	13 ± 2
2979	4.6 ± 0.4			
3141	10.4 ± 0.6		7	14 ± 2
3195	2.5 ± 0.3			
3212	7.7 ± 0.3		6	
3248	DEP		5	12 ± 2
3272	1.3 ± 0.3			
3349	2.9 ± 0.3			
3526	1.7 ± 0.4			
3635	1.8 ± 0.2			
3674	2.5 ± 0.2			
3775	0.40 ± 0.18			
3949				24 ± 2

tions as being populated by both the 100-second and 85-second isomeric states. The half-life of the long-lived isomeric state was determined to be 85.2 ± 1.8 seconds from a weighted average of the half-lives for the 1247-, 1321-, 2289-, and 2415-keV transitions.

Decay curves for the 197- and 381-keV transitions, populated by the short half-life isomeric state, are also shown in Figure 11. The half-life value obtained from averaging the values for these two transitions was 44.8 ± 1.0 seconds.

Examples of the coincidence spectra used to construct the level scheme are shown in Figure 12. The gates used and the coincidences observed in each of these gates are tabulated in Table XI.

The percent beta feeding and log*ft* values for the levels from the two iscmers are presented in Table XII. Log*ft* limits were specified for some of the levels asscciated with multiply placed transitions. A Q-value of 6890 keV (accepted by the Nuclear Data Sheets (13)) was used for both isomers. The ground-state beta feeding from the low-spin isomer was assumed to be less than 2% as deduced by Johnson and O'Kelley (6) and accepted by the Nuclear Data sheets (13).

Only one level scheme is presented because of the complex nature of the feeding to the ^{136}Xe levels from the two isomers. The proposed level scheme is shown in Figure 13. A comparison of the levels obtained in this study to levels obtained in previcus decay studies (10,11,12) and (p,p') experiments (20,21) is shown in Figure 14. A level by level dis-

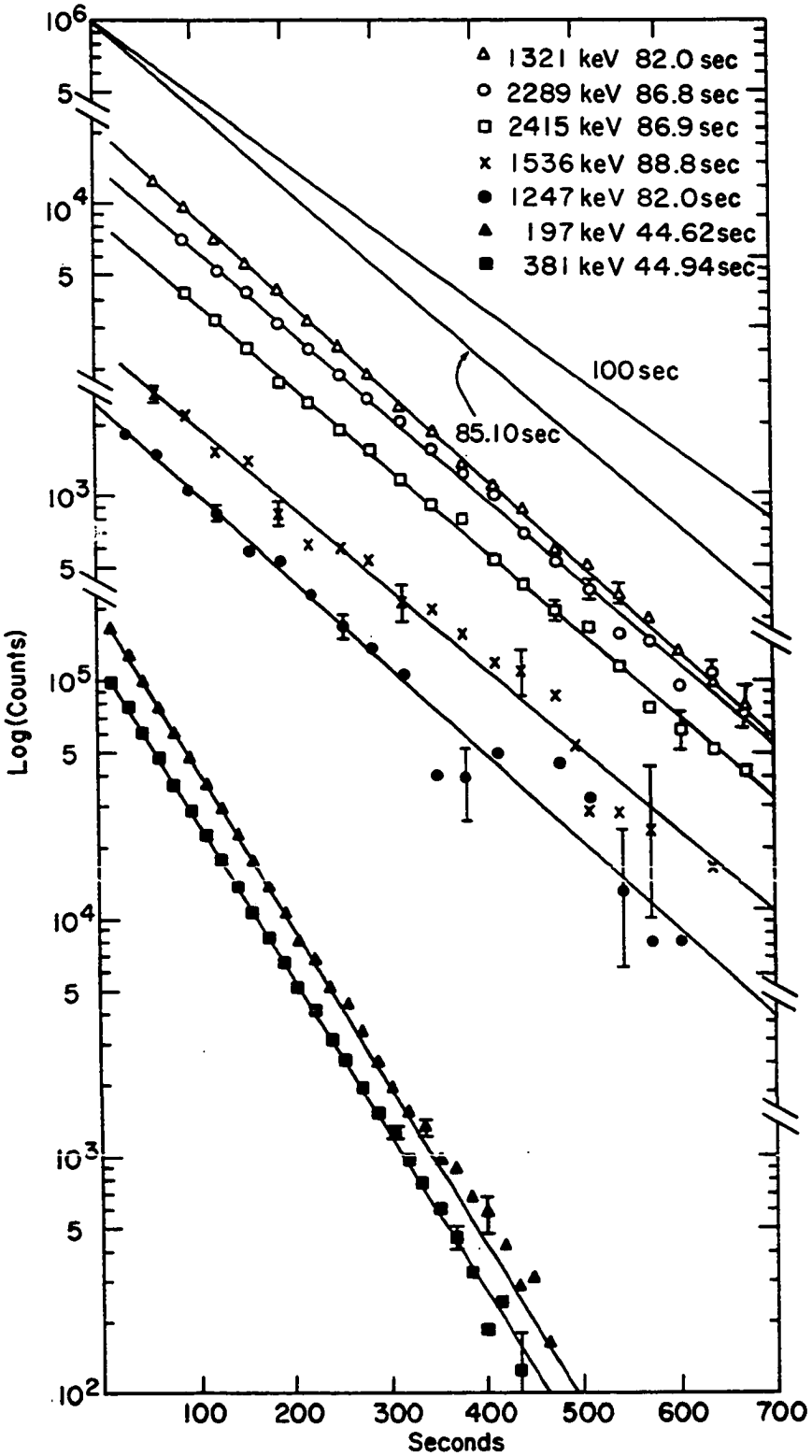

Figure 11. Decay curves for the 45- and 85-second ^{136}I isomers

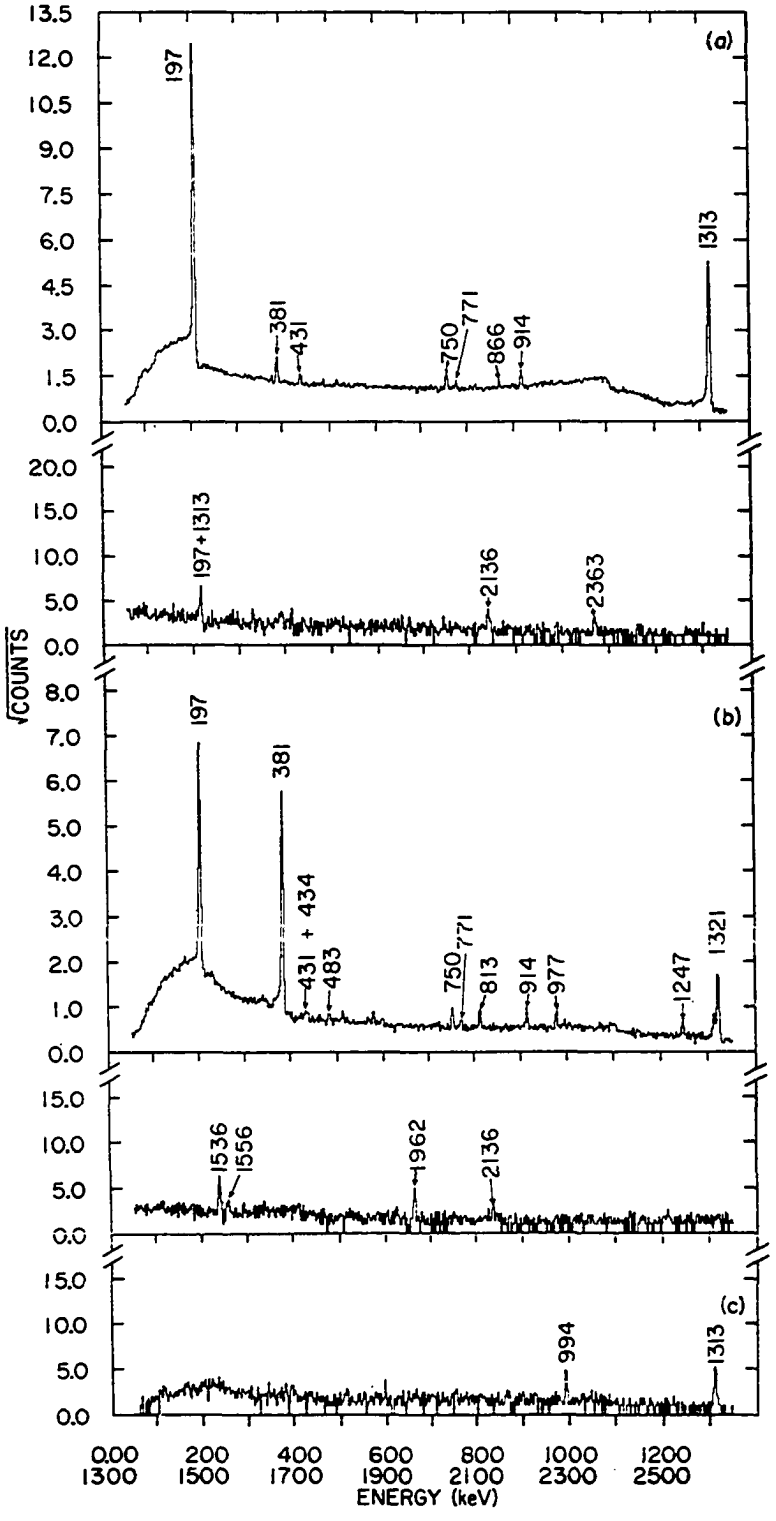

Figure 12. Gamma spectra in coincidence with the (a) 381-, (b) 1313-, and (c) 1962-keV gamma rays from ^{136}I

Table XI. Coincidences observed in ^{136}I decay

Gating Energy (keV)	Definite Coincidences (keV)	Possible Coincidences (keV)
197	381, 1313	
219	2415	1101, 1313
345+347	370, 976, 2290	
370	183, 347	1796
381	197, 431, 750, 771, 866, 914, 1313, 2136, 2363	396, 483, 2178
431	381, 434, 483, 1313	319
434	309, 431, 813	381
483	431, 813, 1313	381
750	164, 381, 1313	
771	381, 1313	
813	319, 434, 483, 1313	339
914	381, 1313	
976	309, 345, 1313	
994	1313, 1962	
1247	309, 1313, 1709	
1313	197, 381, 431, 434, 483, 750, 771, 813, 914, 976, 1247, 1321, 1536, 1556, 1962, 2956, 3141	309, 994, 2136
1321	1313	1635, 1820
1536	1313	362
1962	994, 1313	396, 598
2290	345	270, 1980
2415	219	
2634		1635
2956	1313	
3141	1313	

cussion follows.

Ground state. The spin and parity of the ^{136}Xe ground state is assumed to be 0^+ since it is an even-even nucleus. The spins of the 85- and 45-second ^{136}I states have not been

Table XII. Beta feeding and log*ft*'s for ^{136}I decay

Level energy (keV)	85-second isomer[1] % beta branching	85-second isomer[1] Log*ft*	45-second isomer[1] % beta branching	45-second isomer[1] Log*ft*
0.0	<2.0	>8.6		
1313.07 ± 0.08	30. ± 4.	7.1	<4.7	>7.6
1694.44 ± 0.09	0.0		<4.5	>7.5
1891.77 ± 0.10			67. ± 8.	6.2[2]
2125.77 ± 0.10	<0.2	>8.9	<1.5	>7.8
2261.86 ± 0.11			12.1 ± 1.2	6.8
2289.54 ± 0.11	10.2 ± 0.9	7.2		
2414.77 ± 0.13	6.2 ± 0.5	7.3		
2444.50 ± 0.11			6.8 ± 0.7	7.0
2465.13 ± 0.13			1.12 ± 0.12	7.8
2559.93 ± 0.10	2.6 ± 0.3	7.7		
2608.63 ± 0.11			9.0 ± 0.7	6.8
2634.18 ± 0.10	34. ± 3.	6.5[2]		
2849.39 ± 0.15	1.10 ± 0.12	7.9		
2869.05 ± 0.13	4.6 ± 0.5	7.3		
2979.1 ± 0.3	0.32 ± 0.05	8.4		
3211.9 ± 0.3	0.23 ± 0.07	8.4		
3275.2 ± 0.4	0.0			
3830.1 ± 0.4			1.02 ± 0.10	7.2

[1]Spread of % beta feeding and log*ft* values due to multiple placement of some gamma rays

[2]Logf_1t < 8.5 so beta transition has spin change < 2

Table XII. (continued)

Level energy (keV)	85-second isomer % beta branching	85-second isomer Logft	45-second isomer % beta branching	45-second isomer Logft
3873.1 ± 0.2	0.19 ± 0.08	8.1		
4057.8 ± 0.3			1.33 ± 0.13	6.9[2]
4269.35 ± 0.15	4.8 ± 0.5	6.5[2]		
4454.0 ± 0.2	1.3 - 1.8	6.9[2] - 6.8[2]		
4474.0 ± 0.3	0.37 ± 0.04	7.5		
4545.0 ± 0.5	0.15 ± 0.03	7.8		
4711.2 ± 0.4	0.05 ± 0.02	8.1		
4947.4 ± 0.3	0.17 - 0.45	7.4 - 7.0[2]		
5017.0 ± 0.3	0.51 ± 0.09	6.9[2]		
5217.8 ± 0.5	0.03 - 0.12	8.0 - 7.3[2]		
5321.1 ± 0.3	0.24 ± 0.03	6.9[2]		
5608.3 ± 0.3	0.15 - 0.24	6.8[2] - 6.6[2]		
5760.3 ± 0.3	0.12 - 0.30	6.7[2] - 6.3[2]		
5800.2 ± 0.5	0.30 ± 0.03	6.3[2]		
5832.2 ± 0.6	0.10 ± 0.02	6.7[2]		
5861.8 ± 0.5			0.14 ± 0.02	6.2[2]
5870.8 ± 1.2	0.03 ± 0.02	7.2[2]		
5968.5 ± 1.0	0.014 ± 0.012	7.3[2]		
6013.0 ± 1.0	0.015 ± 0.012	7.3[2]		
6052.6 ± 0.4	0.16 ± 0.02	6.1[2]		
6091.4 ± 0.3			0.03 - 0.29	6.6[2] - 5.5[2]
6103.9 ± 0.3	0.24 ± 0.03	5.9[2]		
6114.4 ± 0.7	0.07 ± 0.02	6.4[2]		
6126.4 ± 0.5	0.09 ± 0.03	6.3[2]		
6169.8 ± 0.8	0.014 ± 0.004	7.0[2]		

Table XII. (continued)

Level energy (keV)	85-second isomer % beta branching	85-second isomer Log*ft*	45-second isomer % beta branching	45-second isomer Log*ft*
6186.5 ± 0.4				
6200.0 ± 1.3	0.011 ± 0.005	7.0[z]		
6253.4 ± 0.8	0.034 ± 0.010	6.5[z]		
6394.8 ± 0.6	0.13 ± 0.03	5.5[z]		
6409.0 ± 0.8	0.02 - 0.05	6.3[z] - 6.0[z]		
6412.3 ± 0.4				
6624.1 ± 0.4	0.54 ± 0.04	4.2[z]		

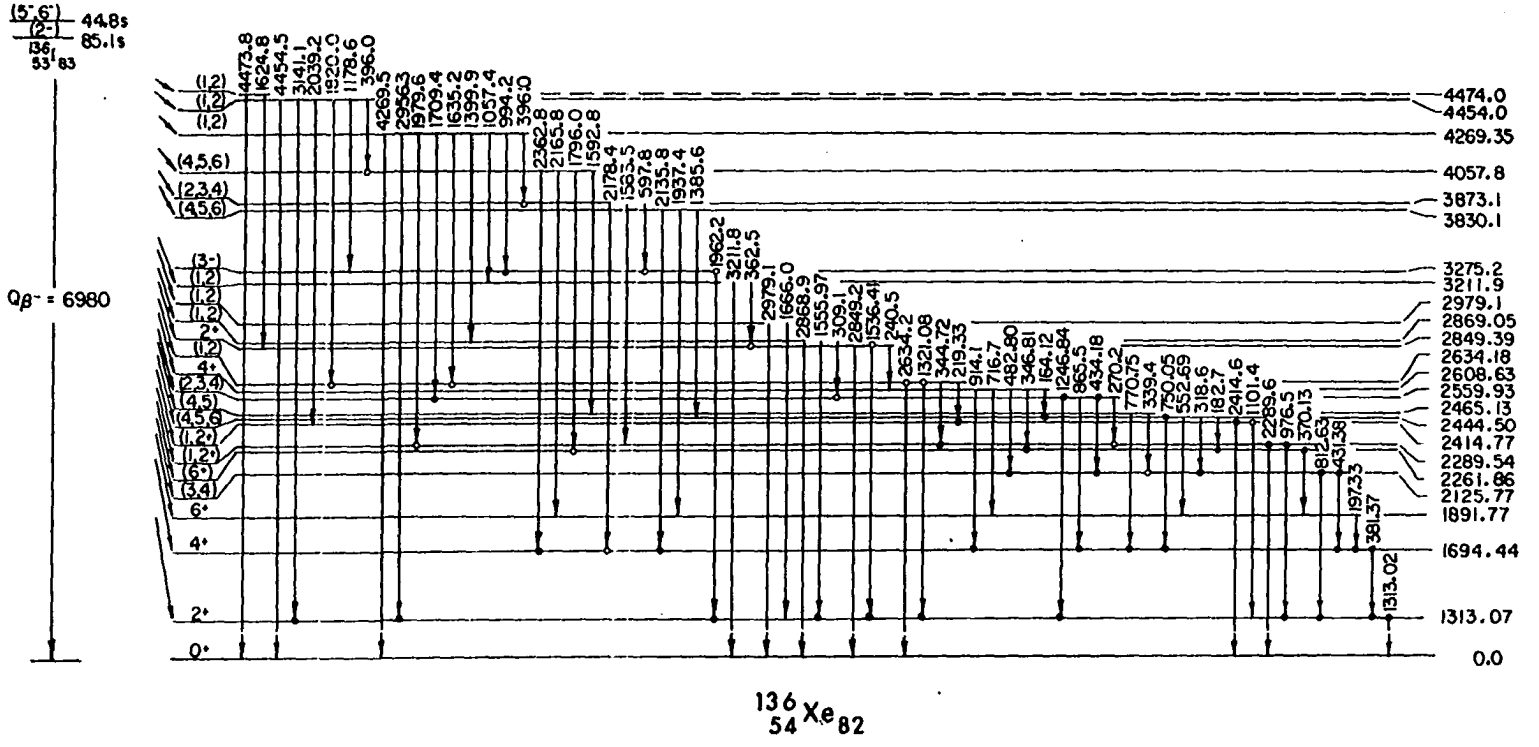

Figure 13. Proposed decay scheme of ^{136}I

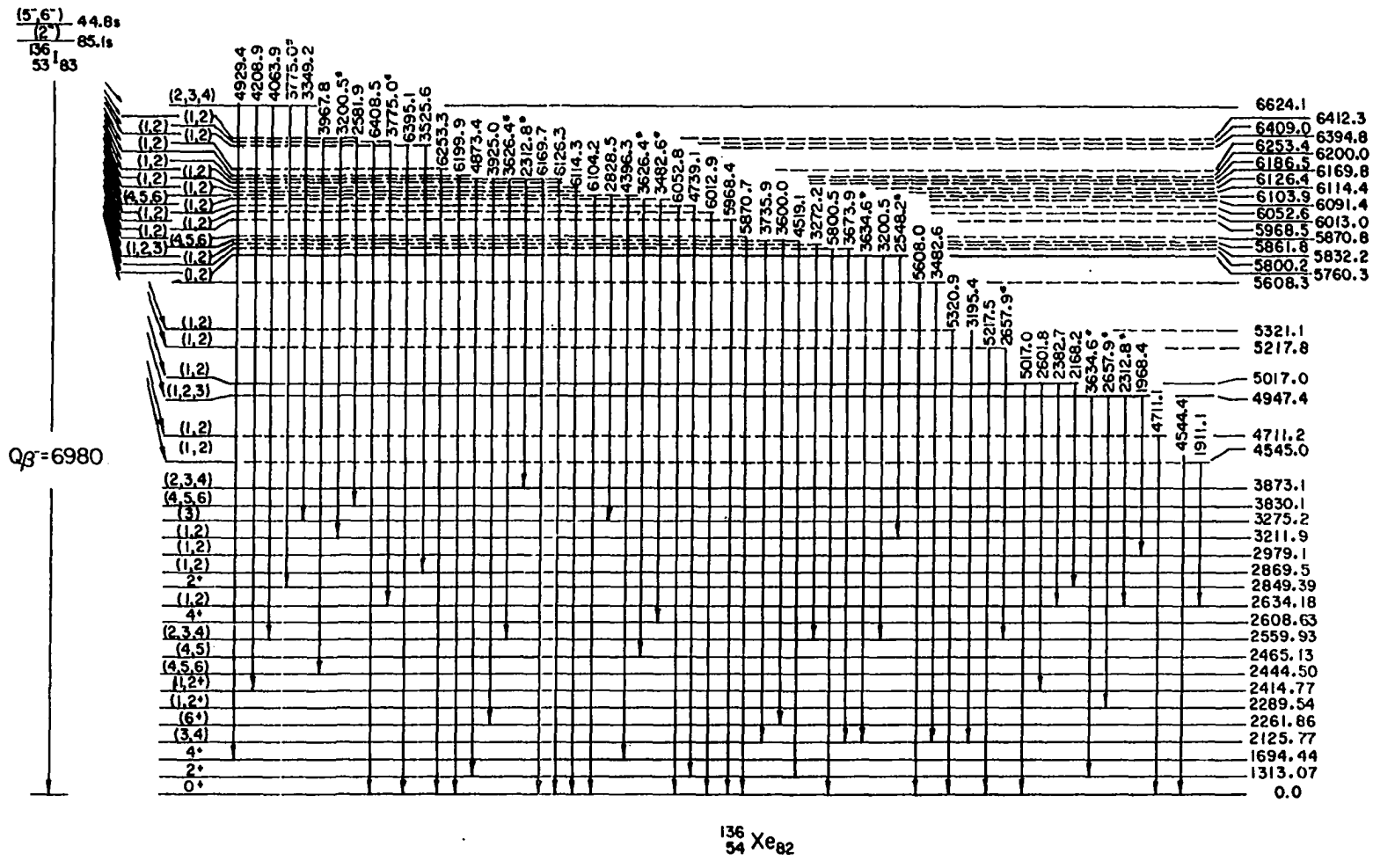

Figure 13. (continued)

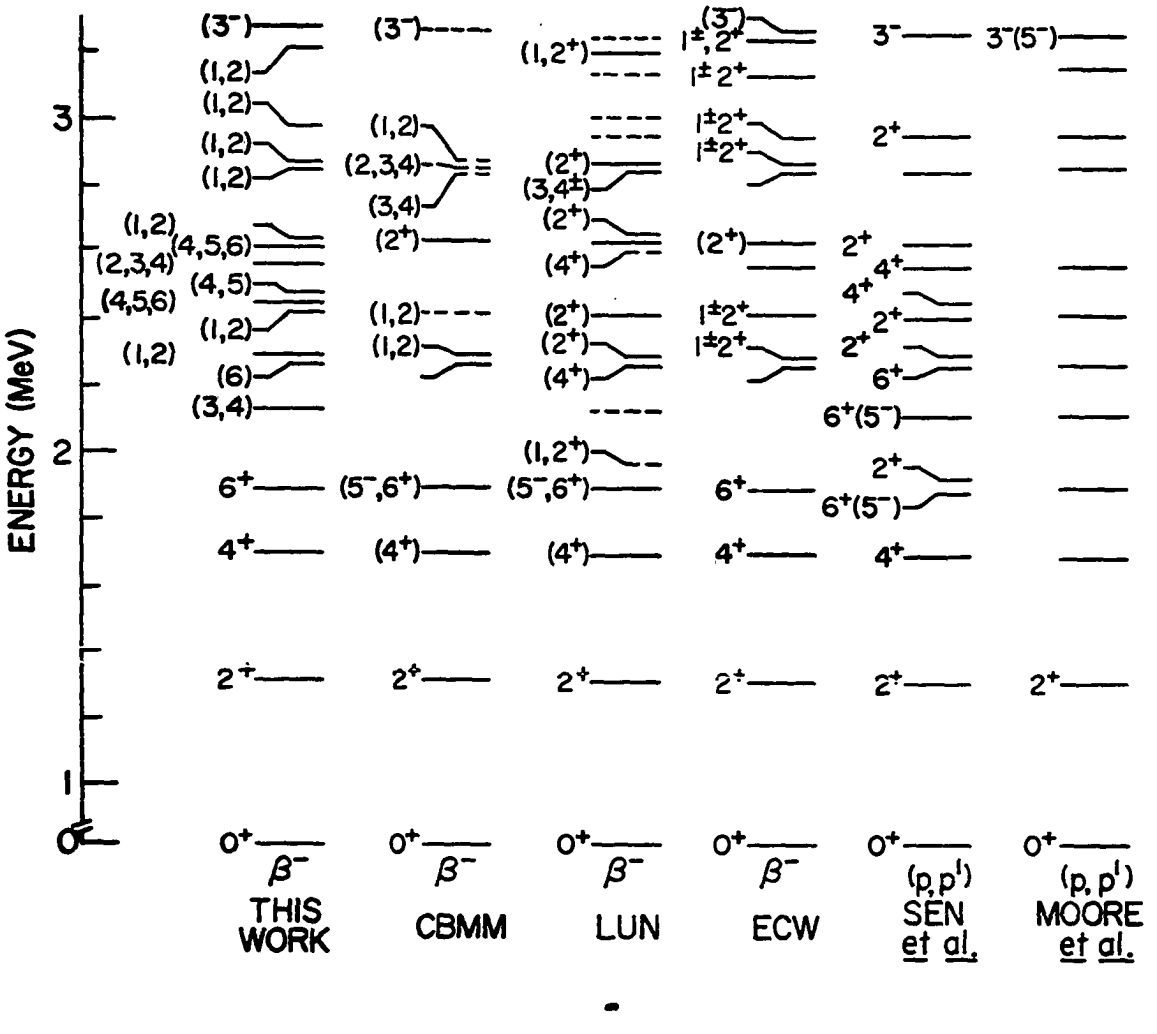

Figure 14. Comparison of ^{136}Xe levels with those from previous studies

measured but the logft values to the excited levels limit the possible spin assignments.

The 2634-keV level, which is fed by the low-spin isomer, decays directly to the 0+ ground state, thus its spin is 1 or 2. A logf_1t value of 8.2 for the beta feeding to this level limits the spin of the 85-second, low-spin isomer to between 0 and 3. The absence of any measured beta feeding to the ground state (6) or to the 4+ level at 1694 keV favors a spin of 2. Negative parity is favored from shell model arguments for both the 85- and 45-second isomeric states.

The spin of the 45-second isomeric state is limited to 5, 6, or 7 by a logf_1t value of 8.0 for beta feeding to the 6+ level at 1892 keV. A spin of 5 was favored by Nuclear Data Sheets (13) on the basis of significant beta feeding to the 4+ 1694-keV level as reported by previous decay studies (10,11,12). After consideration of internal conversion coefficients and feeding from higher levels, no evidence for beta feeding to the 1694-keV level was seen. A lower limit of 9.4 for the logf_1t value was obtained; thus there is no reason to favor spin 5 for the 45-second isomer. If an assignment of 4+ as indicated by (p,p') data (21) for the 2444-keV level is accepted, then the observed beta feeding to this level would eliminate spin 7 for the 45-second isomer. Since the spin of the 2126-keV level is limited to 2, 3, or 4, the small amount of beta feeding to this level does not

support an assignment of 7 to the 45-second isomer.

1313.07 ± 0.08-keV level. This well-established level has been accepted as a 2^+ state by Nuclear Data Sheets (13) which is consistent with the systematics of other N=82 nuclei and the even Xe isotopes. The beta feeding is from only the low-spin isomer. Edvardson and Norlin (17) reported the B(E2) value of the ground-state transition to be 0.17 ± 0.03 e^2b^2 from a Coulomb excitation experiment. They also reported a lifetime for this level of 0.59 ± 0.15 picoseconds.

1694.44 ± 0.09-keV level. This level is established by a strong coincidence of the 381-keV transition with the 1313-keV transition. The spin and parity assignment of 4^+ for this level is confirmed by its observation as a member of the YRAST band by Cheifetz et al. (16). This assignment is also confirmed in inelastic proton scattering and is consistent with the systematics of the N=82 isotones. No beta feeding to this level from the 45-second isomer was observed in disagreement with earlier decay work.

1891.77 ± 0.10-keV level. This level is established by a strong coincidence between the 197- and 381-keV transitions. Based on the E2 character of 197-keV transition, the observation of this level as a member of the YRAST band in ^{252}Cf(SF) studies (15,16), and the systematics of the N=82 isotones, the spin and parity for this level is probably 6^+. The half-life of this level has been measured using delayed

beta-gamma, gamma-gamma and fission-gamma coincidences (10,11,15). The value accepted by Nuclear Data Sheets (13) is 3.0 ± 0.2 microseconds.

Lundan (11) postulated a level at 1962 keV which was depopulated only by a 1962-keV transition. In this work, the 1962-keV transition was seen in coincidence with the 1313-keV transition and was placed depopulating a level at 3275 keV, consistent with the results of Carraz et al. (10) and Erten et al. (12).

2125.77 ± 0.10-keV level. This level is established by the depopulating transitions at 431 and 813 keV which are seen in coincidence with the 381- and 1313-keV transitions respectively. The level was postulated by Lundan (11), but was not observed by Carraz et al. (10) or Erten et al. (12) or accepted by Nuclear Data Sheets (13). The 431- and 813-keV transitions have been measured as having both half-life components and populate the 4+ and 2+ levels at 1694 and 1313 keV respectively; thus the spin is limited to 2, 3, or 4. A spin of 3 or 4 is favored for this level on the basis of a small amount of beta feeding from the high-spin isomer. A level at 2108 keV was seen in the (p,p') studies (20,21) and was assigned a spin of 5 or 6 by Sen et al. (21). This is inconsistent with the results of this work if the levels are the same.

2261.86 ± 0.11-keV level. This level is established by the de-excitation transition at 370 keV which is strong and decays with a 45-second half-life. It is not seen in prompt coincidence with the 197-, 381-, or 1313-keV transitions, because it is assumed to feed the 6^+ level at 1892 keV which has a 3 microsecond half-life (13). The 2262-keV level was reported by the three decay studies (10,11,12) and was seen in both (p,p') experiments (20,21). An assignment of 6^+ was made by Sen et al. (21) which is consistent with this work.

2289.54 ± 0.11-keV level. This level is established by a ground-state transition and a 976-keV transition which is seen in coincidence with the 1313-keV transition. This level was reported by earlier decay studies (10,11,12) and by Sen et al. (21) who assigned it a spin of 2. The existence of a strong ground-state transition limits the spin to 1 or 2, so an assignment of 2^+ is favored for this level.

2414.77 ± 0.13-keV level. This level was seen by the earlier decay studies (10,11,12) and by both (p,p') studies (20,21). A ground-state transition limits the spin to 1 or 2. Since the reaction assignment is 2^+ for this level, a spin of 2 is favored.

2444.50 ± 0.11-keV level. This level is established by coincidence between the 750- and 381-keV transitions. Since it depopulates to levels with spins of 4 and 6, the possible spins are 4, 5, and 6. This level has been seen only in the

(p,p') work of Sen et al. (21) who reported it as a 4+ level, hence a spin of 4 is favored for this level. Multiscale data on the 750-keV transition confirms that the level is fed by the high-spin isomer.

2465.13 ± 0.13-keV level. This new level, which has not been reported in earlier work, is established by a definite coincidence of the 770- with the 381-keV transition.

2559.93 ± 0.10-keV level. This level is established by a definite coincidence between the 1247- and 1313-keV transitions and by other coincidences. It was proposed by Erten et al. (12) and reported in the (p,p') work (20,21). Transitions to the 2+ level at 1313 keV and the 4+ level at 1894 keV limit the spin to 2, 3, or 4. An assignment of 4+ is favored based on an assignment by Sen et al. (21).

2608.63 ± 0.11-keV level. This level is established by several coincidences and was postulated by Lundan (11) but not accepted by Nuclear Data Sheets (13). It is fed by the high-spin isomer and transitions to the 4+ and 6+ levels at 1694 and 1892 keV, respectively, limit the spin assignment to 4, 5, or 6. A transition from the 2849-keV level, which decays also to the ground state, further restricts the spin to 4+.

2634.18 ± 0.10-keV level. This level was seen in earlier decay work (10,11,12) and a strong ground-state transition limits the spin to 1 or 2. A spin of 2 is favored

based on the results of Sen et al. (21). The 1321-keV transition was placed as depopulating this level, so no level doublet was required as proposed by Lundan (11).

2849.39 ± 0.15-keV level. This level was postulated in previous decay studies (10,11,12). Multiscale data on the 1536-keV transition indicates that this level is fed by only the low-spin isomer and a ground-state transition limits the spin of the level to 1 or 2. An additional transition to the 4+ level at 2609 keV restricts the spin to 2+.

The level proposed by Carraz et al. (10) at 2854 keV is not accepted in this work. The 219-keV transition was placed on the basis of coincidence results as depopulating the 2634-keV level and a small peak at 567 keV was measured as being long-lived relative to 85 seconds.

2869.05 ± 0.13-keV level. Earlier beta-decay studies have established this level (10,11,12). The presence of a ground-state transition limits the spin to 1 or 2. The broad peak in the (p,p') data (20,21) at approximately 2855 keV probably results from the excitation of both the 2849- and 2869-keV levels.

A level postulated at 2956 keV in earlier decay studies (11,12) and accepted by Nuclear Data Sheets (13) was not supported in this study. The 2956-keV transition was seen in coincidence with the 1313-keV transition and is postulated to depopulate a level at 4269 keV.

The levels below 2900 keV are considered to be well-established from energy sums and coincidence information. Levels above 2900 keV are in many cases less well-established because of poor statisics for gamma transitions greater than 2 MeV in the coincidence spectra and the larger uncertainties in energies for transitions greater than 3.5 MeV.

2979.1 ± 0.3-keV level. This level was not reported in previous decay studies. The existence of a ground-state transition limits the spin to 1 or 2. A reaction level observed in the (p,p') work of Sen et al. (21) at 2969 keV with a spin of 2 may correspond to this level.

A level prcposed by Lundan (11) at 3006 keV was not supported by the results of this study. The doublet at 345, 347 keV was not resolved in his study and the coincidence observed in this study is between the 370- and the 347-keV transition rather than the one at 345 keV as reported by Lundan (11). No coincidences with other transitions depopulating the 2634-keV level were observed.

Another level at 3141 keV was postulated by Lundan (11) and Erten et al. (12) and accepted by Nuclear Data Sheets (13). It was not accepted in this study. The 3141-keV transition was observed in coincidence with the 1313-keV transition and was placed as depopulating a level at 4454 keV.

3211.9 ± 0.3-keV level. Lundan (11) proposed this level on the basis of the energy sum of the 1962- and 1247-keV

transitions and on the existence of a ground-state transition. In this work, the 1247- and 1962-keV transitions are placed elsewhere. The 3211-keV ground-state transition limits the spin to 1 or 2.

Lundan (11) and Erten et al. (12) proposed a level at 3243 and 3250 keV respectively that was accepted by Nuclear Data Sheets (13). This level is not supported in this work. The peak observed in this work at 3247 keV was identified as the double-escape peak of the 4269-keV transition.

3275.2 ± 0.4-keV level. This level is established from the coincidence of the 1962- and 1313-keV transitions and was postulated in the earlier decay studies of Carraz et al. (10) and Erten et al. (12). Within the uncertainty limits of this study, the beta feeding to this level is zero. Based on the (p,p') data (20,21), Nuclear Data Sheets (13) accepted an assignment of 3^-. This is consistent with the observation of de-excitation only to the 1313-keV level. Moore et al. (20) has interpreted this level as an $f_{7/2}s_{1/2}$ neutron particle-hole configuration with a small admixture of $f_{7/2}d_{3/2}$. It is the highest level reported in previous decay studies.

3830.1 ± 0.4-keV level. This level is established by a coincidence between the 2136- and 381-keV transitions. The de-excitation pattern is only to high-spin levels and multiscale data on the 2136-keV transition indicates that the level is fed by only the high-spin isomer of ^{136}I. The spin

is restricted to 4, 5, or 6 by transitions to the 4^+ and 6^+ levels at 1694 and 1892 keV respectively.

3873.1 ± 0.2-keV level. Three possible ccincidences establish this level. It is postulated that it is fed by only the low-spin isomer on the basis cf its de-excitation pattern. Transitions to the 1694- and 2289-keV levels limit the possible spin assignments to 2, 3, or 4. This is consistent with a 3^- or 4^- assignment by Moore et al. (20) from (p,p') data. They interpreted this level to be predominantly a $f_{7/2}d_{\bar{3}/2}$ neutron particle-hole state with a small admixture of $f_{7/2}s_{\bar{1}/2}$.

4057.8 ± 0.3-keV level. A coincidence between the 2363- and 381-keV transitions confirms the existence of this level. The de-excitation pattern of this level indicates the beta feeding to be from the high-spin isomer. Depopulating transitions to the 4^+ and 6^+ levels at 1694 and 1892 keV limit the spin to 4, 5, or 6. From the (p,p') data of Moore et al. (20), this level has been interpreted as predominantly a $f_{7/2}s_{\bar{1}/2}$ neutron particle-hole state with small admixtures of $f_{7/2}d_{\bar{3}/2}$ and $p_{3/2}d_{\bar{3}/2}$. The 3^- assignment from reaction studies (20) is not consistent with the results from gamma de-excitation. A 4^- assignment is possible from a $f_{7/2}s_{\bar{1}/2}$ state but would imply an M2 transition between the 4058- and 1892-keV levels. It is also possible that the level seen in the (p,p') work (20) is not the same as one seen in beta

decay.

4269.35 ± 0.15-keV level. Three definite coincidences confirm the existence of this level. Multiscale measurements on the 994-keV transition indicate this level to be fed only by the low-spin isomer. The presence of a ground-state transition limits the spin to 1 or 2. About one third of the beta feeding from the low-spin isomer of ^{136}I to levels above 3 MeV goes to this state giving it a low log*ft* value of 6.5. The level has been interpreted (20) as a $f_{7/2}d_{3/2}^{-1}$ plus a $p_{3/2}d_{3/2}^{-1}$ neutron particle-hole state with a small admixture of the $p_{3/2}s_{1/2}^{-1}$ state. Their 2^- assignment is consistent with the results of this work but would require that the ground-state transition be M2. It is interesting to note that the strongest transition which depopulates this level (its placement is confirmed by coincidence results) is to the level at 3275 keV which has also been interpreted as a neutron particle-hole state.

4454.0 ± 0.2-keV level. This level is confirmed by a coincidence between the 3141- and 1313-keV transitions. The de-excitation pattern indicates that this level is fed by the low-spin isomer and the presence of a ground-state transition limits the spin to 1 or 2. From (p,p') experiments (20), this level has been interpreted as a mixed $p_{3/2}s_{1/2}^{-1}$ plus $p_{3/2}d_{3/2}^{-1}$ neutron particle-hole configuration, and their assignment of 1^- or 2^- is consistent with the results of this

decay study.

4474.0 ± 0.3-keV level. This less well-defined level is indicated by a dashed line on the decay scheme. A ground-state transition from the 4474-keV level limits its spin to 1 or 2.

4545.0 ± 0.5- and 4711.2 ± 0.4-keV levels. These levels are also dashed. Both levels have ground-state transitions which limit their spin assignments to 1 or 2. They have been interpreted (20) to have major $p_{3/2}s_{\bar{1}/2}$ and $p_{3/2}d_{\bar{3}/2}$ neutron particle-hole components. The 4711-keV state was postulated (20) to have an additional component of $p_{1/2}d_{\bar{3}/2}$ and small admixtures of $f_{5/2}j^{-1}$ neutron particle-hole states.

4947.4 ± 0.3-keV level. A $\log ft$ value of less than 8.5 limits the spin assignment to 1, 2, or 3 and the decay pattern indicates beta feeding from only the low-spin isomer. The neutron particle-hole interpretation postulated for the level (20) is a complex mixture of configurations involving $p_{3/2}$, $p_{1/2}$, and $f_{5/2}$ particle states. Their proposed assignment of 2^- is consistent with these beta-decay results.

5017.0 ± 0.3-, 5760.3 ± 0.3-, and 6624.1 ± 0.4-keV levels. These are the only undashed levels above 5 MeV. De-excitation patterns indicate that all are fed by the low-spin isomer. A ground-state transition from the 5017-keV level limits the spin to 1 or 2. Transitions to the 4^+ level at 1694 and the low-spin level at 2414 keV limit the spin of the

6624-keV level to 2, 3, or 4.

5217.8 ± 0.5-, 5321.1 ± 0.3-, and 5608.3 ± 0.3-keV levels. All of these levels have ground-state transitions which indicate that they are fed by the low-spin isomer. This limits their spin to 1 or 2.

5832.2 ± 0.6-keV level. The decay pattern of this level indicates that it is fed by the low-spin isomer. A spin of 1, 2, or 3 is favored based on a $\log f_1 t$ value of 7.3.

5861.8 ± 0.5- and 6091.4 ± 0.3-keV levels. These two levels appear to be the only levels above 5 MeV that are fed by only the high-spin isomer. Transitions from the 5862-keV level to the 4^+ and 6^+ levels at 2126 and 2262 keV respectively limit the spin assignment to 4, 5, or 6. The spin of the 6092-keV level is limited to 4, 5, or 6 by a $\log f_1 t$ value < 7.1 and a transition to the 4^+ level at 1694 keV.

6186.5 ± 0.4- and 6412.3 ± 0.4-keV levels. The de-excitation patterns for these levels imply possible beta feeding from both isomers. Because the splitting of the beta feeding to these levels is not known, no beta feedings or $\log ft$ values were calculated.

5800.2 ± 0.5-, 5870.8 ± 1.2-, 5968.5 ± 1.0-, 6013.0 ± 1.0-, 6052.6 ± 0.4-, 6103.9 ± 0.3-, 6114.4 ± 0.7-, 6126.4 ± 0.5-, 6169.8 ± 0.8-, 6200.0 ± 1.3-, 6253.4 ± 0.8-, 6394.8 ± 0.6-, and 6409.0 ± 0.8-keV levels. Because Nuclear Data Sheets (13) has accepted a Q-value for ^{136}I of 6980 keV, any

transition with energy greater than (6980 - 1313) keV must depopulate a level of the same energy. Thirteen such levels were observed and their spins are limited to 1 or 2.

B. Decay of ^{138}I

The prompt singles spectrum for the decay of ^{138}I (spectrum A of Table III.) is shown in Figure 15 and the fits for the 831-, 1278-, 1463-, and 1810-keV peaks are shown in Figure 16. Other activities observed in this spectrum include ^{137}Xe, ^{138}Xe, ^{139}Xe, ^{138}Cs, and ^{136}I. Eight gamma transitions were assigned to ^{138}I decay. The energies, relative intensities, and placements of these transitions are listed in Table XIII. Other weak transitions with short half-lives were observed which may belong to the decay of ^{138}I, but the statistics were insufficient to make a definitive assignment on the basis of half-life, and no other supporting evidence was found. The energies of these transitions are 2302, 2544, 2572, 2836, 3297, 3310, 3496, and 4089 keV.

A comparison of the results of this study with those of previous workers is given in Table XIV. The transitions reported by Kratz et al. (23) at 295.4, 370.4, and 466.1 keV were not seen in this study. An upper limit was obtained for the intensity of the 466-keV transition but not for the 295- and 370-keV transitions, since they were obscured by transi-

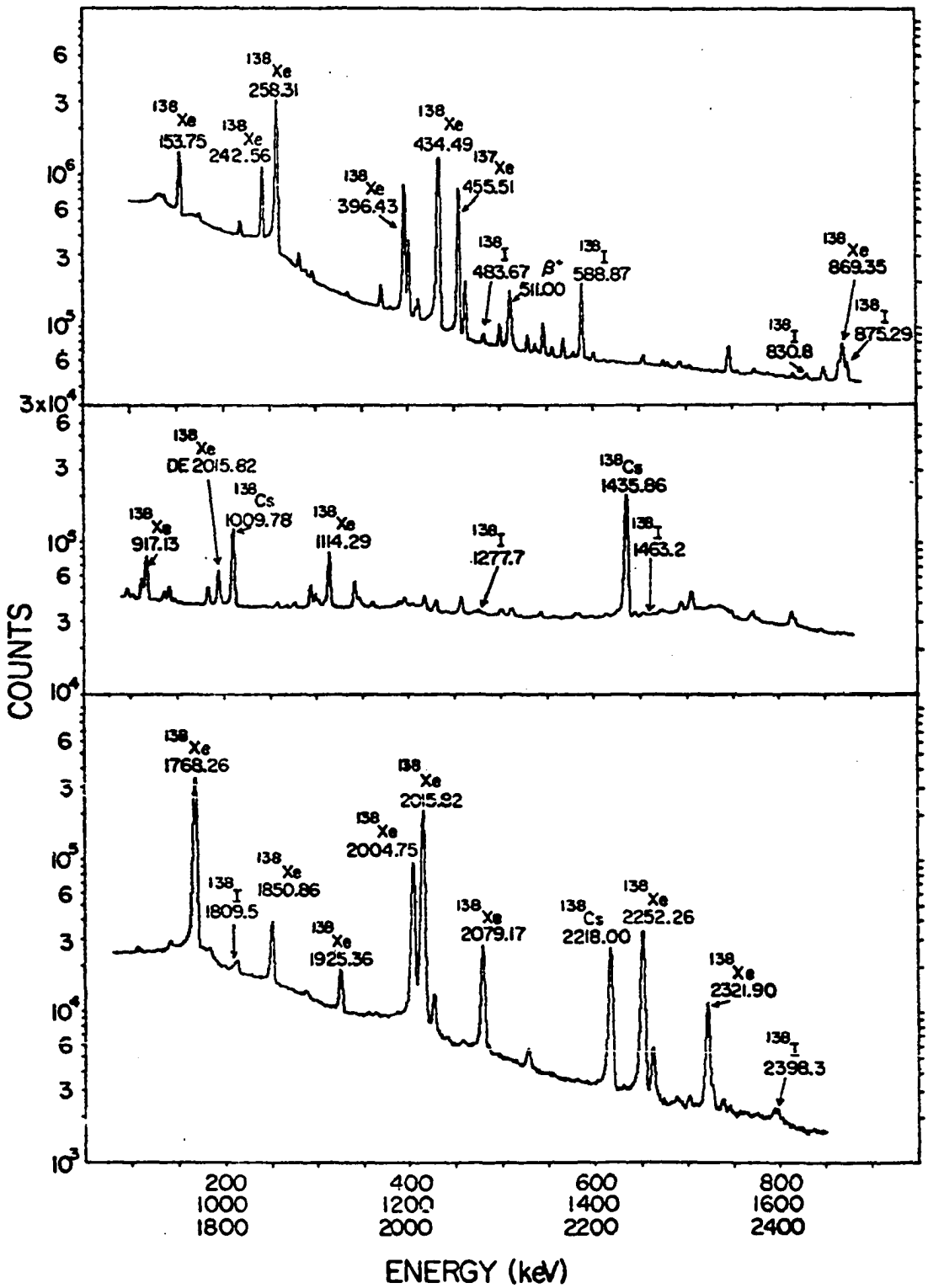

Figure 15. Gamma-ray spectrum from the decay of ^{138}I

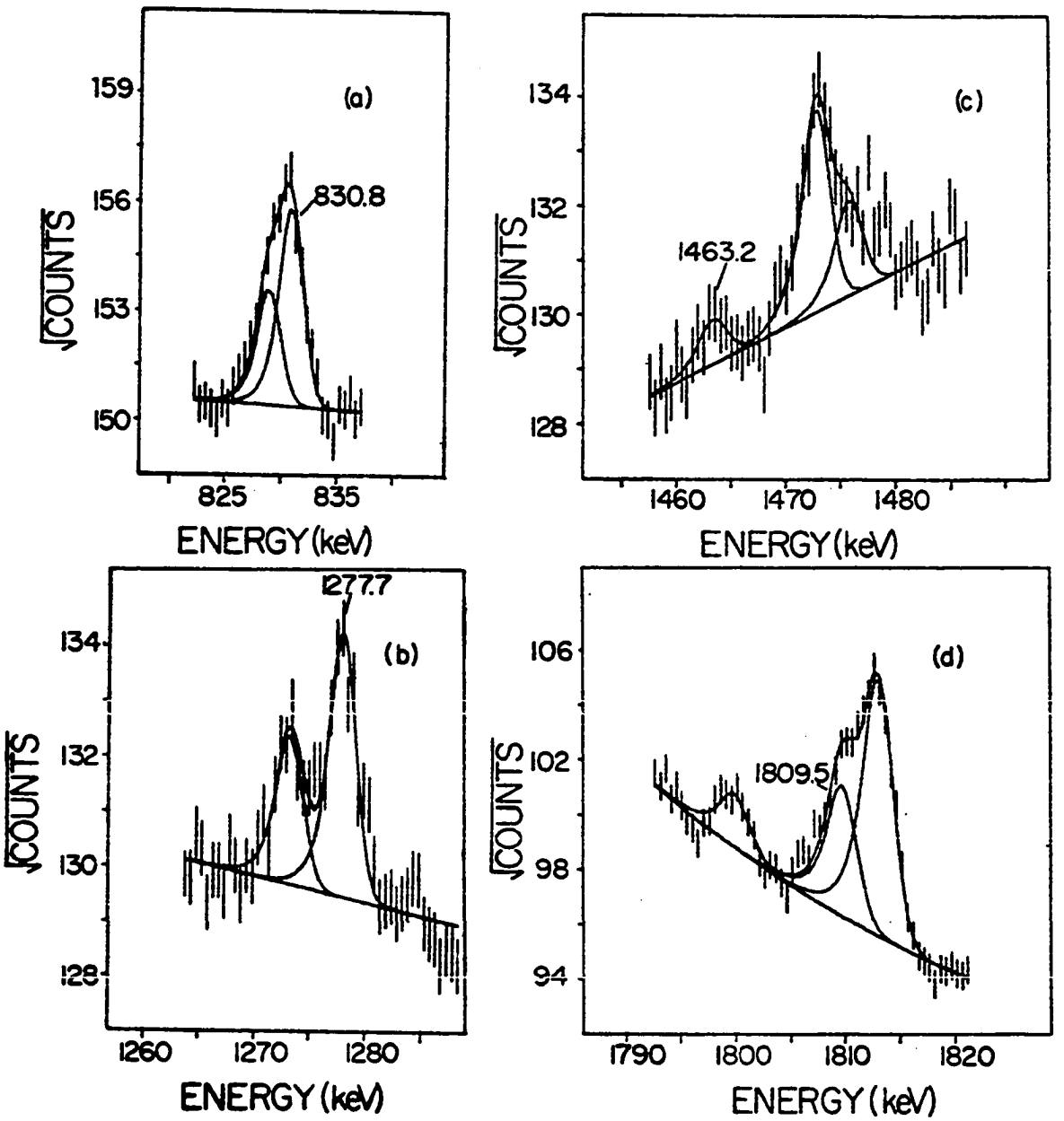

Figure 16. Detailed gamma-ray spectra for the (a) 831-, (b) 1278-, (c) 1463-, and (d) 1810-keV peaks in ^{138}I

Table XIII. Gamma transitions observed in ^{138}I decay

Energy (keV)	Relative intensity[1]	Placement
483.67 ± 0.10	72 ± 8	1073 --> 589
588.87 ± 0.08	1000	589 --> 0
830.8 ± 0.3	39 ± 7	1903 -->1073
875.29 ± 0.15	186 ± 20	1464 --> 589
1277.7 ± 0.3	50 ± 7	1867 --> 589
1463.2 ± 1.2	8 ± 6	1464 --> 0
1809.5 ± 0.5	58 ± 10	2398 --> 589
2398.3 ± 0.5	16 ± 4	2398 --> 0

[1]Intensity normalized to 1000 for the 589-keV gamma transition.

Table XIV. Comparison with previous ^{138}I studies

Energy[1] (keV)	Relative Intensity[1]	Energy[2] (keV)	Relative Intensity[2]	Energy[3] (keV)
		295.4 ± 0.5	50	
		370.4 ± 0.5	50	
466	<30	466.1 ± 0.5	50	
483.67 ± 0.10	72 ± 8	482.7 ± 0.3	150	482 ± 1
588.87 ± 0.08	1000[4]	588.7 ± 0.1	1000[4]	589.5 ± 0.5

[1]Results from this work.
[2]Results from Reference 23.
[3]Results from Reference 16.
[4]Intensity normalized to 1000 for the 589-keV gamma transition.

Table XV. Coincidences observed in ^{138}I decay

Gating Energy (keV)	Coincident Transitions (keV)
484	589, 831
589	484, 831, 875, 1278, 1810
831	484, 589
875	589
1278	589

tions at 296.5 and 371.4 keV from ^{139}Xe and ^{138}Xe respectively. Intensities reported by Cheifetz *et al.* (16) cannot be compared directly with those from beta decay, since the population mechanism is different.

A level scheme was constructed using the coincidence data summarized in Table XV. The spectrum of gamma transitions observed in coincidence with the most intense ^{138}I transition (589 keV) is shown in Figure 17, and the spectra observed in coincidence with the gamma transitions at 484, 831, 875, and 1278 keV are shown in Figure 18. The level scheme for the decay of ^{138}I is shown in Figure 19.

Although the percent beta feeding to the ground state was not measured, the log*ft* values were calculated assuming no ground-state beta feeding. The results are given in Table XVI. The Q value of 7.8 MeV used in this calculation was obtained from the mass tables of Garvey *et al.* (38). The as-

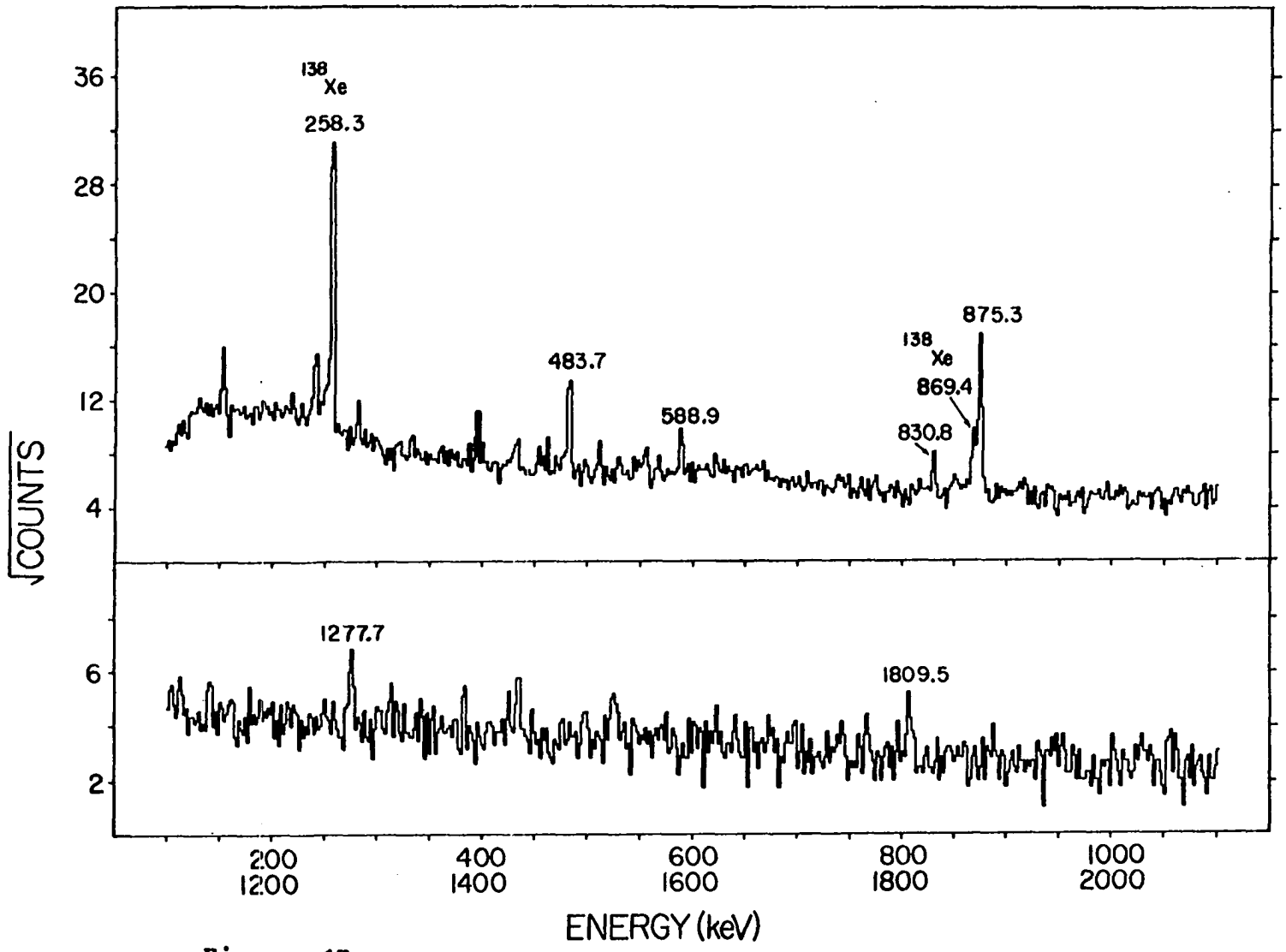

Figure 17. Gamma spectrum in coincidence with the 589-keV gamma ray from ^{138}I

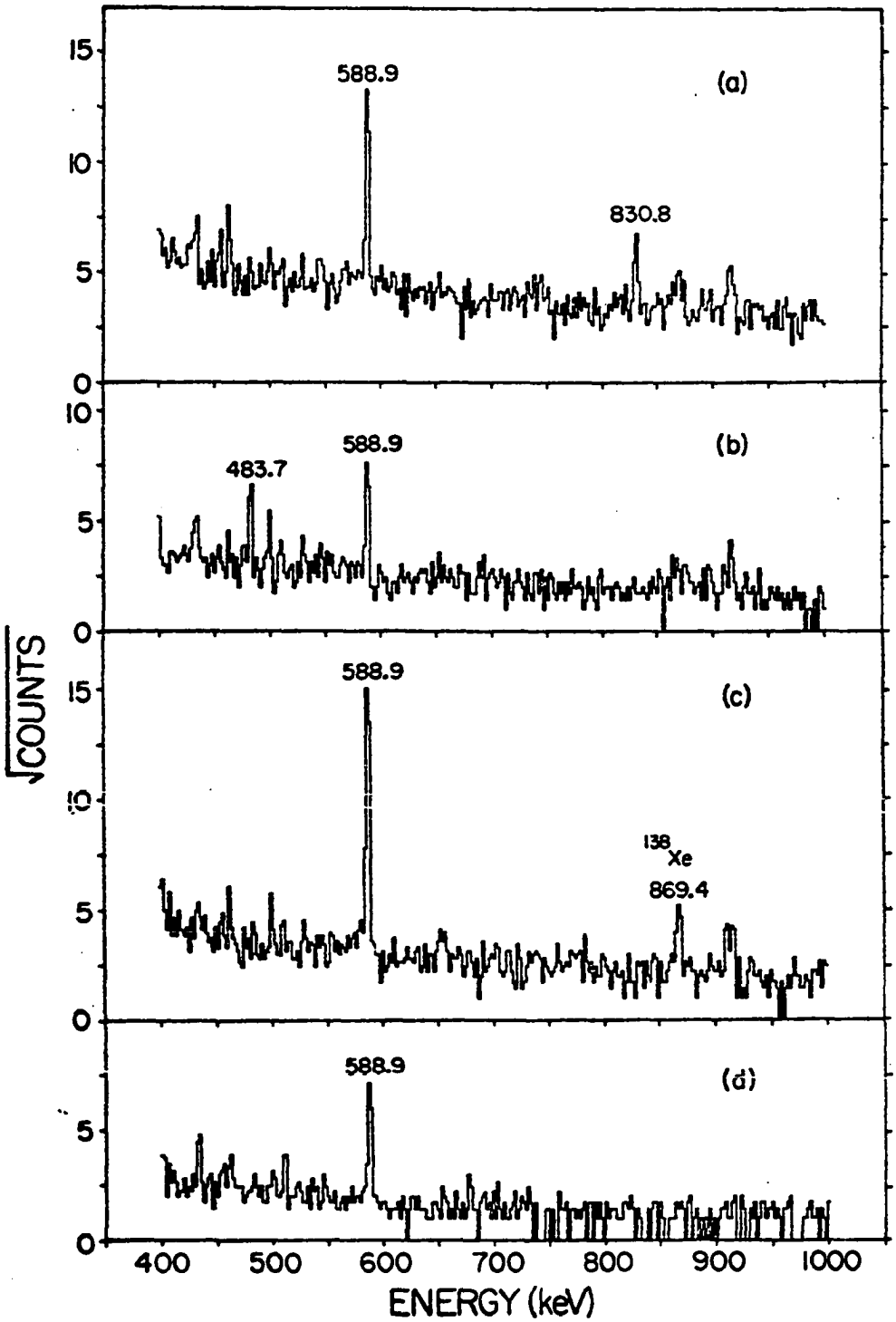

Figure 18. Gamma spectra in coincidence with the (a) 484- (b) 831- (c) 875-, and 1278-keV gamma rays from ^{138}I

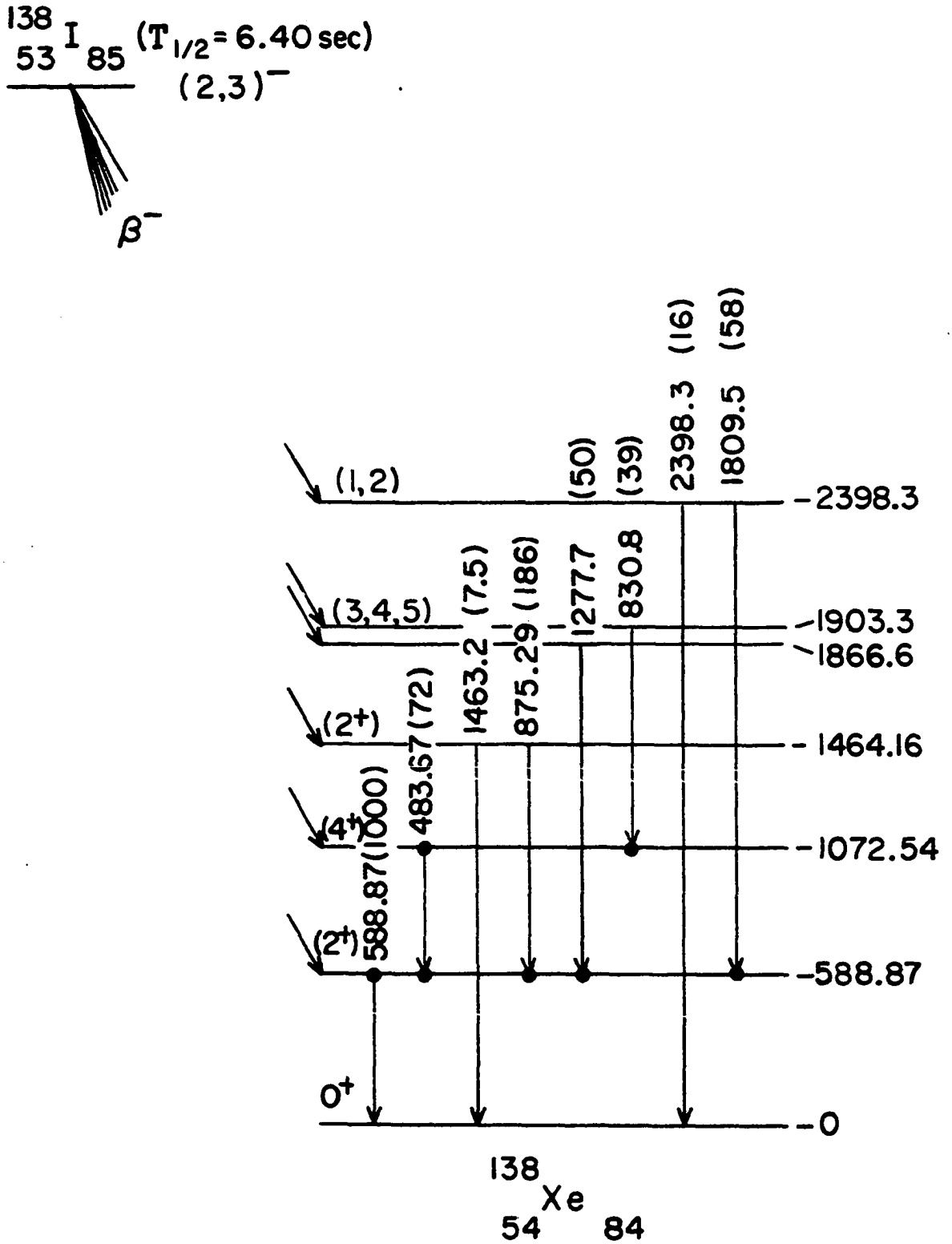

Figure 19. Proposed decay scheme of ^{138}I

sumption of zero feeding to the ground state is based on the beta feeding to the 1072-keV level which has a preferred assignment of 4^+. A detailed discussion of the observed ^{138}Xe excited states follows.

Table XVI. Beta feeding and logft values for ^{138}I decay

^{138}I Levels (keV)	Percent Beta Branching[1]	Logft[2]	Logf_1t[2]
588.87 ± 0.10	62 ± 6	6.1	8.2
1072.54 ± 0.14	3.2 ± 1.0	7.2	9.3
1464.14 ± 0.18	18.9 ± 2.0	6.4	8.4
1866.55 ± 0.31	4.9 ± 0.7	6.8	8.8
1903.34 ± 0.32	3.8 ± 0.7	6.9	8.9
2398.34 ± 0.31	7.2 ± 1.1	6.5	8.3

[1]Assumed ground-state feeding is 0%.
[2]Q-value of 7.8 MeV obtained from reference 38.

Ground state. The spin and parity for ^{138}Xe is assumed to be 0^+ since it is an even-even nucleus. The ground-state spin for ^{138}I has not been measured but the beta feeding to the excited levels of ^{138}Xe limits the possible values as described below.

588.87 ± 0.10-keV level. The most intense transition is the 589-keV transition which is assumed to establish the first excited state in agreement with the YRAST sequence pro-

posed by Cheifetz et al. (16). The preferred assignment of 2^+ for this level is consistent with the results for all known even-even Xe isotopes and N=84 isotones. The $\log f_1 t$ value of 8.2 limits the spin of the ^{138}I ground state to 1, 2, or 3. This conclusion is valid for ground-state beta feedings up to 45%.

1072.54 ± 0.14-keV level. The 1073-keV level is established from the observed coincidences between the 484-, 589-, and 831-keV transitions and the fact that the 484-keV transition is more intense than the 831-keV transition. The preferred assignment of 4^+ for this level is based on systematics and the absence of an observed transition to the ground state. It is also in agreement with the assignment by Cheifetz et al. (16) as the 4^+ member of the YRAST band. A $\log ft$ value of 7.2 limits the spin of the ^{138}I ground state to the range 2 to 6 with a preferred value of 2 or 3.

1464.14 ± 0.18-keV level. This level is established by the observation of only the 589-keV transition in coincidence with the 875-keV transition. The observation of a weak gamma transition to the ground state eliminates a spin 0 assignment for this level and makes an assignment of 3 or 4 unlikely. From systematics, the preferred assignment is 2^+. A $\log f_1 t$ value of 8.4 is consistent with this assignment.

1866.55 ± 0.31-keV level. This level is established by the observation of the 1277-keV transition in coincidence

with the 589-keV transition.

1903.34 ± 0.32-keV level. The observed coincidence of the 831-keV gamma transition with both the 589- and 484-keV transitions establishes this level. Since the only observed decay of this level is to the (4+) level at 1073 keV, an assignment of spin 3 or higher is implied, but the spin is limited to less than 6 by a log*ft* value of 6.9.

2398.34 ± 0.31-keV level. Observation of the 1810-keV transition in coincidence with the 589-keV transition establishes this level. Because a ground-state gamma transition of 2398 keV was observed, a spin of 0 is eliminated and a value of 1 or 2 is favored.

C. Decay of ^{137}Xe

A gamma singles spectrum (spectrum A of Table IV.) for energies less than 1620 keV is shown in Figure 20. The observed contaminants included ^{41}Ar, ^{60}Co, and ^{137}Cs. A second singles spectrum (spectrum D of Table IV.) was collected through an absorber. The energy range of 1200 to 4200 keV from this spectrum is shown in Figure 21. The absorber consisted of 7 millimeters of lead followed by 2 millimeters cadmium and was used to suppress counts from the intense 456-keV transition and enhance counts from weak gamma transitions above 3 MeV. Strong contaminant peaks were observed from ^{140}La decay that was present upstream in the switch magnet from preceding experiments. Other background activi-

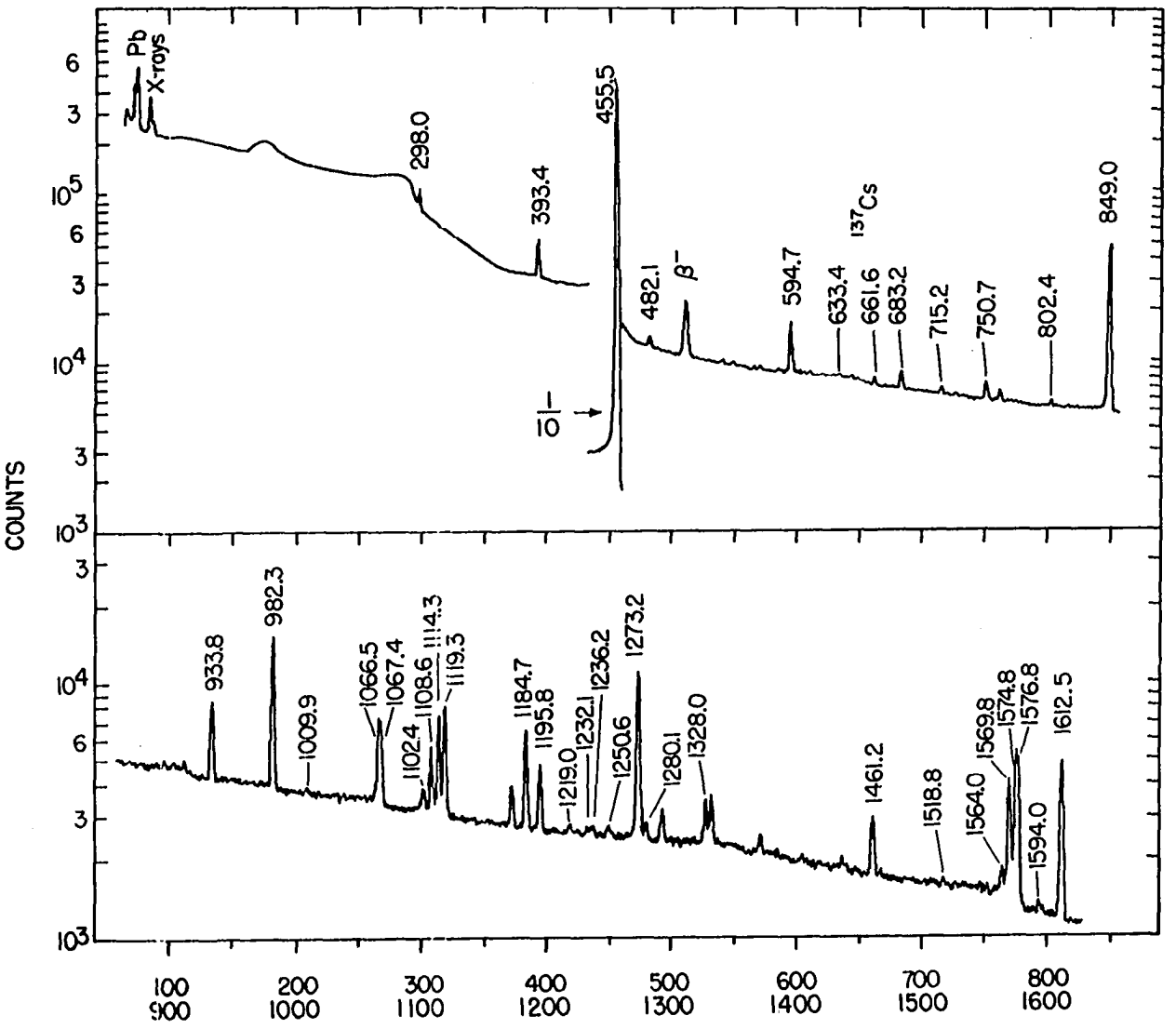

Figure 20. Spectrum of gamma rays with energies less than 1620 keV from the decay of ^{137}Xe

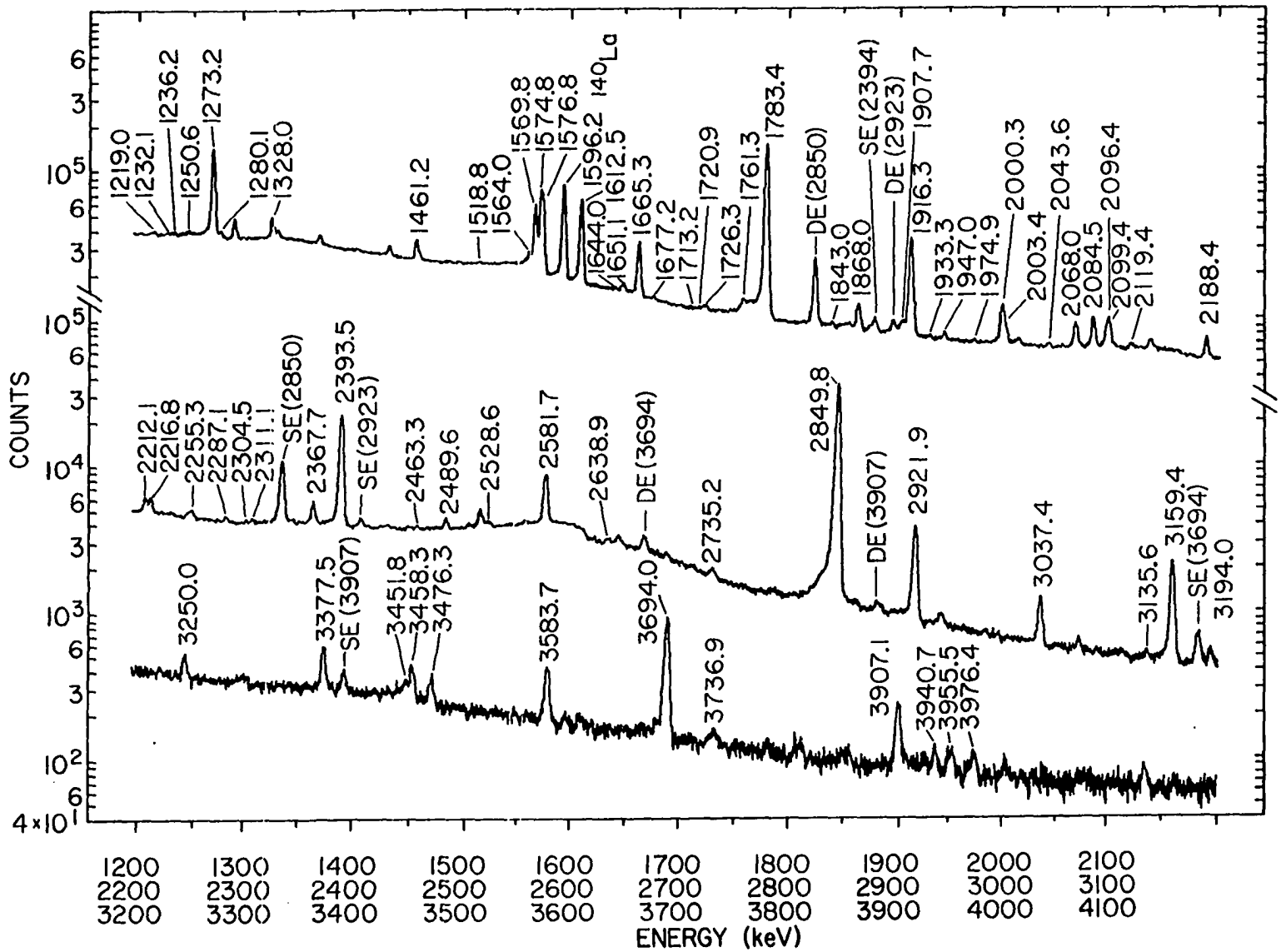

Figure 21. Spectrum of gamma rays with energies greater than 1200 keV from the decay of ^{137}Xe

ties observed included ^{138}Xe and ^{138}Cs. Approximately 15% of the peak at 1461 keV is background activity from ^{40}K.

A total of 94 gamma transitions were assigned to the decay of ^{137}Xe. The energies, relative intensities and placements of these transitions are given in Table XVII. Also included in this table for comparison are the energies and relative intensities reported by Monnand et al. (25) and Holm (24). Several of the intensities quoted by Monnand et al. (25) are stated as being <0.1 even though the peaks are clearly labeled and visible in their singles spectrum. A few peaks reported by Reference 25 were not seen in this study and upper limits are given. Three other peaks reported in Reference 25 were interpreted as being escape peaks. The 933-keV peak was interpreted as a singlet rather than a doublet and the ones at 1234 and 2099 keV were interpreted as doublets. The 1067-keV doublet presented a problem in this study because the energy obtained for the high-energy component with the centroids free to vary during the fitting process was about 1 keV larger than the placement energy indicated by the coincidence results. This result was true for both spectra A & D. An acceptable fit was obtained for this doublet with the centroid fixed at the placement energy and the height constrained to vary with the height of the 1066-keV peak.

Table XVII. Gamma transitions observed in ^{137}Xe decay

Energy[1] (keV)	Relative Intensity[1]	Energy[2] (keV)	Relative Intensity[2]	Energy[3] (keV)	Relative Intensity[3]	Placement
298.00 ± 0.07	3.8 ± 0.3	297.6 ± 0.6	3.0			1868 --> 1570
393.35 ± 0.06	4.5 ± 0.3	393.5 ± 0.3	4.3	394	5.7	849 --> 456
455.51 ± 0.04	1000.[4]	455.45 ± 0.10	1000.[4]	456	1000.[4]	456 --> 0
482.14 ± 0.12	0.48 ± 0.10	481.9 ± 0.3	0.5			2850 --> 2368
	<0.05	526.8 ± 0.5	0.2			
DEP (1570)		547.3 ± 0.5	∿0.1			
	<0.04	584.5 ± 0.5	<0.1			
594.70 ± 0.06	2.7 ± 0.3	594.5 ± 0.2	2.7	595	3.	1868 --> 1273
633.4 ± 0.5	0.08 ± 0.04					2850 --> 2217
DEP (1665)		644.0 ± 1.0	0.2			
683.2 ± 0.1	0.65 ± 0.07	683.0 ± 0.3	0.7	684	0.7	1868 --> 1185
	<0.04	700.0 ± 1.0	<0.1			
715.2 ± 0.2	0.21 ± 0.05	715.4 ± 0.5	∿0.1			1564 --> 849
750.65 ± 0.1	0.67 ± 0.07	750.6 ± 0.3	0.8			2850 --> 2099
802.4 ± 0.4	0.13 ± 0.04	802.0 ± 1.0	<0.1			1651 --> 844
848.95 ± 0.06	20. ± 1.	849.0 ± 0.2	22.8	849	21.7	849 --> 0
	<0.04	865.0 ± 1.0	∿0.1			

[1]Results from this work.
[2]Results from Monnand *et al.* (25).
[3]Results from Holm (24).
[4]Intensities normalized to 1000 for the 456-keV transition.

Table XVII. (continued)

Energy[1] (keV)	Relative Intensity[1]	Energy[2] (keV)	Relative Intensity[2]	Energy[3] (keV)	Relative Intensity[3]	Placement
933.82 ± 0.06	2.7 ± 0.2	933.3 ± 0.3	0.7	934	2.3	2850 --> 1916
		934.4 ± 0.3	2.3			
	<0.04	954.0 ± 1.0	<0.1			
982.25 ± 0.05	6.7 ± 0.4	982.4 ± 0.2	7.3	982	7.3	2850 --> 1868
1009.9 ± 0.2	0.13 ± 0.03	1007.5 ± 0.6	<0.1			
	<0.04	1024.0 ± 0.6	<0.1			
	<0.04	1037.4 ± 0.5	<0.1			
1066.5 ± 0.2	1.74 ± 0.3	1066.6 ± 0.3	2.0			2850 --> 1783
1067.4 ± 0.2	1.57 ± 0.3	1067.8 ± 0.3	1.7	1068	2.7	1916 --> 849
	<0.03	1097.0 ± 0.5	≈0.1			
1102.42 ± 0.10	0.53 ± 0.05	1102.4 ± 0.4	0.6			3952 --> 2850
1108.63 ± 0.06	1.64 ± 0.15	1108.6 ± 0.4	1.8	1107	2.3	1564 --> 456
1114.32 ± 0.06	2.96 ± 0.2	1114.5 ± 0.3	3.3			1570 --> 456
1119.33 ± 0.06	3.43 ± 0.2	1119.5 ± 0.3	3.9	1117	6.7	1575 --> 456
	<0.03	1139.5 ± 1.0	≈0.1			
1184.70 ± 0.06	2.7 ± 0.3	1184.6 ± 0.3	2.9	1185	2.7	1185 --> 0
1195.75 ± 0.06	1.54 ± 0.1	1195.5 ± 0.3	1.7	1197	2.3	1651 --> 456
1219.0 ± 0.4	0.09 ± 0.02	1219.0 ± 0.6	≈0.1			2068 --> 849
1232.1 ± 0.7	0.05 ± 0.02	1234.0 ± 1.0	≈0.1			2796 --> 1564
1236.2 ± 0.4	0.11 ± 0.02					3104 --> 1868
1250.6 ± 0.4	0.21 ± 0.03	1251.0 ± 1.0	≈0.1			2099 --> 849
1273.23 ± 0.1	7.3 ± 0.7	1273.2 ± 0.2	7.5	1275	8.3	1273 --> 0
1280.05 ± 0.15	0.30 ± 0.03	1280.0 ± 0.6	0.2			2850 --> 1570
1327.98 ± 0.06	0.94 ± 0.08	1328.0 ± 0.5	1.0	1330	0.7	1783 --> 456
1461.16 ± 0.2	0.55 ± 0.07					1916 --> 456

Table XVII. (continued)

Energy[1] (keV)	Relative Intensity[1]	Energy[2] (keV)	Relative Intensity[2]	Energy[3] (keV)	Relative Intensity[3]	Placement
1518.8 ± 0.5	0.06 ± 0.02	1519.0 ± 1.0	0.2			2368 --> 849
	<0.02	1529.0 ± 1.0	0.1			
1564.0 ± 0.2	0.32 ± 0.04	1564.0 ± 1.0	0.3			1564 --> 0
1569.77 ± 0.07	2.74 ± 0.2	1569.8 ± 0.3	3.0			1570 --> 0
1574.83 ± 0.15	2.3 ± 0.3	1575.0 ± 0.4	1.7			1575 --> 0
1576.75 ± 0.10	3.3 ± 0.3	1576.9 ± 0.4	3.9	1576	5.7	2850 --> 1273
1594.0 ± 0.6	0.10 ± 0.02	1594.0 ± 0.6	0.1			3377 --> 1783
1612.52 ± 0.06	4.0 ± 0.3	1612.6 ± 0.3	4.5	1615	5.3	2068 --> 456
1644.0 ± 0.8	0.028 ± 0.015					2099 --> 456
1651.14 ± 0.2	0.14 ± 0.02	1650.7 ± 0.7	0.1			1651 --> 0
1665.30 ± 0.07	1.7 ± 0.1	1665.4 ± 0.3	2.0	1668	2.7	2850 --> 1185
1677.2 ± 0.6	0.032 ± 0.013					
1713.2 ± 0.8	0.024 ± 0.015					
1720.9 ± 0.6	0.035 ± 0.015					3938 --> 2217
1726.3 ± 0.3	0.077 ± 0.013					3377 --> 1651
1761.3 ± 0.3	0.19 ± 0.05	1761.0 ± 1.0	0.2			2217 --> 456
1783.43 ± 0.06	13.3 ± 0.6	1783.4 ± 0.2	15.3	1784	16.0	1783 --> 0
1843.0 ± 0.4	0.046 ± 0.012	1843.0 ± 1.0	<0.1			
	<0.02	1857.6 ± 1.0	<0.1			
1867.96 ± 0.08	0.52 ± 0.05	1868.0 ± 0.4	0.6			1868 --> 0
1907.7 ± 0.2	0.17 ± 0.02					3824 --> 1916
1916.31 ± 0.08	3.1 ± 0.4	1916.5 ± 0.3	3.2	1918	3.7	1916 --> 0
1933.3 ± 0.4	0.043 ± 0.012					3584 --> 1651
1947.0 ± 0.2	0.085 ± 0.011	1947.0 ± 1.0	<0.1			2796 --> 849
1974.9 ± 0.5	0.038 ± 0.012					3159 --> 1185

Table XVII. (continued)

Energy[1] (keV)	Relative Intensity[1]	Energy[2] (keV)	Relative Intensity[2]	Energy[3] (keV)	Relative Intensity[3]	Placement
2000.3 ± 0.2	0.57 ± 0.06	2001.0 ± 0.5	0.7			2849 --> 849
2003.4 ± 0.3	0.21 ± 0.04					3787 --> 1783
2043.6 ± 0.3	0.057 ± 0.012	2043.2 ± 1.0	<0.1			
2068.0 ± 0.2	0.33 ± 0.03	2068.0 ± 0.4	0.4			2068 --> 0
2084.47 ± 0.10	0.44 ± 0.03	2084.5 ± 0.3	0.5			3952 --> 1868
2096.4 ± 0.3	0.23 ± 0.03					2945 --> 849
2099.42 ± 0.15	0.43 ± 0.04	2098.6 ± 0.3	0.6			2099 --> 0
2119.4 ± 0.4	0.055 ± 0.012					
2188.44 ± 0.10	0.26 ± 0.03	2188.6 ± 0.4	0.4			3037 --> 849
2212.1 ± 0.2	0.13 ± 0.02	2212.8 ± 0.6	0.1			3787 --> 1575
2216.8 ± 0.4	0.076 ± 0.03					2217 --> 0
2255.3 ± 0.3	0.08 ± 0.01	2255.5 ± 1.0	0.1			3104 --> 849
2287.1 ± 0.4	0.045 ± 0.008					3938 --> 1651
2304.5 ± 0.8	0.018 ± 0.008					3955 --> 1651
2311.1 ± 0.5	0.031 ± 0.008					3584 --> 1273
2367.65 ± 0.2	0.21 ± 0.03	2368.0 ± 0.6	0.2			2368 --> 0
2393.53 ± 0.15	2.6 ± 0.2	2393.6 ± 0.3	2.9	2396	3.3	2849 --> 456
2463.3 ± 0.7	0.023 ± 0.009					3737 --> 1273
2489.6 ± 0.2	0.088 ± 0.010	2489.4 ± 1.0	<0.1			2945 --> 456
2528.6 ± 0.6	0.047 ± 0.011					3377 --> 849
2581.71 ± 0.1	0.75 ± 0.07	2581.8 ± 0.3	0.8			3037 --> 456
2638.9 ± 0.7	0.029 ± 0.011					3824 --> 1185
2735.2 ± 0.4	0.044 ± 0.009					3584 --> 849
2849.80 ± 0.1	5.9 ± 0.3	2850.0 ± 0.2	7.6	2852	8.7	2850 --> 0
2921.9 ± 0.2	0.57 ± 0.05	2922.1 ± 0.3	0.7	2924	1.0	3377 --> 456

Table XVII. (continued)

Energy[1] (keV)	Relative Intensity[1]	Energy[2] (keV)	Relative Intensity[2]	Energy[3] (keV)	Relative Intensity[3]	Placement
3037.4 ± 0.2	0.14 ± 0.02	3037.4 ± 0.6	0.2			3037 --> 0
3135.6 ± 0.7	0.012 ± 0.005					
3159.4 ± 0.2	0.38 ± 0.04	3159.6 ± 0.6	0.5	3162	0.3	3159 --> 0
3194.0 ± 0.4	0.029 ± 0.006	3195.5 ± 1.0	<0.1			
3250.0 ± 0.4	0.034 ± 0.006	3250.3 ± 1.0	<0.1			
3377.4 ± 0.2	0.064 ± 0.008	3377.8 ± 0.8	<0.1			3377 --> 0
		3396.0 ± 1.5	<0.1			
3451.8 ± 0.8	0.015 ± 0.007					3907 --> 456
3458.3 ± 0.4	0.041 ± 0.007	3458.5 ± 1.0	<0.1			
3476.3 ± 0.4	0.028 ± 0.006	3475.5 ± 1.5	<0.1			
3583.7 ± 0.3	0.063 ± 0.009	3583.0 ± 2.0	0.1			3584 --> 0
3694.0 ± 0.3	0.20 ± 0.02	3693.5 ± 1.0	0.3	3697	0.3	3694 --> 0
3736.9 ± 0.7	0.010 ± 0.003					3737 --> 0
	<0.003	3797.0 ± 3.0	<0.1			
3907.1 ± 0.4	0.043 ± 0.007	3907.5 ± 3.0	<0.1	3914		3907 --> 0
3940.7 ± 0.9	0.008 ± 0.004					3941 --> 0
3955.5 ± 0.8	0.011 ± 0.004					3955 --> 0
3976.4 ± 0.8	0.010 ± 0.004					3976 --> 0

The proposed level scheme is supported by the coincidence results contained in Table XVIII. The 982-keV transition was observed to be in coincidence with the 456-keV transition and hence cannot be a ground-state transition. This fact results in significant differences from previous work (24,25). This coincidence was confirmed by a careful analysis of accidental coincidences and gamma singles intensities. The spectrum seen in coincidence with the 456-keV transition is shown in Figure 22 and the spectra seen in coincidence with the 849- and 982-keV gates are shown in Figure 23. As a consequence of the 982-456 coincidence, several of the gamma cascades proposed by Monnand et al. (25) are inverted in this study. The proposed level scheme for ^{137}Xe decay is shown in Figure 24. The levels proposed in this study are compared in Figure 25 to the beta decay results of Monnand et al. (25) and the proton-transfer experiments of Wildenthal et al. (19).

Percent beta feedings and log*ft* values were calculated using a ground-state beta branching of 67 ± 3% as measured by Onega and Pratt (39). A Q-value of 4.15 MeV was used in the log*ft* calculation. The results of the percent beta feeding and log*ft* calculations are tabulated in Table XIX.

The accepted assignment of $7/2^+$, for the ground state of ^{137}Cs, has been obtained by atomic-beam methods and shell-model arguments. From the angular distributions of the

Table XVIII. Coincidences observed in ^{137}Xe decay

Gating Energy (keV)	Definite Coincidences (keV)	Possible Coincidences (keV)
298	982, 1114, 1570	456
393	456	1067
456	298, 393, 982, 1066, 1067, 1109, 1114, 1119, 1196, 1328, 1461, 1613, 2394, 2582, 2922	934, 3452
595	982, 1273	
683	982, 1185	
849	1067, 2000, 2188	934, 1219, 2096
934	849, 1067, 1461, 1916	456
982	298, 456, 595, 1114, 1185, 1273, 1570	683, 1868
1066	1328, 1783	456
1067	849, 934	393, 456
1114	298, 456, 982	
1119	456	2212
1185	683, 982, 1665	1102
1196		456
1273	595, 982, 1577	
1328	456, 1066	
1461	456, 934	
1570	298, 982	1280
1577		1273
1613	456	
1665	1185	
1783	1066	2003
1868	982	
1916	934	
2394		456

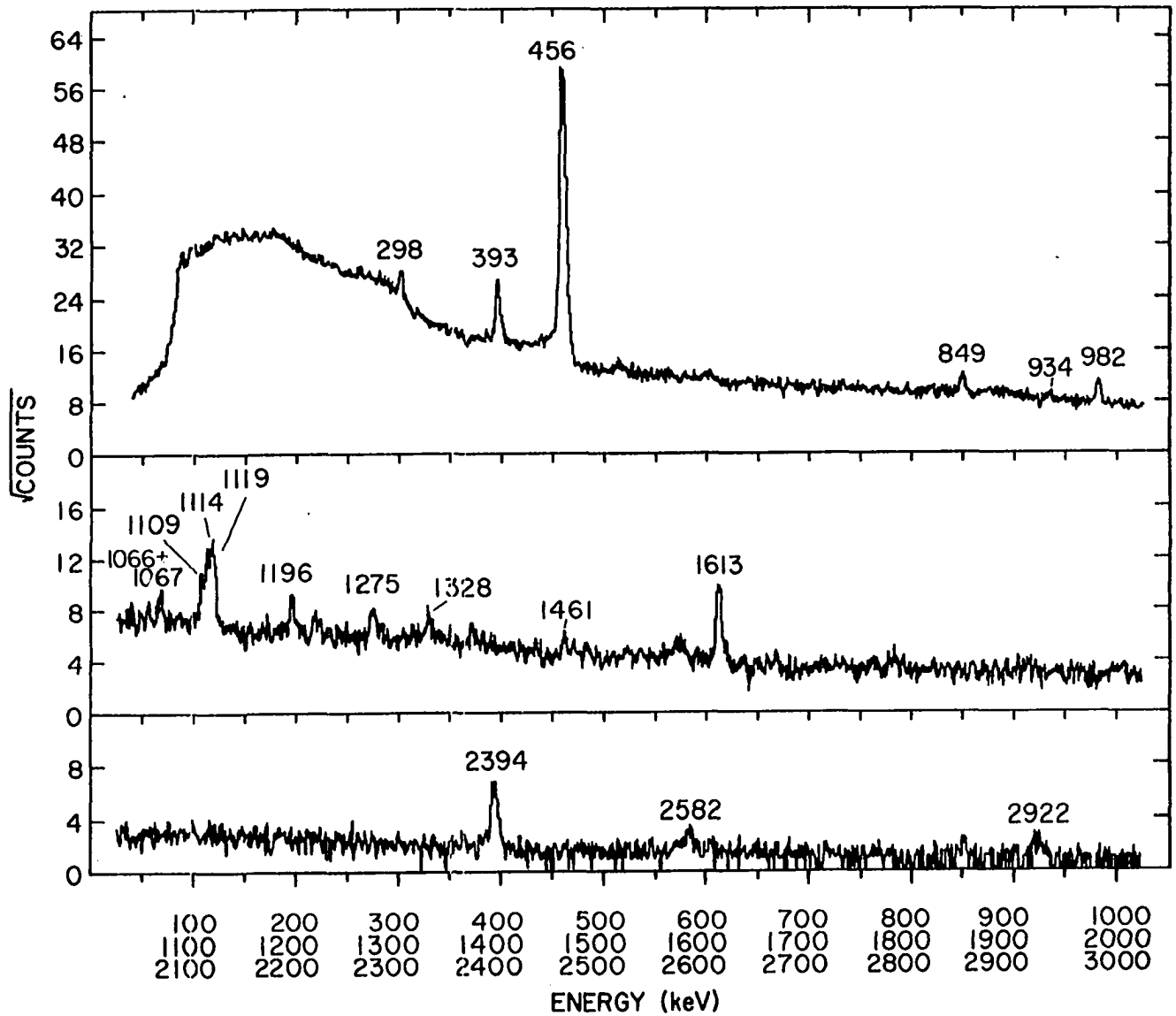

Figure 22. Gamma spectrum in coincidence with the 456-keV gamma ray from ^{137}Xe

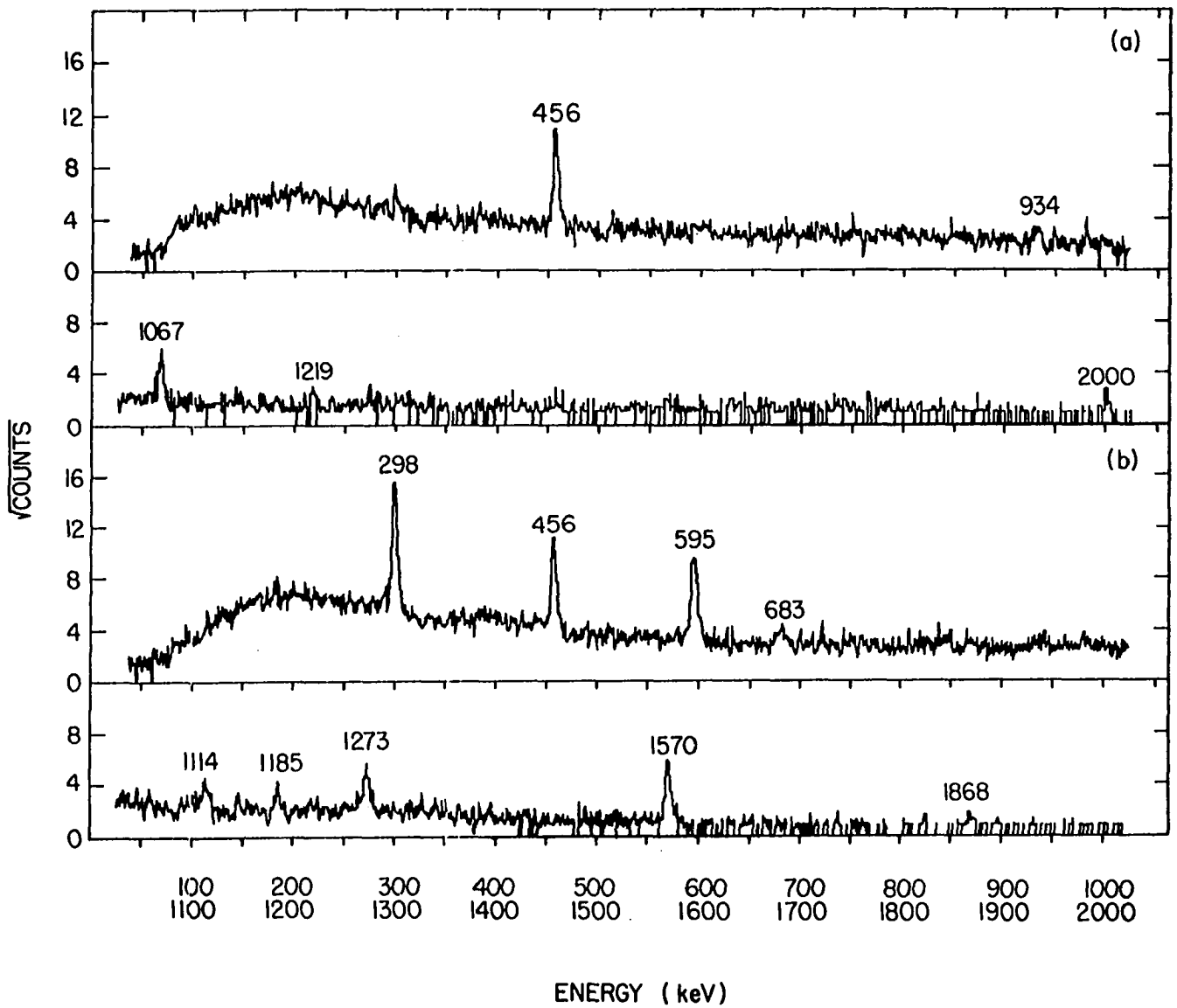

Figure 23. Gamma spectra in coincidence with the (a) 849- and (b) 982-keV gamma rays from ^{137}Xe

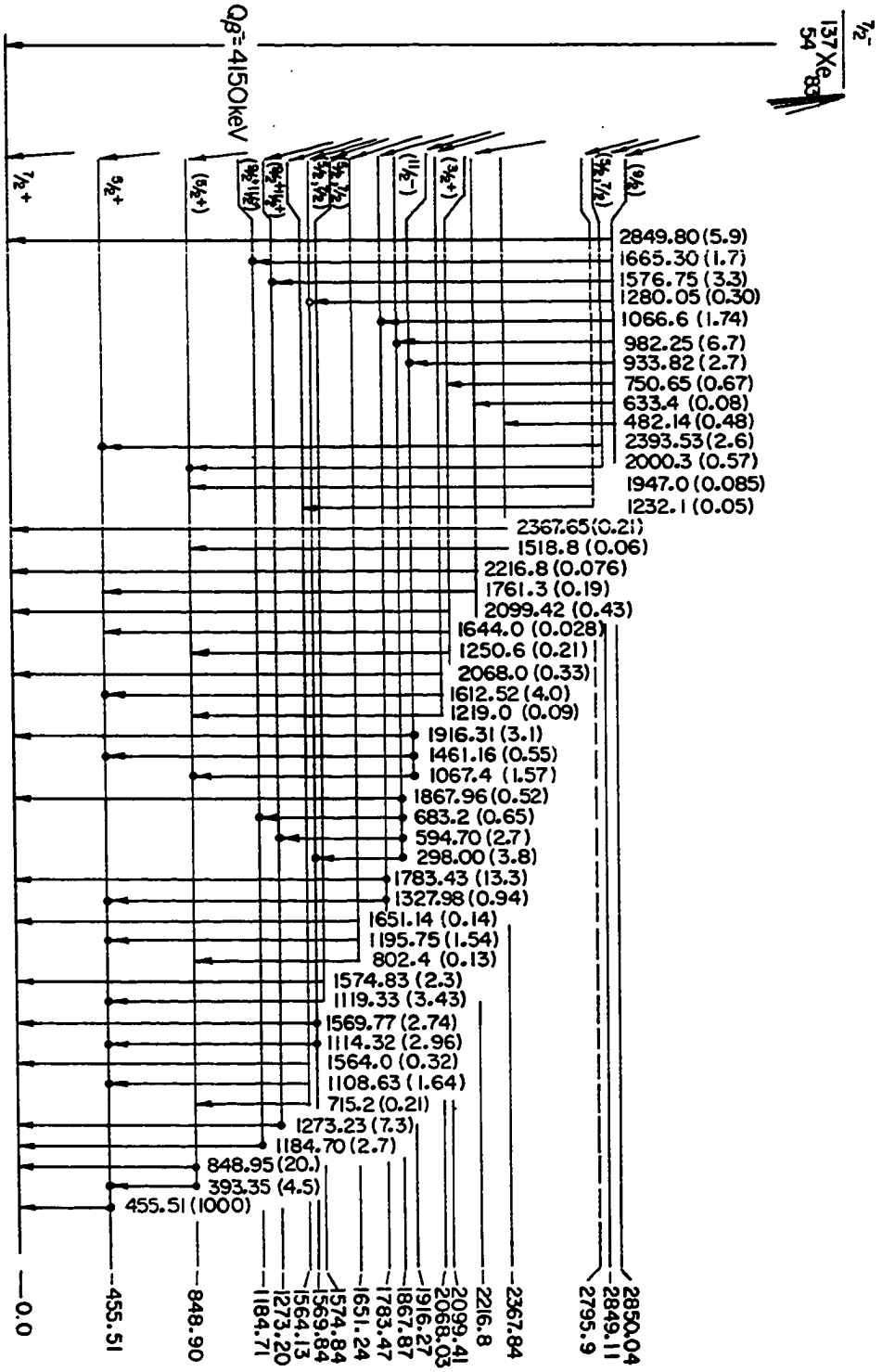

Figure 24. Proposed decay scheme of ^{137}Xe

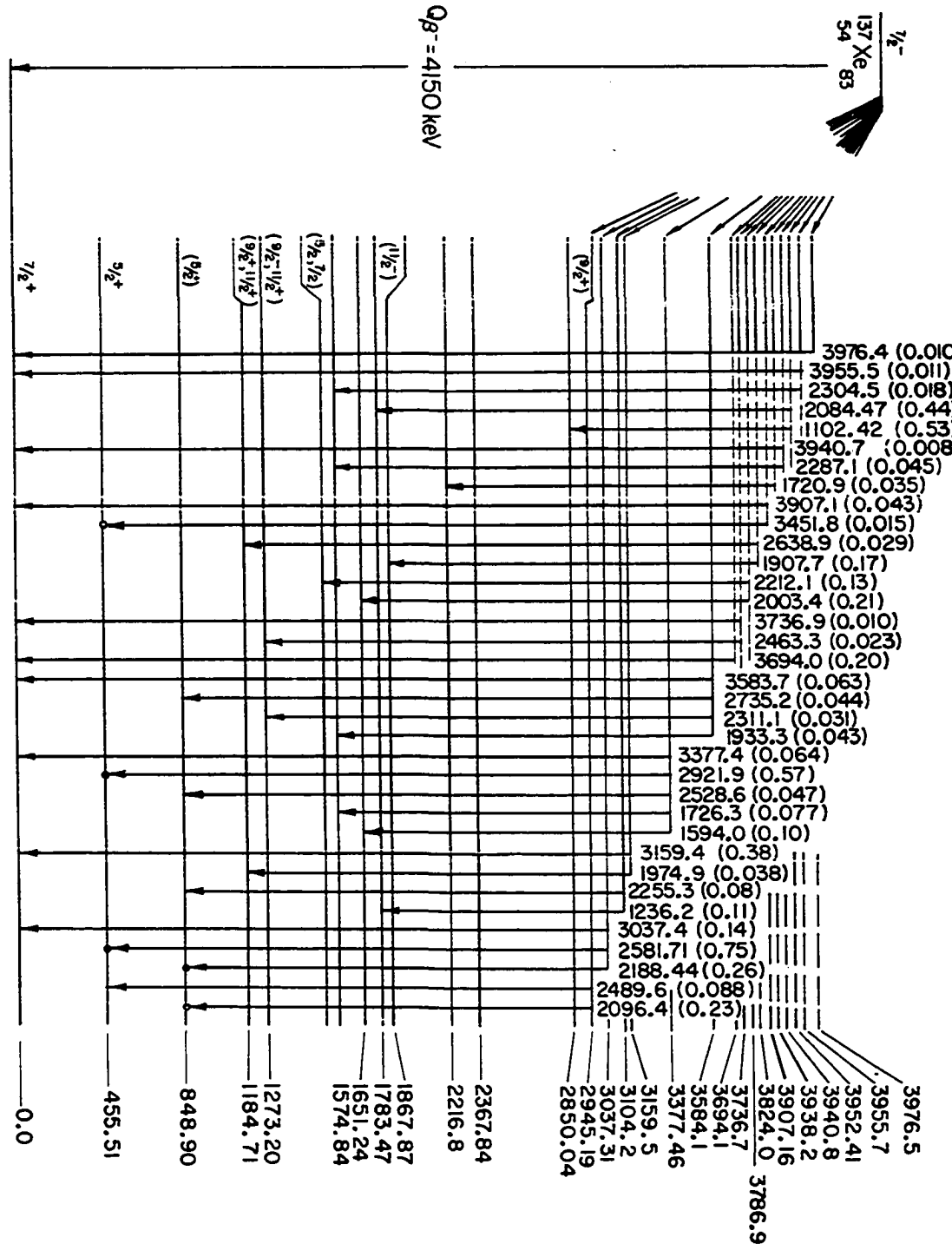

Figure 24. (continued)

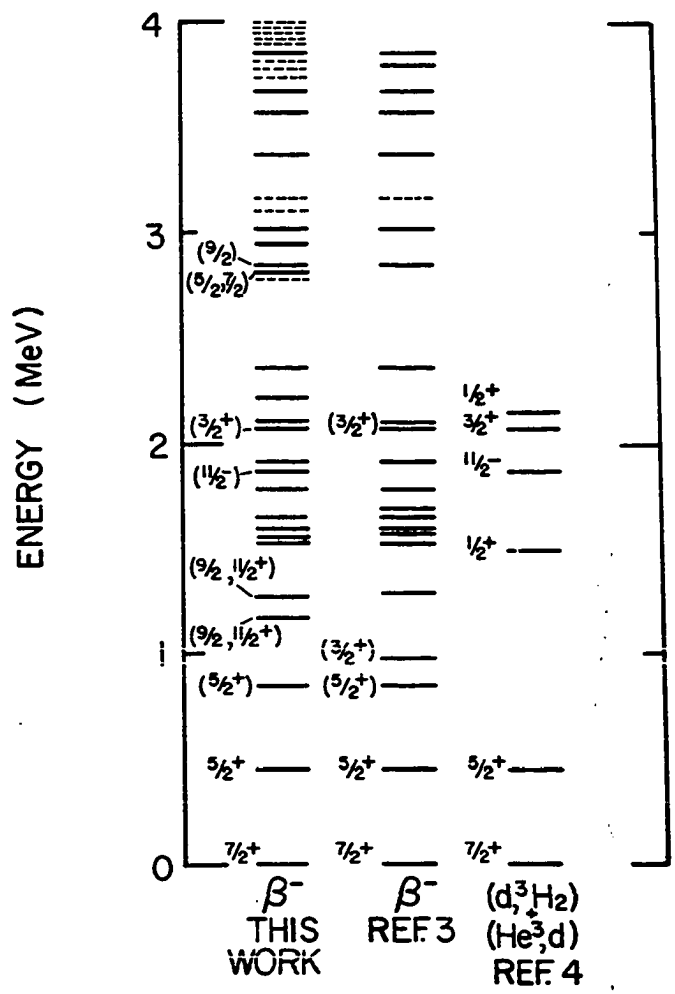

Figure 25. Comparison of ^{137}Cs levels from this work with previous studies

Table XIX. Beta feeding and log*ft* values for ^{137}Xe decay

^{137}Cs Levels (keV)	Percent Beta Branching	Log*ft*
0.0	67.0 ± 3.0	6.6[1]
455.51 ± 0.05	30.4 ± 3.1	6.7[1]
848.90 ± 0.06	0.65 ± 0.08	8.2
1184.71 ± 0.05	<0.02	>9.5
1273.20 ± 0.06	0.04 ± 0.03	9.1
1564.13 ± 0.06	0.066 ± 0.01	8.7
1569.84 ± 0.06	0.050 ± 0.014	8.8
1574.84 ± 0.06	0.17 ± 0.03	8.3
1651.24 ± 0.08	0.051 ± 0.007	8.8
1783.47 ± 0.05	0.38 ± 0.05	7.8
1867.87 ± 0.07	<0.03	>8.8
1916.27 ± 0.10	0.073 ± 0.02	8.4
2068.03 ± 0.07	0.14 ± 0.02	8.0
2099.41 ± 0.09	<0.003	>9.7
2216.8 ± 0.2	0.005 ± 0.002	9.3
2367.84 ± 0.11	<0.003	>9.3
2795.9 ± 0.2	0.004 ± 0.001	8.8
2849.11 ± 0.13	0.100 ± 0.015	7.4[1]
2850.04 ± 0.09	0.72 ± 0.08	6.5[1]
2945.19 ± 0.17	0.010 ± 0.002	8.2
3037.31 ± 0.09	0.036 ± 0.005	7.5[1]
3104.2 ± 0.3	0.006 ± 0.001	8.2
3159.5 ± 0.2	0.013 ± 0.002	7.8[1]
3377.46 ± 0.14	0.027 ± 0.004	7.1[1]
3584.1 ± 0.4	0.0056 ± 0.001	7.3[1]
3694.1 ± 0.4	0.0062 ± 0.001	6.9[1]
3736.7 ± 0.6	0.0010 ± 0.0004	7.6[1]
3786.9 ± 0.2	0.011 ± 0.002	6.4[1]
3824.0 ± 0.2	0.0061 ± 0.0011	6.5[1]
3907.16 ± 0.13	0.0018 ± 0.0006	6.6[1]
3938.2 ± 0.4	0.0025 ± 0.001	6.3[1]
3940.8 ± 1.0	0.0002 ± 0.0001	7.2[1]
3952.41 ± 0.15	0.030 ± 0.004	5.1[1]
3955.7 ± 0.6	0.0009 ± 0.0003	6.6[1]
3976.5 ± 0.9	0.0003 ± 0.0001	6.9[1]

[1]Log*f*$_1$*t* value less than 8.5

^{136}Xe(d,p)^{137}Xe reaction (40) and shell-model considerations, an assignment of $7/2^-$ is preferred for the ^{137}Xe ground state. This assignment is consistent with a log$\underline{f}_1\underline{t}$ value of 8.2 for the beta transition to the ^{137}Cs ground state (spin parity rules are summarized in Table VII). Some preferred assignments of spin and parity can be made on the basis of reaction studies (19), de-excitation patterns and low log$\underline{f}_1\underline{t}$ values. A discussion of these levels follows.

455.51 ± 0.05-keV level. This level is well-established by previous studies (19,24,25,26,39). Single proton transfer reactions (19) indicate that this level contains most of the $d_{5/2}$ single-particle strength, therefore an assignment of $5/2^+$ is preferred for this level. This assignment is consistent with a log$\underline{f}_1\underline{t}$ value of 8.2 to this level.

848.90 ± 0.06-keV level. This level has been observed in previous decay studies (24,25) and in a muon capture study (26). A spin and parity assignment of $5/2^+$ is favored from the results of shell-model calculations of the second excited state. These calculations will be discussed later.

A major difference in the results of this work compared to previous decay studies (24,25) is the absence of a level at 982 keV. The 982-keV transition was placed as depopuating the 2850-keV level instead of a ground-state transition primarily because of an observed coincidence of the 456- and 982-keV transitions. A careful analysis of the intensity of

the 456-keV peak in both the 982- and 849-keV gates shows that in the spectrum resulting from the 982-keV gate, 40% of the counts in the 456-keV peak are true coincidences. These counts cannot be attributed to either accidental or Compton background coincidences. A supporting argument is the fact that the 456- and 982-keV transitions were seen to be in strong coincidence with the 1114-keV transition but no 527-keV transition connecting the proposed 982-keV level to to the 456-keV level was observed. According to the decay scheme of Monnand et al. (25) the 456- and 527-keV transitions would be seen at about equal intensity, but the 982-keV coincidence would be much stronger. The only other possibility for a coincidence with the 456-keV transition is a 133-, 393-keV cascade through the 849-keV level. A 133-keV gamma ray was not observed and neither transition was seen in coincidence with the 1114-keV gamma ray.

The placement of the 982-keV transition as depopulating the 2850-keV level results in a reversed order of transitions seen in cascade from the 2850-keV level compared to the level scheme of Monnand et al (25). The order proposed in this work for these four cascades is supported by several observed coincidences and results in non-zero beta feeding for two of the intermediate levels.

1184.71 ± 0.05 and 1273.20± 0.06-keV levels. These levels decay only to the ground state and do not have a low

log*ft*. This suggests that they are of spin 9/2 or greater and may correspond to the lowest 9/2+ and 11/2+ levels obtained in shell-model calculations. Because all of the experimental levels in this region have logf_1t values greater than 8.5, their spin assignments are not well determined. All of these levels except those at 1868, 2368, and 2796 keV decay both to the 7/2+ ground state and the 5/2+ first excited state. Their spin assignments are therefore restricted to the range 3/2 to 9/2. All except the 2099- and 2217-keV levels are confirmed by definite coincidences with the 456-keV transition.

1569.84 ± 0.06-keV level. This level is strongly fed by the 1868-keV level. If the 1868-keV level is accepted as the 11/2- state, then the assignment for this level is restricted to 7/2 or 9/2. Since the de-excitation of this level to the 5/2+ level is stronger than to the 7/2+ ground state, an assignment of 7/2 is preferred.

1574.84 ± 0.06-keV level. An assignment of 5/2 or 7/2 is preferred because this level strongly depopulates to both the 7/2+ ground state and the 5/2+ 456-keV level.

1867.87 ± 0.07-keV level. This level probably corresponds to the 1.85-MeV $h_{11/2}$ state seen in the proton transfer experiments of Wildenthal *et al.* (19). This correspondence is consistent with a de-excitation pattern which includes the 7/2+ ground state and levels proposed as 9/2+

and 11/2+ at 1185 and 1273 keV respectively. A beta feeding that is zero within experimental uncertainties is also consistent with this assignment.

2068.03 ± 0.07-keV level. This level may correspond to the $d_{3/2}$ single-particle level seen at 2.07 MeV in proton transfer reactions (19). This assignment is consistent with the observation that the level depopulates strongly to the 5/2+ single particle state at 456 keV and only weakly to the 7/2+ ground state.

2849.11 ± 0.13- and 2850.04 ± 0.09-keV levels. A level doublet is postulated here where previous studies (24,25) have reported a single level. The 2849-keV level results from the lower energy for the 2393.53- + 455.51- and 2000.3- + 848.95-keV sums. Both levels have $\log f_1 t$ values less than 8.5 which restrict the possible spin assignments to 5/2, 7/2, or 9/2 if the assignment for the ^{137}Xe ground state is 7/2−. The strongest depopulating transition for the 2849-keV level is to the 5/2+ single-particle state at 456-keV and no transition to a higher-spin level was observed. An assignment of 5/2 or 7/2 is thus preferred for this level. For the 2850-keV level, the strongest depopulating transitions are to the 7/2+ ground state and the 11/2− level at 1868 keV. An assignment of 9/2 is preferred for this level.

All of the levels above 3 MeV, with the exception of the 3104-keV level, have $\log f_1 t$ values less than 8.5. If the as-

signment for the ^{137}Xe ground state is 7/2$^-$ then the assignments for these levels are restricted to 5/2, 7/2, or 9/2. The large number of high-lying levels with low log*ft* values is similar to observations made for the N=82 nucleus ^{136}Xe where an allowed beta decay of a core neutron to create neutron particle-hole states was proposed to explain these observations.

V. DISCUSSION

A. The Shell Model in this Region

The nuclei studied in this work are near the doubly magic ^{132}Sn nucleus. There has been considerable interest in this region as a test of the shell model. The shell model states between the magic numbers 50 and 82 are $g_{7/2}$, $d_{5/2}$, $h_{11/2}$, $d_{3/2}$ and $s_{1/2}$. The states between 82 and 126 are $f_{7/2}$, $h_{9/2}$, $f_{5/2}$, $p_{3/2}$, $i_{13/2}$, and $p_{1/2}$. For the nuclei studied in this work, the expectation is that the protons above Z=50 will occupy predominantly the $g_{7/2}$ and $d_{5/2}$ single-particle states for the low-lying excited states. From the observed systematic trends, the $h_{11/2}$ state may be an important component in the wavefunctions of the low-lying levels as will be more completely discussed later. Two of the decays studied (^{136}I,^{137}Xe) populate levels in N=82 closed-shell nuclei. The neutron components of the wavefunction are not expected to be significant for the lower excited levels, but they are expected to play an important role in the structure of ^{138}Xe levels and levels above the core breaking threshold for ^{136}Xe and ^{137}Cs.

B. Systematics for Even-Even Nuclei in the N=82 Region

The levels proposed for the decay of ^{138}I are important because they extend the known systematics of the Xe isotopes

to the neutron-rich side of N=82. They also extend the systematics of the N=84 nuclei to within four protons of Z=50. It is helpful to compare the N=82 and N=84 and the Xe and Ba systematics. A comparison of the lowest 2^+, 4^+, and 3^- states for N=82 and N=84 nuclei is shown in Figure 26. As expected, the energies of the levels for the N=84 nuclei are lower than for the N=82 nuclei. The similarity of the trends suggests that the structural dependence on Z is not significantly altered by the addition of two neutrons.

Contrary to what might be expected, the energy of the 2^+ and 4^+ levels increases as the number of protons above Z=50 is increased. A possible explanation of this increase is as follows. The $h_{11/2}$ single-particle energy is observed to decrease with increasing Z for the N=82 isotones as confirmed by proton-transfer experiments (19) and illustrated in Figure 27. The decrease results in an increasing admixture of two $h_{11/2}$ protons coupled to spin 0 in the ground-state wavefunction. The pairing energy associated with the ground state increases with the increasing $h_{11/2}$ admixture, therefore the gap between the 0^+ ground state and first excited 2^+ level increases.

The systematics for Xe and Ba (shown in Figure 28) are also similar. The difference in the level spacing below N=82 compared to above N=82 is of significant interest. The neutron pairs added above N=82 fill the high-spin $f_{7/2}$ and

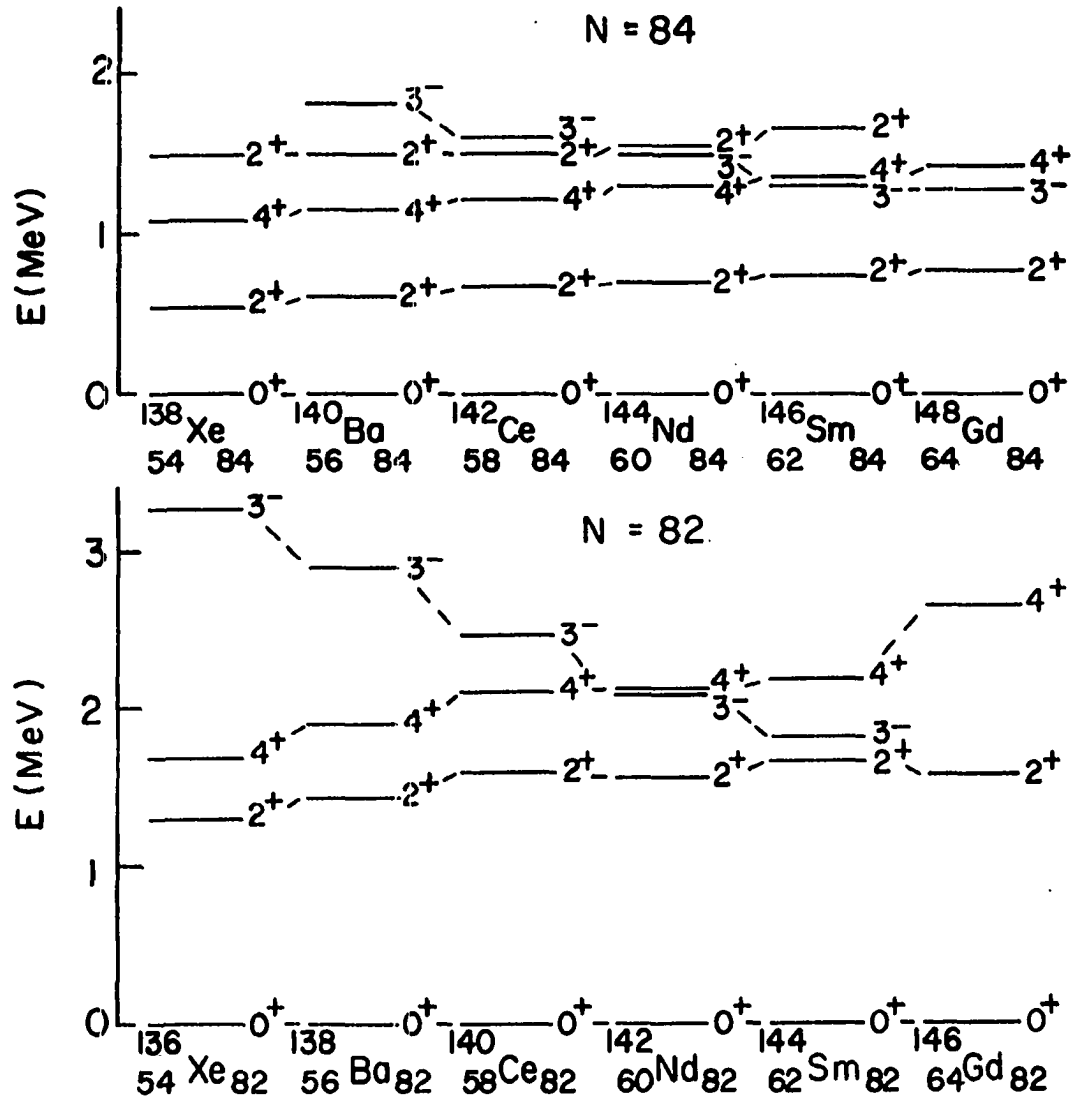

Figure 26. Systematics of low-lying levels for even-even N=82 and N=84 nuclei

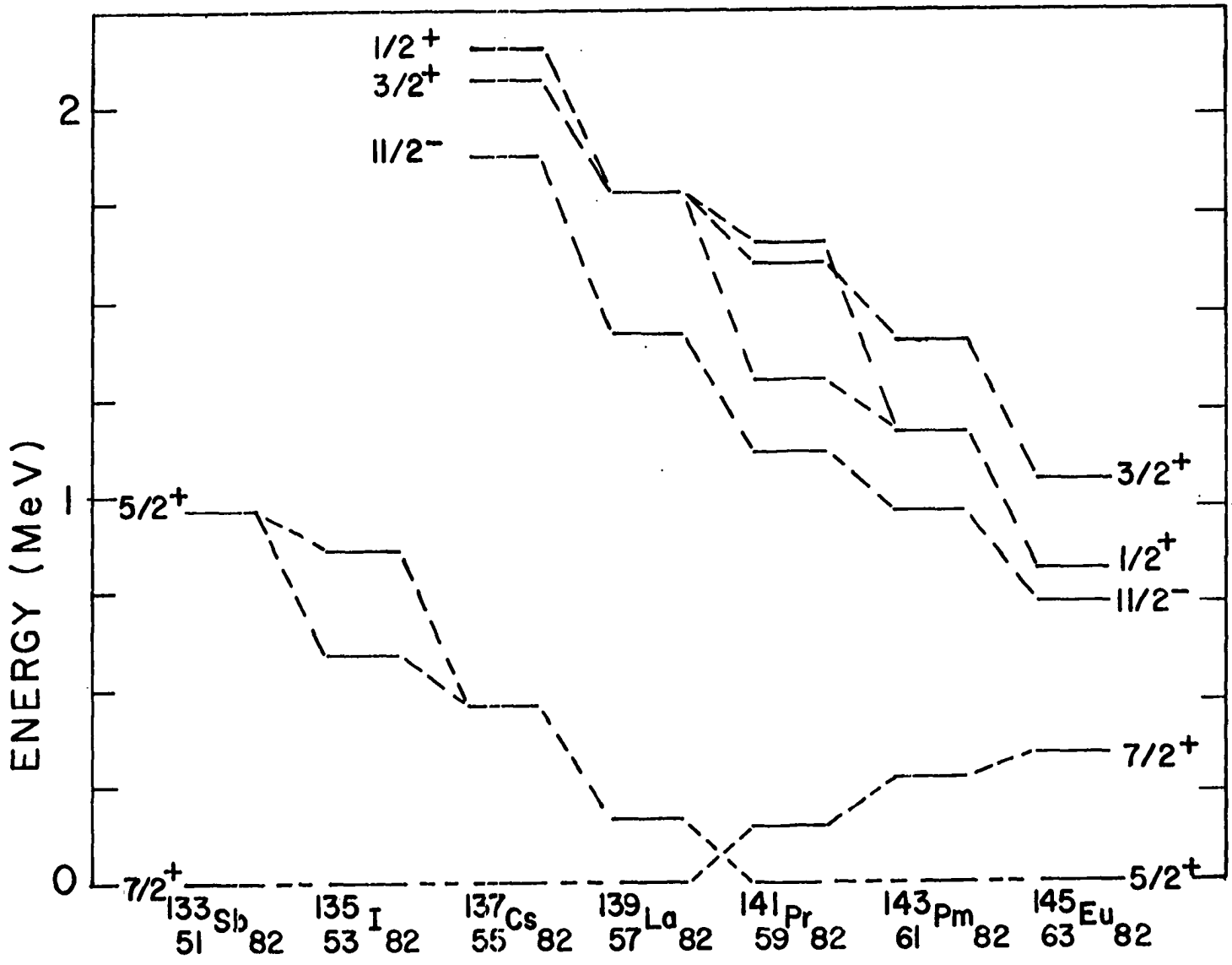

Figure 27. Relative energies of proton single-particle states seen in odd-A N=82 nuclei

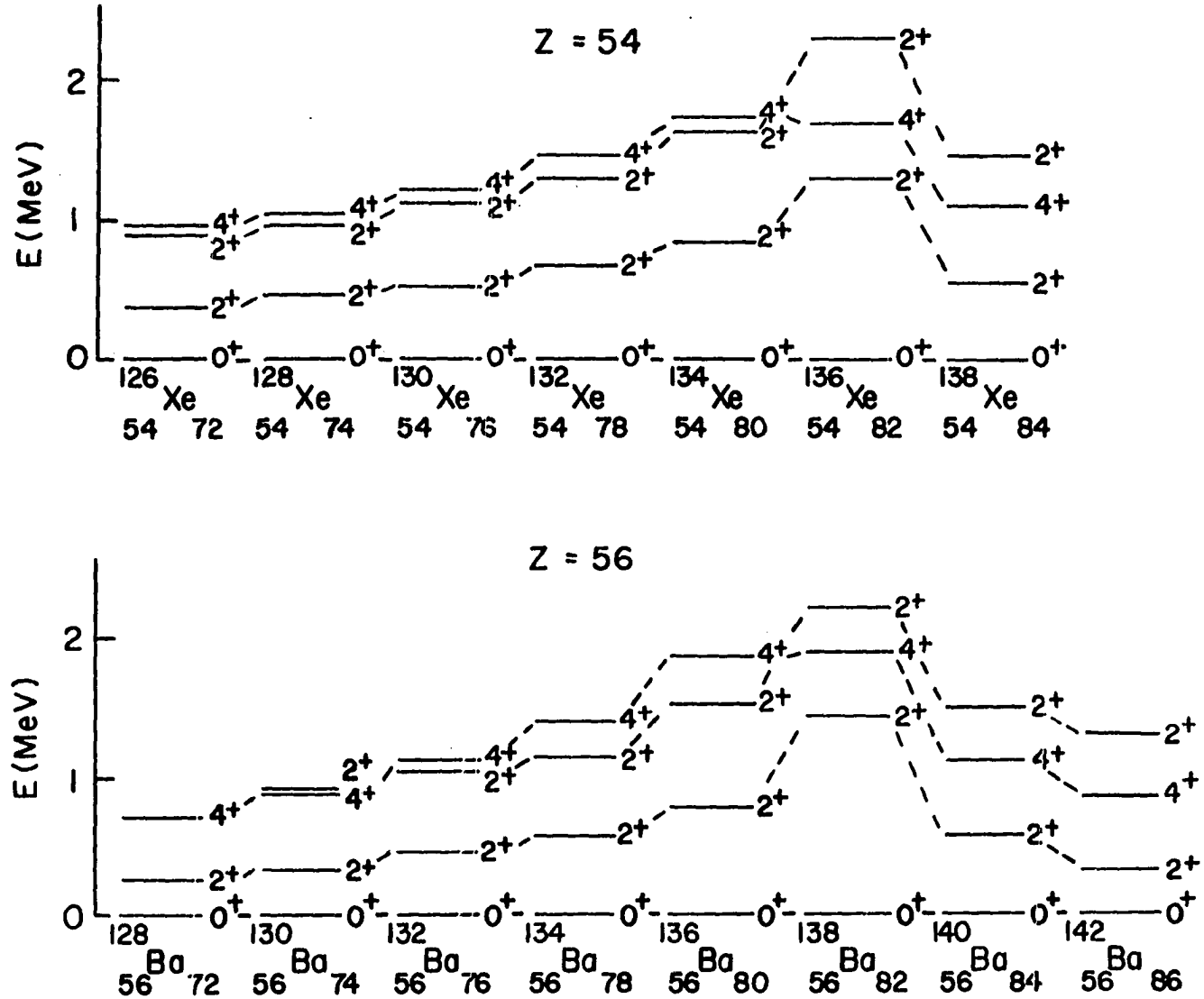

Figure 28. Systematics of the even Xe and Ba isotopes

$h_{11/2}$ orbitals, while the hole states below N=82 occupy the low-spin $s_{1/2}$ and $d_{3/2}$ orbitals. The pairing energy associated with the 0^+ ground state increases with increasing j thus enlarging the gap between the 0^+ level and the higher spin levels as j increases. The dependence on j of the pairing interaction is opposed by the nuclear quadrupole interaction. The quadrupole interaction is the "long range" part of the interaction. Coherent effects involving many particles may result which compete with the pairing force and produce large ground-state deformations and collective levels for nuclei far from the magic numbers. Also, the number of available states that the interacting particles can scatter into is larger for the particles above N=82 than for the hole states where the Pauli principle restricts the available phase space. The observed behavior suggests that the quadrupole interaction predominates over the pairing interaction as one moves away from doubly-magic ^{132}Sn. Additional support for this hypothesis is illustrated in Figure 29, where the excitation energies of the first excited 2^+ level for N=78, 80, 82, 84, and 86 are compared. For Z=54 and 56 the asymmetry about N=82 is evident but decreases until by Z=62 there is symmetry. As more protons are added to Z=50 collective effects increase until they begin to dominate for Z=62 and N≠82.

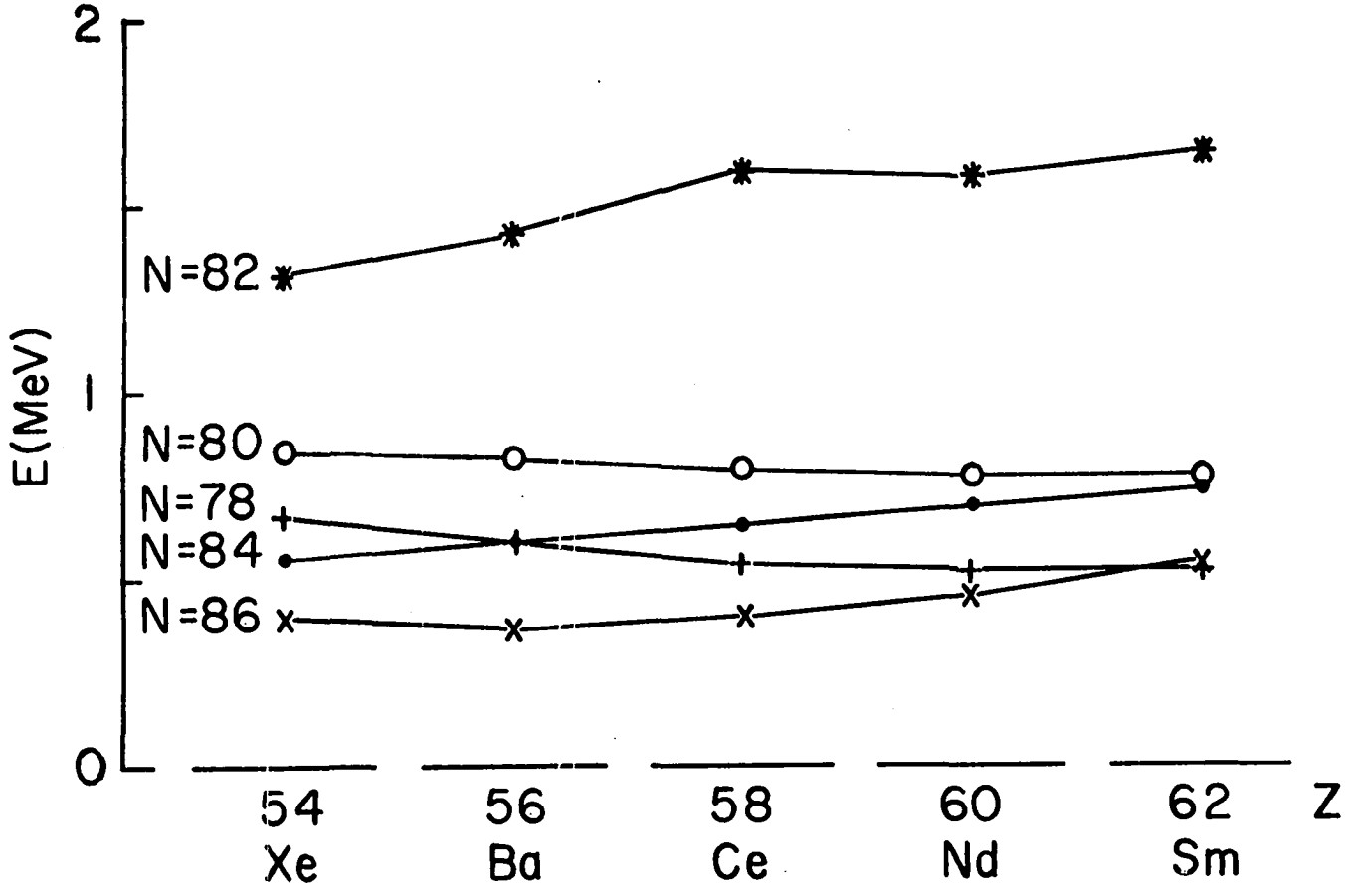

Figure 29. Systematics of the first excited 2^+ levels for N=78, 80, 82, 84, and 86 nuclei

Other effects involving core excitations are seen at higher energies. The high-lying states of ^{136}Xe and ^{138}Ba have been investigated using (p,p') reactions populating isobaric analog resonances (20,41). Several levels above 3 MeV were interpreted as containing significant neutron particle-hole configurations.

Several of these particle-hole states appear to be populated by beta decay. A comparison of the beta decay results with the results of (p,p') scattering for levels above 3 MeV is shown in Figure 30. Over a quarter of all the beta feeding to levels above 3 MeV for ^{136}Xe is to the 4269-keV level which has been interpreted as a particle-hole state. This large feeding can be explained as an allowed beta decay of one of the core neutrons leaving the daughter nucleus in a neutron particle-hole configuration with an excited proton. As an example the $f_{7/2}d_{3/2}^{-1}$ particle-hole state could be formed by allowed beta decay of a $d_{3/2}$ neutron in ^{136}I into a $d_{3/2}$ proton resulting in a $d_{3/2}^{-1}$ neutron hole.

The states which have been identified as having neutron particle-hole components prefer to decay to other particle-hole levels. For example, the 4269-keV level appears to predominantly decay via a 994-keV transition to the 3272-keV level which has also been interpreted as a neutron particle-hole level. Similar observations have been made for the ^{138}Ba levels (42,43).

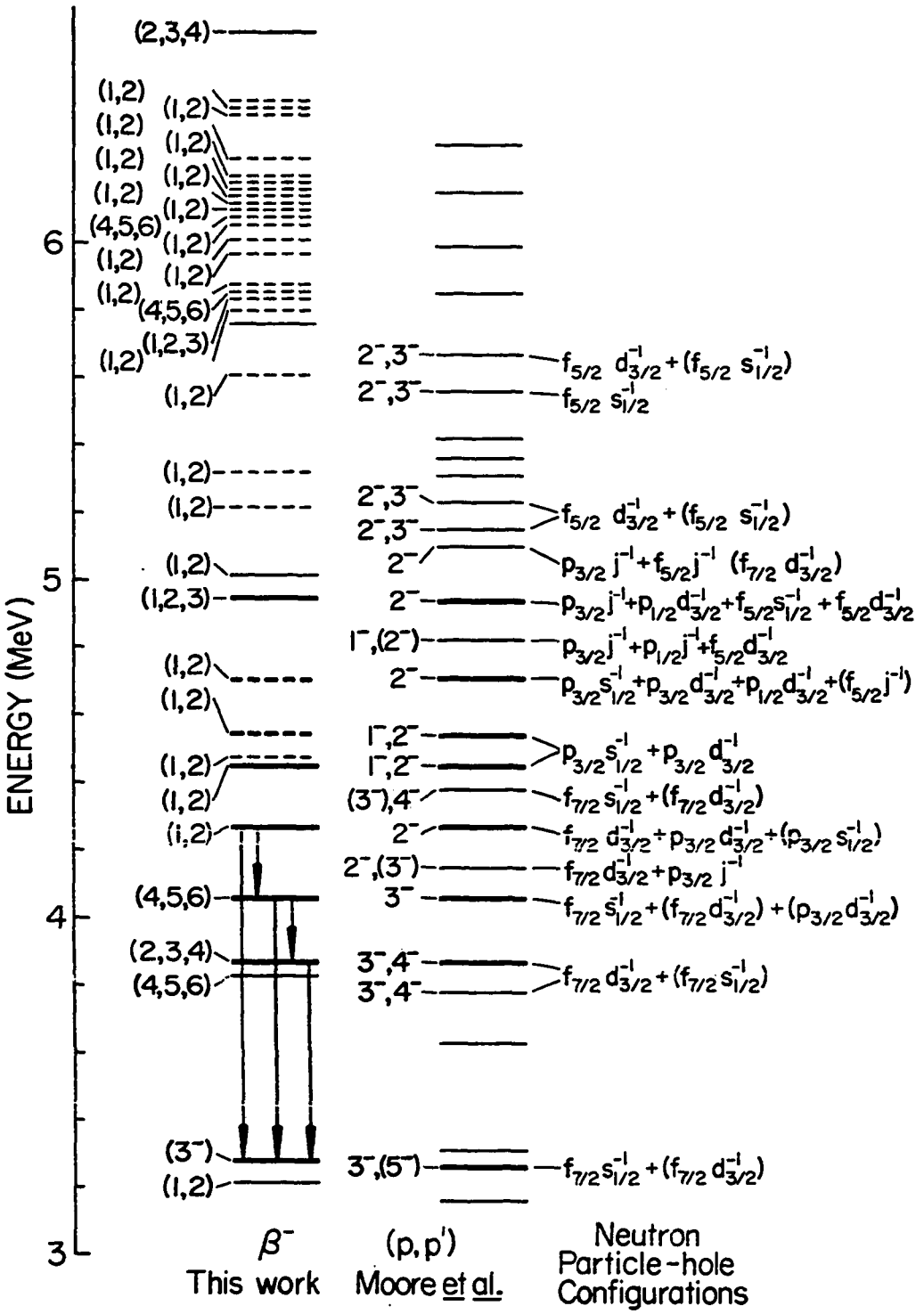

Figure 30. Particle-hole states in ^{136}Xe

The level at 3275 keV is believed to be the 3^- octupole state. It is interesting that this level also appears to have a neutron particle-hole component. Small admixtures of specific configurations can have significant effects on both the beta and gamma transition probabilities so that the neutron particle-hole interpretation is not inconsistent with a collective octupole interpretation.

C. Theoretical Calculations for Even-A N=82 Nuclei

Theoretical calculations for the N=82 nuclei have paralleled the development of experimental information. The first N=82 nuclei for which experimental information was available contained several protons outside the Z=50 shell. Quasi-particle calculations were performed for these nuclei and were later made for ^{136}Xe levels. Lombard (44) performed a two quasi-particle calculation in 1968 using as a basis all of the single-particle states between Z=50 and 82. A gaussian type residual interaction was used and levels for spins 0^+ through 4^+ and 3^- were calculated.

Another quasi-particle calculation for N=82 even-even nuclei was made by Waroquier and Heyde (45) using the same subspace as Lombard. Calculations were made using both a surface-delta interaction and a gaussian force as the residual nucleon-nucleon interaction. They obtained a set of single-particle energies from the experimental level schemes

for the odd proton N=82 nuclei by inverting the gap equations. In a separate publication, Heyde et al. (46) gave a two quasi-particle analysis of the isomeric states observed in even-even N=82 nuclei. Only a gaussian interaction was used for the residual interaction, and the parameters used were the same as for the previous paper.

A shell-model calculation for ^{136}Xe levels has been performed by Wildenthal and Larson (47,48) using four protons outside the doubly-magic ^{132}Sn core. The configuration space included all configurations of $g_{7/2}$ and $d_{5/2}$ plus those with one proton in either the $s_{1/2}$ or $d_{3/2}$ orbital. The residual interaction used was an isospin-dependent surface-delta interaction (modified surface-delta interaction MSDI). The strength of the interaction and the single-particle energies were chosen to optimize the agreement between the model and experimental level energies for positive-parity states in N=82 nuclei with A=136-140. A comparison of these calculations with the experimental results is shown in Figure 31.

The calculations confirm that the predominant configuration for the ground state is $g_{7/2}$. Lombard (44) does not give any wavefunctions or significant components but has the best energy fit for the first 2^+ and 4^+ levels. Although the $h_{11/2}$ orbital was not included in Wildenthal and Larson's calculation (47), the resulting set of levels has the highest first excited 2^+ level. Their reported calculation for ^{134}Te

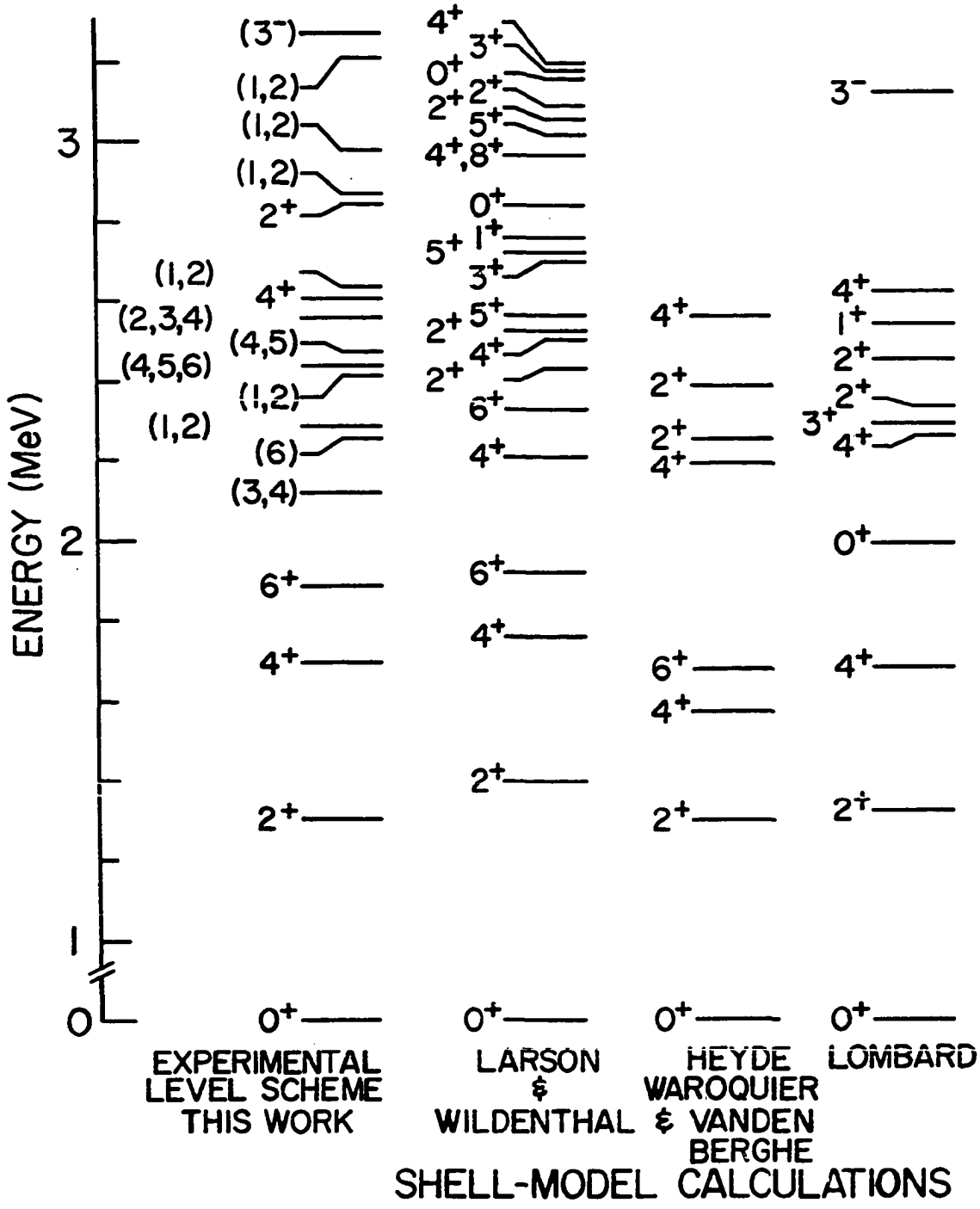

Figure 31. Comparison of ^{136}Xe levels with shell-model calculations

(47) gave level energies too high for the YRAST sequence. These two calculations illustrate the short-range pairing nature of the MSDI and may be an additional indication of the importance of the long-range quadrupole components of the residual interaction. Lombard (44) predicts a 0^+ level at about 2 MeV which was not seen in this work. All of the calculations have a 4^+ level at about 2.2 MeV probably corresponding to the experimental 2126-keV level. A second 6^+ level was reported by Wildenthal and Larson (47,48) at 2.33 MeV which may correspond to the experimental level at 2262 keV. Additional possible correspondences are difficult to establish because of the high level density and the uncertainty as to the spins and parities of the experimental levels. The 3^- level of Lombard (44) is the only negative-parity state calculated. The only odd-parity orbital included was the $h_{11/2}$ proton.

No theoretical calculation has been published specifically for ^{138}Xe levels. Vanden Berghe (49) has published a unified-model calculation of the N=84 nuclei. The parameters chosen result in a level spectrum which is most consistent with experiment for ^{144}Nd and ^{146}Sm. The model couples the two neutrons outside the N=82 core to quadrupole vibrations. The results of this calculation give wavefunctions which show substantial mixing of single-particle states resulting from the coupling of core excitations.

D. Interpretations of ^{137}Cs Levels

Most of the levels observed in the beta decay of ^{137}Xe were not observed in the proton transfer experiments of Wildenthal *et al.* (19). The levels at 0-, 456-, 1868- and 2068-keV appear to correspond to the single-particle levels identified in Reference 19. The systematics for the relative energies of the proton single-particle states is shown in Figure 27. The large number of levels between 1 and 2 MeV for the odd-A N=82 nuclei and the limited number of spin and parity assignments inhibits any attempt to construct comprehensive level systematics for the odd-A nuclei. The low-lying levels of ^{137}Cs can probably be interpreted as an extra proton coupled to a ^{136}Xe core. A consequence of this interpretation is that some similarities would be expected in comparing the ^{137}Xe and ^{136}I decay schemes.

Approximately 36% of all beta feeding to levels above 1 MeV is to the 2850-keV level. A similar observation was made earlier (in this chapter) for the N=82 isotone ^{136}Xe in which a level at 4269 keV was strongly populated by beta decay and was interpreted by isobaric analogue resonance (p,p') experiments as having a neutron particle-hole character. A possible interpretation of the 2850-keV level is that of a neutron particle-hole state coupled to the ground-state proton configuration. Since the strongest depopulating transition for

the 2850-keV level is to the $h_{11/2}$ 1868-keV level, another possible interpretation is that the 2850-keV level is a three quasi-particle state in which one of the quasi-particles is $h_{11/2}$.

E. Theoretical Calculations for ^{137}Cs Levels

Theoretical calculations of the levels in ^{137}Cs have been performed by Heyde and Waroquier (50) and by Wildenthal and Larson (48). A comparison of these calculations with the experimental results is shown in Figure 32.

The first calculation is a quasi-particle treatment which includes all one and three quasi-particle configurations of the protons in the states between Z=50 and Z=82. A central force of gaussian shape with spin exchange was used as the residual nucleon-nucleon interaction.

Wildenthal and Larson performed a shell-model calculation in which all five protons outside the Z=50 shell were included. The basis used included all configurations of the $d_{5/2}$ and $g_{7/2}$ orbitals and configurations in which one proton was excited to the $d_{3/2}$ or $s_{1/2}$ orbitals. A modified surface-delta interaction was used.

It is not possible to make a detailed comparison with experimental levels because the number of known spin and parity assignments for the experimental levels is limited and the density of experimental and theoretical levels is high.

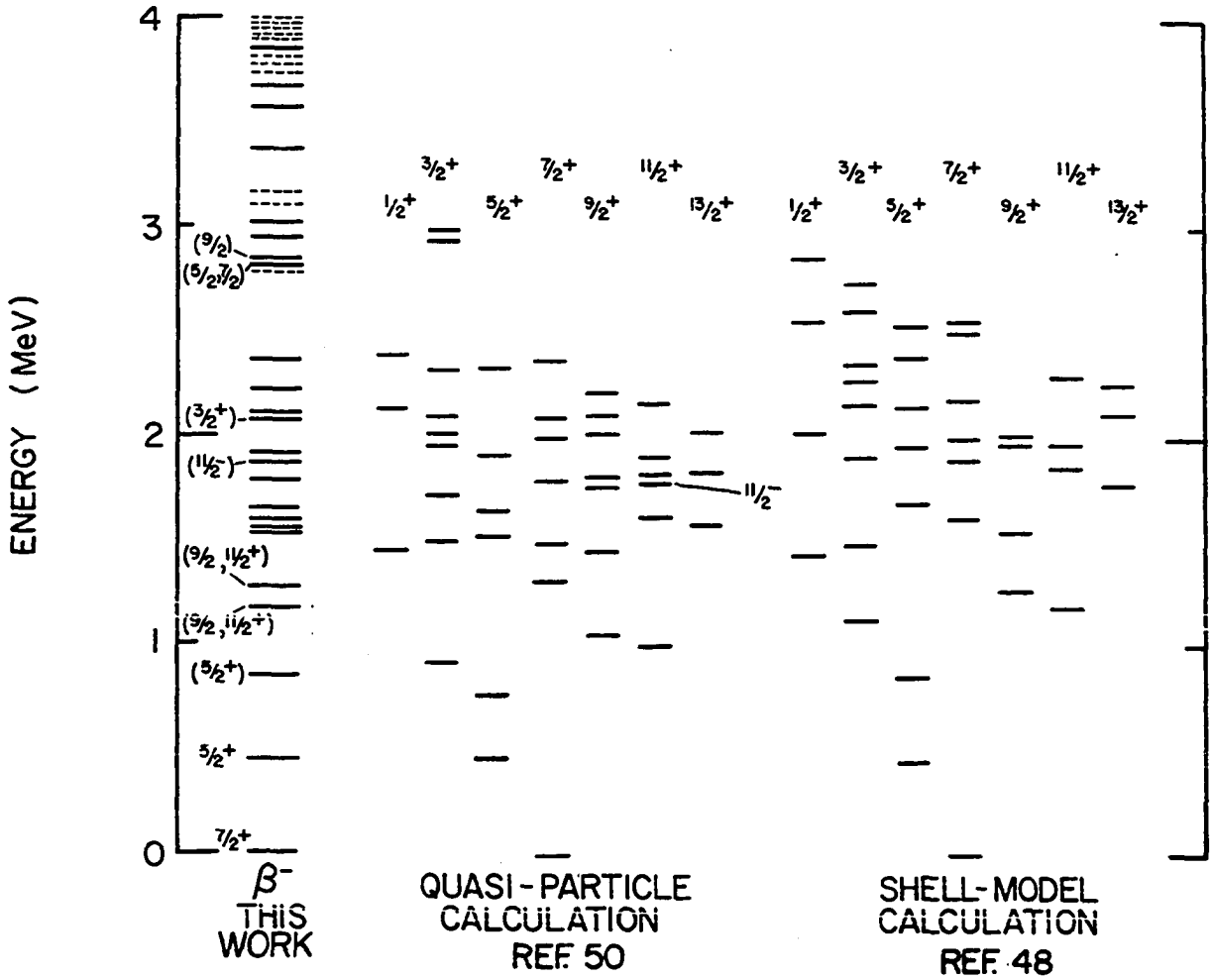

Figure 32. Comparison of ^{137}Cs levels with shell-model calculations

A low-lying $3/2^+$ state is predicted at about 1 MeV. This level was not observed in this study probably because it would be fed by a first-forbidden unique beta transition. Above this level, the density of states from the theoretical calculations is in good agreement with the observed experimental level density and spin assignments.

VI. CONCLUSIONS

The results of this study clarify many discrepancies between previous studies of ^{136}I decay. A proposed 100-second isomer was not observed, and the placement of most transitions connecting low-lying levels was established. The spin and parity of the high-spin isomer cannot be limited to 5^-, since beta feeding to the 4^+ level at 1694 keV was not observed.

Many new transitions with energy greater than 3 MeV were observed and many new levels above 3.3 MeV were proposed. Some of these levels appear to correspond to neutron particle-hole states seen in (p,p') isobaric analogue resonance experiments. A similar observation can be made for a few levels in ^{138}Ba (42,43). It would be interesting to study the decay of ^{134}Sb in order to search for similar levels and to examine their systematics.

Levels corresponding to single-particle states identified in proton-transfer experiments (19) were observed in the decay scheme for ^{137}Xe. The 2850-keV level was observed to be strongly populated by beta decay and possible interpretations as a neutron particle-hole state or a three quasiparticle state containing some $h_{11/2}$ single-particle strength were proposed.

The level systematics for the N=84 and Xe isotopes were extended by the construction of the first decay scheme for ^{138}I. Further study of this decay with sources containing a larger ratio of I to Xe is necessary for a more comprehensive extension of the Xe and N=84 systematics.

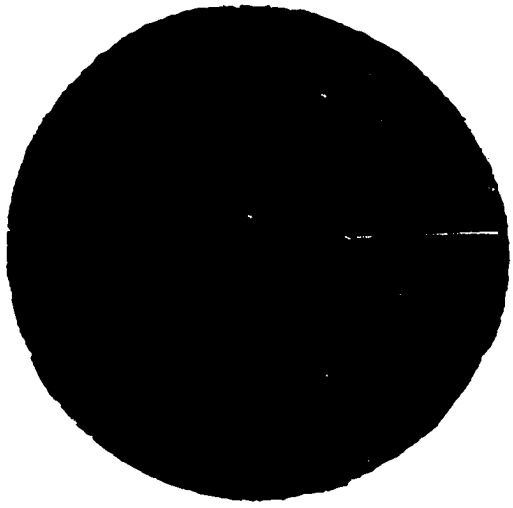

The level systematics for the N=84 and Xe isotopes were extended by the construction of the first decay scheme for ^{138}I. Further study of this decay with sources containing a larger ratio of I to Xe is necessary for a more comprehensive extension of the Xe and N=84 systematics.

VII. APPENDIX: COMPUTER CODES

New computer codes have been developed to assist in the analysis of the experimental data. These codes are discussed below.

A. ENERGY Code

The code ENERGY was developed to simplify the calculation of gamma energies and to expedite the analysis of the energies of gamma peaks above 3.5 MeV using a bootstrapping procedure. The output cards from the peak-fitting codes were used to enter the peak centroids into the ENERGY code, and the energies were entered on standardized energy calibration cards. The code has two modes of operation. The first mode successively performs a weighted least-squares fit of the differential nonlinearity to polynomials of increasing order. The argument of the polynomial is the least-squares line energy. The nonlinearity was calculated relative to a least-squares line determined from a specified subset of the ordered pairs in the input data. The resulting polynomial and nonlinearity are plotted for each degree (≤ 7) of the polynomial to determine the order of polynomial which gives the best fit. The uncertainty in the nonlinearity value is specified as half of the difference between two polynomials (of the same order as the nonlinearity polynomial) which are

the weighted least-squares fits to the points of the upper and lower error limits respectively.

The other mode of operation is to use the polynomial of optimum order to evaluate the energy of unknown peaks. The nonlinearity polynomial was obtained from peaks in the calibration spectrum. The code adds the polynomial value of the nonlinearity to the least-squares line energy to obtain the energy of the unknown peak.

If a peak is labeled as a double- or single- escape peak, (DEP or SEP) ENERGY calculates the single-escape and photo-peak (PP) energies. If succeeding cards contain the SE and or PP and these peaks are within the specified range of the nonlinearity, then a weighted average of the PP energy is performed. This calculated PP energy could be used to extend the nonlinearity curve.

B. Multiscale Codes

The code TRANSF16 was used to sum and transfer the 16K multiscale data sets from magnetic tape onto a private disk pack. This code is a modification of an earlier code which was adapted to process 16K data sets. The code can be used to correct for overflows of channel zero in each time slice.

A special plotting code (PLTMULTI) was developed to plot and list selected energy regions of the multiscale data, summed over selected time intervals. These plots were used

to determine the placement of windows on the background above and below the peak and on the peak itself.

The code HALFLIFE performs the analysis required to obtain the dead-time corrected areas of a peak as a function of time and plots a single half-life fit to the decay curve. Peak areas are determined by subtracting the area under the background line in the peak window from the sum of the counts in the peak window. The background line is the least-squares line through the counts in both background windows. Counts from the oscillator stored in channel 0 are normalized to the counts stored for the last time interval, and the peak areas are divided by this normalization to obtain the dead-time corrected areas. Punched cards were generated containing the time, counts in the peak window, background counts in the peak window, uncertainty of this background and the dead-time correction factor. Two different methods are used to fit a single half-life to the decay curve. The first is a least-squares line fit to the logarithm of the decay curve. The second method performs a Newton's method minimization of the chi-square as a function of the decay constant.

If the decay curve could not be fit with a single half-life, then the punched card output was analyzed using the code MULTLMDA. This code constructs a decay curve from the card input and minimizes the chi-square value by performing a stepping search on the decay-constant parameters. The calcu-

lated decay curve can contain up to a maximum of ten components and can include daughter activities which grow in during the multiscale cycle. The code can plot and list the fit obtained using the initial guess for the parameters in addition to the fit obtained with the final parameter values.

VIII. BIBLIOGRAPHY

1. Chart of the Nuclides, Knolls Atomic Power Laboratory, Education Relations, General Electric Co., Schenectady, N.Y.

2. F. Strassmann and O. Hahn, Naturwissenschaften 28, 817 (1940)

3. N. Sugarman, J. Chem. Phys. 17, 11 (1949)

4. W.Seelmann-Eggebert and H. J. Born, Naturwissenschaften 31, 59 (1943)

5. M. McKeown and S. Katcoff, Phys. Rev. 94, 965 (1954)

6. N. R. Johnson and G. D. O'Kelley, Phys. Rev. 114, 279 (1959)

7. R. L. Bunting, Nuclear Data Sheets 15, 335 (1975)

8. G. B. Holm, U. Fägerquist and I. Bergström, Phys. Letters 6, 324 (1963)

9. A. Lundan and A. Siivola, Ann. Acad. Sci. Fennicae, Ser, A VI, No. 288 (1968)

10. L. C. Carraz, J. Blachot, E. Monnand and A. Moussa, Nucl. Phys. A158, 403 (1970)

11. A. Lundan, Z. Phys. 242, 107 (1971)

12. H. N. Erten, C. D. Coryell and W. B. Walters, J. Inorg. Nucl. Chem. 33, 4005 (1971)

13. R. L. Bunting and J. J. Kraushaar, Nuclear Data Sheets 13, 191 (1974)

14. E. Achterberg, F. C. Iglesias, A. E. Jech, J. A. Moragues, D. Otero, M. L. Perez, A. N. Proto, J. J. Rossi, W. Scheuer and J. F. Suarez, Phys. Rev. C5, 1759 (1972)

15. W. John, F. W. Guy and J. J. Wesolowski, Phys. Rev. C2, 1451 (1970)

16. E. Cheifetz, J. B. Wilhelmy, R. C. Jared and S. G. Thompson, Phys. Rev. C4, 1913 (1971)

17. L. O. Edvardson and L. O. Norlin, (Sweden Uppsula Univ. Fysiska Inst.) Dept. NTIS 15p. April 1974

18. B. H. Wildenthal, E. Newman and R. L. Auble, Phys. Lett. 27B, 628 (1968)

19. B. H. Wildenthal, E. Newman and R. L. Auble, Phys. Rev. C3, 1199 (1971)

20. P. A. Moore, P. J. Riley, C. M. Jones, M. D. Mancusi and J. L. Foster Jr., Phys. Rev. C1, 1100 (1970)

21. S. Sen, P. J. Riley and T. Udagawa, Phys. Rev. C6, 2201 (1972)

22. A. Lundan and K. Anttila, Nucl. Inst. Meth. 79, 333 (1970)

23. K. -L. Kratz, W. Lauppe and G. Herrmann, Inorg. Nucl. Chem. Letters 11, 331 (1975)

24. G. Holm, Arkiv Fysik 37, 1 (1968)

25. E. Monnand, R. Brissot, J. Crancon, Ch. Ristori, F. Schussler and A. Moussa, J. Phys. (Paris) 36, 1 (1975)

26. G. R. Lucas Jr., P. Martin, G. H. Miller, R. E. Welsh, D. A. Jenkins, R. J. Powers and A. R. Kunselman, Phys. Rev. C7, 1678 (1973)

27. J. R. McConnell and W. L. Talbert Jr., Nucl. Instr. Methods 128, 227 (1975)

28. W. L. Talbert, Jr. and D. Thomas, Nucl. Instr. Methods, 38, 306 (1965)

29. W. L. Talbert, Jr. and J. R. McConnell, Arkiv Fysik 36, 99 (1966)

30. J. H. Norman, W. L. Talbert, Jr. and D. M. Roberts, USAEC Report IS-1893 (1968)

31. G. H. Carlson, W. L. Talbert, Jr., and J. R. McConnell, Phys. Rev. C9, 283 (1974)

32. W. C. Schick, Jr., Bettis Atomic Power Laboratory, Westinghouse Electric Corporation, West Mifflin, Pa., Private Communication

33. D. A. Gedcke and W. J. McDonald, Nucl. Instr. Meth., 55, 377 (1967)

34. D. A. Gedcke and W. J. McDonald, Nucl. Instr. Meth., 58, 253 (1968)

35. W. C. Schick, Jr., ERDA Report IS-3636 (1975)

36. W. C. Schick, Jr., USAEC Report IS-3460 (1974)

37. S. Raman and N. B. Gove, Phys. Rev. C7, 1995 (1973)

38. G. T. Garvey, W. J. Gerace, R. L. Jaffe, I. Talmi, and I. Kelson, Rev. Mod. Phys. 41, S1 (1969)

39. R. J. Onega and W. W. Pratt, Phys. Rev. 136B, 365 (1964)

40. P. A. Moore, P. J. Riley, C. M. Jones, M. D. Mancusi and J. L. Foster Jr., Phys. Rev. 175, 1516 (1968)

41. G. C. Morrison, M. Williams, J. A. Nolen, Jr., and D. von Ehrenstein, Phys. Rev. Letters 19, 592 (1967)

42. J. C. Hill and D. F. Fuller, Phys. Rev. C5, 532 (1972)

43. G. H. Carlson, W. L. Talbert, Jr. and J. R. McConnell, Phys. Rev. C9, 283 (1974)

44. R. J. Lombard, Nucl. Phys. A117, 365 (1968)

45. M. Waroquier and K. Heyde, Nucl. Phys. A164, 113 (1971)

46. K. Heyde, M. Waroquier, and G. Vanden Berghe, Phys. Letters 35B, 211 (1971)

47. B. H. Wildenthal and D. Larson, Phys. Letters 37B, 266 (1971)

48. B. H. Wildenthal and D. Larson, Dept. of Phys., Michigan State University, Private Communication

49. G. Vanden Berghe, Z. Physik A272, 245 (1975)

50. K. Heyde and M. Waroquier, Nucl. Phys. A167, 545 (1971)

IX. ACKNOWLEDGMENTS

The author would like to express his appreciation and thanks to all past and present members of the TRISTAN research group for their contributions tc the TRISTAN group and to this study in particular. Additional thanks and appreciation is expressed to the following individuals:

Dr. John C. Hill for the many long and late sessions required to complete this study and for his guidance in completing the analysis of these data.

Dr. W. C. Schick Jr. for his guidance during the first four years of this study.

Dr. W. L. Talbert Jr. for his enccouragement and suggestions during this research and for the suggestion of iodine decays as an interesting research project.

Dr. F. K. Wohn for many useful discussions cn data analysis and computer codes.

J. R. McConnell for his work and skill in developing and operating the TRISTAN system and for his instruction in the operation of it.

D. R. Lekwa, M. A. Cullison and A. R. Landin for their maintenance of TRISTAN and for their assistance in obtaining these data.

Finally, the author would like to express his thanks to his parents, Mr. and Mrs. R. E. Western, for their encouragement and support during this study.